A NONPERTURBATIVE CALCULATION

OF THE ELECTRON'S ANOMALOUS MAGNETIC MOMENT

Approved by:

Dr. Kent Hornbostel

Dr. Werner Horsthemke

Dr. Pavel Nadolsky

Dr. Roberto Vega

A NONPERTURBATIVE CALCULATION OF THE ELECTRON'S ANOMALOUS MAGNETIC MOMENT

A Dissertation Presented to the Graduate Faculty of the

Dedman College

Southern Methodist University

in

Partial Fulfillment of the Requirements

for the degree of

Doctor of Philosophy

with a

Major in Theoretical Physics

by

Sophia S Chabysheva

(B.S., Physics, St. Petersburg State University, Russia, 1991)
(M.S., Physics, St. Petersburg State University, Russia, 1993)

August 4, 2009

ACKNOWLEDGMENTS

This work began under the ever-helpful guidance of Gary McCartor, and, after he was lost to us, continued with the generous help of Kent Hornbostel, who bravely stepped into the role of thesis advisor for a project not quite related to his own work. The project also benefited from advice from John Hiller, a long-time collaborator of Gary's, who worked with the methods involved from the earliest days and also provided sample computer code from a smaller but similar calculation in Yukawa theory, and from Vladimir Klemeshev, who was a great help in the development of a preliminary version of the computer code, as well as the graphic design for several of the figures. The support and encouragement of the Physics Department at Southern Methodist University, particularly from Ryszard Stroynowski, were critical to the continuation and completion of the project. The resources made available by the University of Minnesota-Duluth during the final stages of the work were also very important, particularly for access to the Minnesota Supercomputing Institute, which granted computer time for the project. The work was also supported in part by the US Department of Energy, under Contract No. DE-FG03-95ER40908.

Chabysheva, Sophia S

B.S., Physics, St. Petersburg State University, Russia, 1991
M.S., Physics, St. Petersburg State University, Russia, 1993

A Nonperturbative Calculation
of the Electron's Anomalous Magnetic Moment

Advisor: Associate Professor Kent Hornbostel
Doctor of Philosophy degree conferred August 4, 2009
Dissertation completed August 4, 2009

As a step in the development of a nonperturbative method for the solution of bound-state problems in quantum chromodynamics (QCD), the Pauli–Villars (PV) regularization scheme is applied to a calculation of the dressed-electron state and its anomalous magnetic moment in light-front-quantized quantum electrodynamics (QED) in Feynman gauge. The regularization is provided by heavy, negative-metric fields added to the Lagrangian. The light-front QED Hamiltonian then leads to a well-defined eigenvalue problem for the dressed-electron state expressed as a Fock-state expansion. The Fock-state wave functions satisfy coupled integral equations that come from this eigenproblem. A finite system of equations is obtained by truncation to no more than two photons and no positrons; this extends earlier work that was limited to dressing by a single photon. Numerical techniques are applied to solve the coupled system and compute the anomalous moment, for which we obtain agreement with experiment, within numerical errors. As part of the analysis, the one-photon truncation is reconsidered in detail, and we find that the PV regularization requires a second PV photon flavor to restore the chiral symmetry of the massless-electron limit and to provide for slowly varying dependence on the PV masses. We also discuss the prospects for application of the method to QCD.

TABLE OF CONTENTS

APPENDIX

LIST OF FIGURES

LIST OF TABLES

This dissertation is dedicated to the memory of Gary McCartor, who originated the method that is applied in this work and guided its development for many years until his sudden passing. His strong voice and relentless optimism, even in the face of an early death, are greatly missed. The project described here was proposed by him, and one can only hope that the outcome meets his expectations.

Chapter 1

INTRODUCTION

1.1. Motivation

High-energy scattering experiments have shown conclusively that the strong nuclear force is well described by a generalization of quantum electrodynamics (QED) known as quantum chromodynamics (QCD). The "chromo" prefix refers to a multi-component charge for the fundamental particles that is called color; it is the analog of the single-component positive and negative charges of electrodynamics. The colored particles are spin-1/2 quarks and antiquarks and spin-1 gluons, the analogs of electrons, positrons, and photons, respectively. A key distinction is that gluons carry color charge and therefore interact among themselves, making QCD very nonlinear. The gluon color charge also causes the apparent coupling of quarks to appear weak at short distances, a phenomenon known as asymptotic freedom. Since it is the short distances that are probed by high-energy scattering, QCD can be analyzed perturbatively and compared to experiment.

At longer distances, at the scale of an atomic nucleus or larger, the effective couplings are strong and nonlinear, such that no quark or gluon can appear in isolation. Instead, they are bound to each other in color-neutral (*i.e.*, without any QCD charge) combinations called hadrons, such as pi-mesons, protons and neutrons. It is the hadrons, the bound states of QCD, that one would like to study, to derive their properties directly from the theory.

This is a difficult task. Nonperturbative calculations are always difficult, but for a strongly coupled theory such as QCD, they are worse. For a weakly coupled theory, one can set aside much of the interaction for perturbative treatment and solve only a small core problem nonperturbatively. For QED, this core problem is the Coulomb problem, the binding of particles with opposite ordinary charge by an inverse square force; when combined with high-order perturbation theory, amazingly accurate results can be obtained for bound states of the theory [1]. In a strongly coupled theory one cannot make this separation so easily.

In the work presented here, the purpose is to explore a nonperturbative method that can be used to solve for the bound states of quantum field theories. Although the bound states of QCD are of particular interest, the method is not yet mature enough for application to QCD. Instead, we will continue with the program developed in the earlier work of Brodsky, McCartor, and Hiller [2, 3, 4, 5, 6, 7, 8] and explore the method within QED. This provides an analysis of a gauge theory, which is a critical step toward solving a non-Abelian gauge theory, such as QCD.

The remainder of this chapter is intended as a brief overview of quantum field theory and applications to bound-state problems. Many details, including precise definitions and explanations, are given in the following chapters and appendices and also in the cited references.

1.2. Quantum Field Theory

Another consequence of strong coupling is that the internal velocities of constituents in a bound system are typically relativistic. So, quantum mechanics must be merged with relativistic kinematics, and the result is quantum field theory.

1.2.1. Quantum Mechanics and Relativity

The relativistic analogs of the Schrödinger equation, such as the Dirac equation for spin-1/2 particles, admit not only positive-energy solutions but also a negative spectrum extending to negative infinity. The existence of these negative-energy states eventually leads to inconsistencies, and they must be re-interpreted as positive-energy particles of opposite spin moving backward in time. A consistent formulation of this idea is a quantum field theory, which QED and QCD are.

The price to be paid in this convergence of quantum mechanics and relativity is the loss of particle-number conservation. Electrons and positrons can emit and absorb photons, photons can change to an electron-positron pair, and an electron-positron pair can annihilate to a photon. Analogous processes happen for quarks and gluons in QCD, as well as two gluons annihilating to produce one or two gluons and one gluon producing or absorbing two more gluons. Thus the bound states of a quantum field theory are linear superpositions of states with different numbers of particles. Of course, the possibilities are not limitless; conservation laws such as (total) charge conservation still apply.

1.2.2. Fock-State Expansions

The states with definite particle number and definite momentum for each particle are called Fock states. We will use Fock states as the basis for the expansion of eigenstates. The coefficients in such an expansion are the wave functions for each possible set of constituent particles. These functions describe the distribution of internal momentum among the constituents. Such an expansion is infinite, and we truncate the expansion to have a calculation of finite size.

The wave functions are determined by a coupled set of integral equations which are obtained from the bound-state eigenvalue problem of the theory. Each bound

state is an eigenstate of the field-theoretic Hamiltonian, and projections of this eigenproblem onto individual Fock states yields these coupled equations. Each equation is a relativistic analog of the momentum-space Schrödinger equation, but with terms that couple the equation to other wave functions that represent different sets of constituents, perhaps one gluon more or less or a quark-antiquark pair in place of a gluon or vice-versa.

The solution of such equations, in general, requires numerical techniques. The equations are converted to a matrix eigenvalue problem by some discretization of the integrals or by a function expansion for the wave functions. The matrix is usually large and not diagonalizable by standard techniques; instead, one or some of the eigenvalues and eigenvectors are extracted by the iterative Lanczos process [9, 10]. The eigenvector of the matrix yields the wave functions, and from these can be calculated the properties of the eigenstate, by considering expectation values of physical observables.

1.2.3. Regularization and Renormalization Conditions

Although this may seem straightforward, a serious complication quickly arises: the solutions for the wave functions yield integrals that are not finite. Thus, the integral equations are not consistent. The integrals must be regulated in some way, to make them finite, and then the regulators removed at the end of the calculation by taking a limit. This may require modification of the integral equations with addition of terms (counterterms) that depend on the regulator and that restore symmetries broken by regulating the original integrals. Basically, the original equations are replaced by new equations that return to the original set in some limit, but the limit is not taken until after physical quantities have been calculated.

During the limiting process, the parameters of the theory – coupling strengths and constituent masses – become functions of the regulating parameters and are determined by what are called renormalization conditions, such as requiring fixed values of bound-state masses or scattering cross sections. This rescaling, or renormalization, of the original (also called bare) parameters of the theory is critical for the consistent definition of the limit.

One frequently finds that one or more of the bare parameters is driven to infinity when the limit is taken; however, this is not an inconsistency because the bare parameters are not observable. For example, the physical mass scales of a theory are the eigenmasses of the Hamiltonian, not the mass parameters in the Hamiltonian. In particular, the bare mass of the electron can be quite different from the physical mass of the electron eigenstate, which is a bare electron dressed by many photons and electron-positron pairs, as expressed in a Fock-state expansion.

1.2.4. Pauli–Villars Regularization

The method of regularization that we use is called Pauli–Villars (PV) regularization [11]. The basic idea is to subtract from each integral a contribution of the same form but of a PV particle with a much larger mass. This subtraction will cancel the leading large-momentum behavior of the integrand, making the integral less singular. For example, an integrand of the form $1/(k^2 + m^2)$ would become $1/(k^2 + m^2) - 1/(k^2 + m_{\rm PV}^2) = (m_{\rm PV}^2 - m^2)/[(k^2 + m^2)(k^2 + m_{\rm PV}^2]$, which falls off as $1/k^4$ instead of $1/k^2$. To make an integral finite, more than one subtraction may be necessary, due to subleading divergences. The masses of these PV particles are then the regulators of the re-defined theory, and ideally one would take the limit of infinite PV masses at the end of the calculation.

The usefulness of PV regularization is in the preservation of symmetries of the theory. Any regularization of a field theory should preserve as many symmetries as possible; these include Lorenz symmetry, chiral symmetry, and gauge symmetry. Ordinary cutoffs break symmetries which then require counterterms for their restoration. The determination of the counterterms can be difficult.

Simply adding more particles to the theory will not result in subtractions. There would be only additions, since the pattern of interactions would be the same. Instead, one must arrange for the square of the interaction to have the opposite sign for a PV particle. In theories where all terms have no imaginary part, this can be arranged by assigning an imaginary coupling to the PV particles. The square is then obviously negative. However, the field-theoretic Hamiltonian is typically complex and Hermitian rather than real and the imaginary coupling is not cleanly isolated.

The alternative is to assign the PV particles a negative "metric," in the sense that annihilation of such a particle produces a minus sign, relative to what would happen with an ordinary particle. In this case, the square of an interaction involves first creation of a PV particle and then its annihilation, for an extra net sign of minus. This produces the desired subtractions.

Ordinarily, this method of regularization, being automatically relativistically covariant, preserves the original symmetries of the theory. However, it may happen that the negative-metric PV particles over subtract, in the sense that some symmetry is broken by a finite amount. In such a case, a counterterm is needed, or a positive-metric PV particle can be added to restore the symmetry.

It is interesting to note that the introduction of negative-metric partners has recently been used to define extensions of the Standard Model that solve the hierarchy problem [12]. The additional fields provide cancellations that reduce the ultraviolet divergence of the bare Higgs mass to only logarithmic. This slowly varying dependence

allows the remaining cancellations to occur without excessive fine tuning.

1.2.5. Light-Cone Coordinates

Another serious complication in the use of Fock-state expansions and coupled equations is the presence of vacuum contributions to the eigenstate. The lack of particle-number conservation in quantum field theory means that, in general, even the vacuum can have contributions from non-empty Fock states with zero momentum and zero charge. The basis for a massive eigenstate will include such vacuum Fock states in products with non-vacuum Fock states, since the vacuum contributions do not change the momentum or charge. These vacuum contributions destroy the interpretation of the wave functions.

In order to have well-defined Fock-state expansions and a simple vacuum, we use the light-cone coordinates of Dirac [13, 14]. In these coordinates, $t + z/c$ plays the role of time, with c the speed of light, and the orthogonal spatial coordinate, $t - z/c$, lies along a lightlike path. Both coordinate axes are tangential to the light cone. The trajectory of any massive particle is timelike and inside the forward light cone; therefore, no massive particle can move backwards along the new spatial coordinate x^-. This means that the light-cone momentum $p^+ = E/c + p_z$, with E the energy and p_z the z-component of momentum, which is conjugate to the light-cone spatial coordinate, cannot be negative and there are no vacuum contributions.

An exception to the lack of structure for the vacuum is the possibility of modes with zero longitudinal momentum or, simply, zero modes [15, 14]. They represent an accumulation point for the spectrum of individual light-cone energies $p^- = E/c - p_z$, which are driven to infinity when p^+ goes to zero. How they should be included is not yet well understood, though it is expected that they are responsible for symmetry breaking effects that occur when a broken-symmetry state becomes the lowest

eigenstate of a theory, making it effectively the vacuum. Since this kind of physics is of great interest for the description of fundamental particles, such as the symmetry breaking by the Higgs particle in the Standard Model [16], some work has been done in this direction [17], though in the work reported here zero modes and symmetry breaking are not considered.

Light-cone coordinates also have the advantage of separating the internal and external momenta of a system. The Fock-state wave functions depend only on the internal momenta. The state can then be boosted to any frame without necessitating the recalculation of the wave functions.

1.3. Quantum Electrodynamics

Calculations in QED are of interest in their own right. We will consider the anomalous moment of the electron, for which Feynman made the following challenge at the 12th Solvay Conference [18]: "Is there any method of computing the anomalous moment of the electron which, on first approximation, gives a fair approximation to the α term and a crude one to α^2; and when improved, increases the accuracy of the α^2 term, yielding a rough estimate to α^3 and beyond." Here α is the fine-structure constant, equal to $e^2/4\pi$, with $-e$ the charge of the electron. It sets the scale of perturbative corrections in QED.

The nonperturbative calculations in a sequence of truncations in particle number that we consider in the present work is an attempt to respond to this challenge. A previous try, using sidewise dispersion relations, was considered by Drell and Pagels [19] but was not systematic. Another attempt, by Hiller and Brodsky [20], did use a truncation in particle number, specifically to two photons, but was unsuccessful due to the lack of a consistent regularization scheme. The theory was regulated by a momentum cutoff; counterterms were constructed but without determination of fi-

nite contributions. With our technique for regularization, a sequence of truncations becomes a systematic procedure (though not necessarily successful). Of course, due to limitations on numerical accuracy, we do not expect to be able to compute the anomalous moment as accurately as high-order perturbative calculations [1, 21].

An explicit truncation in particle number, the light-cone equivalent of the Tamm–Dancoff approximation [22], can be made. This truncation has significant consequences for the renormalization of the theory [23, 24], in particular the uncancelled divergences discussed below. It also impacts comparisons to Feynman perturbation theory [25], where the truncation eliminates some of the time-ordered graphs that are required to construct a complete Feynman graph. Fortunately, numerical tests in Yukawa theory [4, 8] indicate that these difficulties can be overcome. The tests show a rapid convergence with respect to particle number.

The standard approach to numerical solution of the eigenvalue problem is the method originally suggested by Pauli and Brodsky [26], discrete light-cone quantization (DLCQ). Periodic boundary conditions are applied in a light-cone box of finite size, and the light-cone momenta are resolved to a discrete grid. Because this method can be formulated at the second-quantized level, it provides for the systematic inclusion of higher Fock sectors. DLCQ has been particularly successful for two-dimensional theories, including QCD [27] and supersymmetric Yang–Mills theory [28]. There was also a very early attempt by Hollenberg *et al.* [29] to solve four-dimensional QCD.

Unfortunately, the kernels of the QED integral operators require a very fine DLCQ grid if the contributions from heavy PV particles are to be accurately represented. To keep the discrete matrix eigenvalue problem small enough, we use instead the discretization developed for the analogous problem in Yukawa theory [8], suitably adjusted for the singularities encountered in QED.

To carry out our calculation in QED, three problems must be solved, as discussed in [7]. We need to respect gauge invariance, interpret new singularities from energy denominators, and handle uncancelled divergences. Although PV regularization normally preserves gauge invariance, the flavor-changing interactions chosen for the PV couplings, where emission or absorption of a photon can change the flavor of the fermion, do break the invariance at finite mass values for the PV fields; we assume that an exact solution exists and has all symmetries and that a close approximation can safely break symmetries. The new singularities occur because the bare mass of the electron is less than the physical mass and energy denominators can be zero; a principal-value prescription is used. These zeros have the appearance of a threshold but do not correspond to any available decay. The uncancelled divergences are handled (as in the case of Yukawa theory [8]), with the PV masses kept finite and the finite-PV-mass error balanced against the truncation error.

In general, physical quantities, such as the anomalous magnetic moment, take the form

$$\lim_{\mu_{\rm PV}\to\infty} \frac{a_1 g^2 \left[+a_2 g^4 \ln \mu_{\rm PV} + \cdots\right]}{1 + b_1 g^2 + b_2 g^2 \ln \mu_{\rm PV} + \cdots} = \begin{cases} 0, & \text{with truncation} \\ \text{finite}, & \text{without truncation}, \end{cases} \tag{1.1}$$

where $\mu_{\rm PV}$ is a PV mass scale and the contents of the square brackets are absent in the case of truncation. When the limit $\mu_{\rm PV} \to \infty$ is taken, the result is either zero or a finite value. In perturbation theory, the order-g^2 terms in the denominator are kept only if the order-g^4 terms are kept in the numerator, and a finite result is obtained. The truncated nonperturbative calculation includes the order-g^2 terms in the denominator but not the compensating order-g^4 terms in the numerator.

This lack of cancellation is handled by not taking the limit of infinite PV masses. For small PV masses, too much of the negatively normed states are included in the eigenstate. For large PV masses, there are truncation errors: the exact eigenstate

has large projections onto excluded Fock sectors. The strategy taken is to include as many Fock sectors as possible and use finite PV mass values for which the two errors are balanced.

For Yukawa theory, the usefulness of truncating Fock space was checked in a DLCQ calculation that included many Fock sectors. The full DLCQ result was compared with results for truncations to a few Fock sectors for weak to moderate coupling strengths and found to agree quite well [4]. We can see in Table 1 of [4] that probabilities for higher Fock states decrease rapidly. This was also checked at stronger coupling by comparing the two-boson and one-boson truncations [8]. Figure 14 of [8] shows that contributions to structure functions from the three-particle sector are much smaller than those from the two-particle sector.

For QED, there has been no explicit demonstration that truncation in Fock space is a good approximation; the two-photon truncation considered here gives the first evidence. The usefulness of truncation is expected for general reasons, but a physical argument comes from comparing perturbation theory with the Fock-space expansion. Low-order truncations in particle number correspond to doing perturbation theory in α to low order, plus keeping partial contributions for all orders in α. As long as the theory is regulated so that the contributions are finite, the contributions of higher Fock states are expected to be small because they are higher order in α.

1.4. Review of Previous Applications

In a series of papers, Brodsky, Hiller, and McCartor developed the light-front PV approach and applied it to simple models with a heavy fermionic source which can emit and absorb bosonic fields [2, 3] and to the dressed-fermion eigenproblem of Yukawa theory [4, 6, 8], and extended it to a one-photon truncation of quantum electrodynamics (QED) [7]. The problem of the dressed electron was considered for

QED in both Feynman gauge and light-cone gauge. There was also some formal work on exact solutions [5], which are possible when the PV particles are degenerate in mass with the physical particles; this is an unphysical limit but has its uses. Many useful lessons were learned as the complexity of the applications grew.

The first test of the method was to consider the one-loop fermion self-energy in Yukawa theory [2]. The one-loop self-energy requires three PV scalars to subtract quadratic and log divergences and to restore chiral symmetry [30]. The usual covariant approach requires only one PV scalar and a symmetric-integration prescription. The addition of PV fields increases the size of the basis in any numerical calculation. Numerical tests of DLCQ calculations of the one-loop self-energy showed that the number of basis states that include PV particles is approximately 60% of the total basis size. Thus the increase in the basis size can be acceptable.

The next step was to consider a soluble model of a heavy source [2]. The model generalized the static-source model of Greenberg and Schweber [31]. The effective light-cone Hamiltonian includes one PV scalar with imaginary coupling. The solution to the eigenvalue problem for this Hamiltonian can be obtained analytically. The Fock-state wave functions factorize into products of wave functions for the individual constituents, and the constituent wave functions are easily found. A numerical solution of the full Hamiltonian eigenvalue problem based on DLCQ showed rapid convergence to the analytic solution and a reasonable basis size, despite the basis states added to include PV particles.

Following this success, the static source was made dynamical by the addition of the correct longitudinal and transverse momentum dependence to its kinetic energy [3]. Again, one PV scalar with imaginary coupling was included. There is no longer an analytic solution, but the numerical solution again shows rapid convergence. With this model Brodsky *et al.* also studied the effects of truncation in particle number

and found that severe truncations can provide good approximations.

The method was then applied to Yukawa theory without antifermions regulated with three PV scalars, two of which are assigned a negative metric [4]. The couplings were arranged to satisfy the constraints that regulate the fermion one-loop self-energy, including preservation of chiral symmetry. An effective interaction to represent the Z graph was also added, to cancel infrared divergences associated with the instantaneous fermion four-point interactions. The numerical quadrature was based on discretized light-cone quantization (DLCQ) [26]. The theory was solved for the dressed fermion state. The Fock wave functions were used to compute various quantities, including average constituent multiplicities, average momenta, structure functions, and a form factor slope. One can also compute entire form factors, though this has not generally been done. Truncations in particle number were again studied; it was found that a truncation to two bosons was sufficient for the regime of moderate coupling strengths, where the nonperturbative and low-order perturbative solutions showed significant differences.

The calculations were significantly improved with the use of one PV scalar and one PV fermion [6, 8], both with negative metric. The interaction term of the Yukawa Lagrangian was generalized to couple zero-norm combinations of the physical and PV fields. The regularization has the advantage that the instantaneous fermion terms cancel in the new Hamiltonian. They arise from the elimination of nondynamical degrees of freedom and are numerically much more expensive to compute than three-point interactions. Fortunately, these terms are independent of mass and have the opposite sign between physical and PV fermions, hence their cancellation. However, chiral symmetry is broken explicitly.

The one-boson truncation admits an analytic solution [6] for the dressed fermion state; this analytic solution and a numerical solution for the two-boson truncation

have been studied closely [8]. The Fock-state expansion is explicitly an eigenstate of J_z, making polar coordinates useful and efficient for the transverse plane. Each wave function has a total L_z eigenvalue equal to 0 for a bare-fermion spin projection of $s_z = +J_z$ and equal to 1 for $s_z = -J_z$.

For the one-boson truncation, the coupled integral equations for the wave functions reduce to algebraic equations in the bare-fermion sector. The solution is similar to the leading-order perturbative solution, except that in light-cone energy denominators the initial energy is determined by the physical mass rather than the bare mass. With these solutions one can investigate the coupling and bare mass as functions of the PV masses.

Two PV mass limits were studied, one where the masses were equal and another where the PV fermion mass was taken to be much larger than the PV boson mass. In the second case, there was found a solution that was much like perturbation theory; however, the problem of uncancelled divergences was encountered.

For the truncation to two bosons, the renormalization must include fermion mass renormalization, due to a divergent self-energy, and include charge renormalization, due to a log divergence in the incomplete cancellation of wave function and vertex renormalizations. The renormalization is done by imposing conditions on the dressed mass M and the Dirac radius $R = \sqrt{-6F_1'(0)}$, and then computing the bare mass m_0 and bare coupling g.

These theories admit exact solutions in the unphysical limit of PV masses being equal to the physical masses [5]. The mass eigenvalue problem becomes triangular, and even operator solutions can be found. It is, however, a very unphysical regime, because negative-metric fields contribute substantially. There is some speculation that a physical regime could be analyzed in terms of perturbations in the mass differences, but the most practical use of these solutions is in providing a limiting case for testing

numerical calculations.

For QED, the PV regularization method has been considered and applied to a one-photon truncation of the dressed electron state [7]. In Feynman gauge, one PV electron and one PV photon were sufficient, and their presence has the convenient feature of not only cancelling the instantaneous fermion interactions but also making the fermion constraint equation explicitly solvable. Ordinarily, in the light-cone quantization of QED [32], light-cone gauge ($A^+ = 0$) must be chosen to make the constraint equation solvable; in Feynman gauge with one PV electron and one PV photon the A^+ terms cancel from the constraint equation. Light-cone gauge has been considered in [7], but the naive choice of three PV electrons for regularization was found insufficient; an additional photon and higher derivative counterterms were also needed. The one-photon truncation yielded an anomalous moment within 14% of the Schwinger term [33]. With two photons, to be considered here, the value for the anomalous moment should be close to the value obtained perturbatively when the Sommerfield–Petermann term [34] is included. However, numerical errors will make this tiny correction undetectable, and we will focus on obtaining better agreement with the leading Schwinger term of $\alpha/2\pi$.

1.5. Prospects for Quantum Chromodynamics

An extension to a two-boson truncation is also very interesting as a precursor to work on QCD. Unlike the one-boson truncation, where QED and QCD are effectively indistinguishable, the two-boson truncation allows three and four-gluon vertices to enter the calculation. A nonperturbative calculation, with these nonlinearities included, could capture much of the low-energy physics of QCD, perhaps even confinement.

One way in which to apply the light-front PV method to QCD is the scheme proposed by Paston *et al.* [35]. It involves the introduction of several PV fields as

well as higher derivative regularization and several counterterms. The formulation is specifically designed to be perturbatively equivalent to covariant Feynman theory. One would then make the assumption that the regularization is sufficient for a nonperturbative calculation and proceed as in the case of QED.

The number of fields and the number of renormalization conditions required by the counterterms in the Paston formulation will make computations quite large. Present computing technology is probably insufficient; however, the reliably steady improvement in computing hardware could make enough resources available by the time a computer code for QCD has been developed. Also, a preliminary step in the study of QCD could be study of a meson model that includes a mechanism for chiral symmetry breaking, proposed by Dalley and McCartor [36].

The approach depends critically on making a Tamm–Dancoff truncation to a finite number of constituents. For QCD this is thought to be reasonable because the constituent quark model was so successful [37]. Wilson and collaborators [38, 24] even argued that a light-cone Hamiltonian approach can provide an explanation for the quark model's success. The recent successes of the AdS/CFT correspondence [39] in representing the light hadron spectrum of QCD also indicates the effectiveness of a truncation; this description of hadrons is equivalent to keeping only the lowest valence light-cone Fock state.

At the very least, the success of the constituent quark model shows that there exists an effective description of the bound states of QCD in terms of a few degrees of freedom. It is likely that the constituent quarks of the quark model correspond to effective fields, the quarks of QCD dressed by gluons and quark-antiquark pairs. From the exact solutions obtained using PV regularization [5], it is known that simple Fock states in light-cone quantization correspond to very complicated states in equal-time quantization, and this structure may aid in providing some correspondence to

the constituent quarks. However, the truncation of the QCD Fock space may need to be large enough to include states that provide the dressing of the current quarks, and perhaps a sufficiently relaxed truncation is impractical. As an alternative, the light-front PV method could be applied to an effective QCD Lagrangian in terms of the effective fields. Some work on developing a description of light-front QCD in terms of effective fields has been done by Głazek *et al.* [40].

1.6. Other Nonperturbative Methods

A directly related Hamiltonian approach is that of sector-dependent renormalization [23], where bare masses and couplings are allowed to depend on the Fock sector. This alternative treatment was used by Hiller and Brodsky [20] and more recently by Karmanov *et al.* [41]. In principle, this approach is roughly equivalent to the approach used here; however, Karmanov *et al.* ignore the limitations on the PV masses that come from having a finite, real bare coupling, as discussed in [20], and do not make the projections necessary to have finite expectation values for particle numbers.

The most developed nonperturbative method is that of lattice gauge theory [42], which has been studied for much longer than nonperturbative light-front methods and has already achieved impressive successes in solving QCD. The lattice is a Euclidean spacetime grid with fermion fields at the vertices and gauge fields on the links between vertices. The continuum Euclidean action $S = \int \mathcal{L} d^4x$ for the Lagrangian $\mathcal{L}$ is approximated by a lattice action $S_{\rm lat}$ that approaches S when the grid spacing goes to zero. An observable is calculated from the expectation value of a suitable operator $\mathcal{O}$, computed as a sum over field configurations U that is weighted by the exponentiation of the action $S_{\rm lat}(U)$

$$\langle \mathcal{O} \rangle = \frac{\sum_U \mathcal{O}(U) e^{-S_{\rm lat}(U)}}{\sum_U e^{-S_{\rm lat}(U)}}. \tag{1.2}$$

The sum is then approximated by random sampling of the possible field configurations. The notion of a wave function does not appear in the lattice approach; to extract a bound-state property from the field configurations requires selection of an appropriate operator. This Euclidean approach has particular difficulty with quantities such as timelike and spacelike form factors, that depend on the signature of the Minkowski metric. In contrast, in a Hamiltonian approach with the original Minkowski metric, a form factor is readily calculated as a convolution of wave functions.

A related method is that of the transverse lattice [43], where light-cone methods are used for the longitudinal direction and lattice methods for the transverse. It is, however, a Hamiltonian approach which results in wave functions. The transverse directions are discretized to a square grid. At each vertex there is a two-dimensional theory, coupled to the theories at nearby vertices by gauge fields on the transverse links. The link fields are replaced by collective variables that represent averages over short-distance fluctuations in the gluon field, and the original gauge group is recovered in the continuum limit. The two-dimensional theories are approximated by DLCQ [14]. The parameters are fixed by requiring restoration of symmetries, particularly Lorentz symmetry. Applications have been to large-N gauge theories and mostly limited to consideration of meson and glueball structure.

Another approach is that of Dyson–Schwinger equations [44], which are coupled equations for the n-point Euclidean Green's functions of a theory, including the propagators for the fundamental fields. Bound states of n constituents appear as poles in the n-particle propagator; in the case of two-body systems, this propagator satisfies the Bethe–Salpeter equation. Solution of the infinite system requires truncation and a model for the highest n-point function. To date the truncation made is at $n = 3$. The model for the 3-point vertex is used to calculate the dressed quark propagator,

and this propagator is used in Bethe–Salpeter equations to study pseudoscalar and vector mesons. Comparisons with lattice results for propagators can be made, to validate the model used for the vertex. Again, as in the lattice approach, there is the limitation to a Euclidean formulation.

The Bethe–Salpeter equation alone can, of course, be used for two-particle states. The kernel is defined perturbatively to include all two-particle irreducible interactions. The interactions that are two-particle reducible are contained implicitly and can be made explicit through iteration of the equation. The perturbative expansion of the kernel must be truncated for practical calculations, a truncation to a single exchange of an intermediate particle, *i.e.* the ladder approximation, being the most common. Any approximation beyond the ladder approximation is very difficult to solve. Also, the interpretation of the solution is made difficult, even in the ladder approximation, by the dependence on a relative time as well as the relative position of the two constituents.

1.7. Outline of Remaining Chapters

In the chapters to follow, we describe the formalism needed to solve the dressed-electron problem in Feynman-gauge QED and apply it to one and two-photon truncations of the Fock space. Chapter 2 contains a discussion of QED quantized on the light cone in Feynman gauge, with a PV electron and two PV photons providing regularization. The eigenproblem for the dressed electron and the expressions to be evaluated for its anomalous magnetic moment are described in Chap. 3.

The analytically soluble one-photon truncation of this eigenproblem is discussed in Chap. 4. Although this one-photon problem was considered in [7], it was done at infinite PV fermion mass. Here we need to be able to make comparisons with the two-photon truncation for which the PV fermion mass must remain finite. Thus,

Chap. 4 contains not only a summary of earlier work but new results for the finite PV mass [45]. In particular, we find that a second PV photon flavor is needed for a sensible calculation.

An analysis of the two-photon truncation is presented in Chaps. 5 and 6. In Chap. 5, we consider only self-energy corrections to the one-photon truncation. This limited form admits a semi-analytic solution and yields results for the anomalous moment that are consistent with experiment to within numerical errors.

In Chap. 6, the full two-photon truncation is kept in the eigenproblem, and the dressed-electron state is computed numerically. The integral equations for the wave functions are discretized to become a matrix eigenvalue problem that is solved by Lanczos iteration [9, 10] and other iterative methods. The results for the anomalous moment are presented and discussed.

Chapter 7 contains a summary of the results and of progress made in developing the light-front PV method, as well as suggestions for additional work on QED and QCD. There are several appendices that contain important proofs, descriptions of numerical methods, and supplemental information that would otherwise interrupt the flow of the main narrative.

Chapter 2

QUANTUM ELECTRODYNAMICS IN FEYNMAN GAUGE

As a starting point for the dressed-electron problem in light-front QED, we provide our definition of light-cone coordinates and construct the light-front Hamiltonian from the QED Lagrangian in Feynman gauge. We also discuss the way in which the gauge condition can be implemented. All of the expressions use units where the speed of light c and Planck's constant $\hbar$ are one.

2.1. Light-Cone Quantization

The calculations here are done in terms of light-cone coordinates [13], which are defined by

$$x^{\pm} \equiv x^0 \pm x^3, \quad \vec{x}_\perp \equiv (x^1, x^2). \tag{2.1}$$

The covariant four-vector is written $x^\mu = (x^+, x^-, \vec{x}_\perp)$. This corresponds to a space-time metric of

$$g^{\mu\nu} = \begin{pmatrix} 0 & 2 & 0 & 0 \\ 2 & 0 & 0 & 0 \\ 0 & 0 & -1 & 0 \\ 0 & 0 & 0 & -1 \end{pmatrix}. \tag{2.2}$$

Dot products are then given by

$$x \cdot y = g_{\mu\nu} x^\mu y^\nu = \frac{1}{2}(x^+ y^- + x^- y^+) - \vec{x}_\perp \cdot \vec{y}_\perp. \tag{2.3}$$

For light-cone three-vectors we use the underscore notation

$$\underline{x} \equiv (x^-, \vec{x}_\perp). \tag{2.4}$$

For momentum, the conjugate to x^- is p^+, and, therefore, we use

$$\underline{p} \equiv (p^+, \vec{p}_\perp) \tag{2.5}$$

as the light-cone three-momentum. A frequently useful variable for a particle in a system is the longitudinal momentum fraction $x \equiv p^+/P^+$, where P^+ is the total plus momentum for the system. The dot product of momentum and position three-vectors is

$$\underline{p} \cdot \underline{x} \equiv \frac{1}{2} p^+ x^- - \vec{p}_\perp \cdot \vec{x}_\perp. \tag{2.6}$$

The derivatives are

$$\partial_+ \equiv \frac{\partial}{\partial x^+}\,, \qquad \partial_- \equiv \frac{\partial}{\partial x^-}\,, \qquad \partial_i \equiv \frac{\partial}{\partial x^i}. \tag{2.7}$$

The natural Lorentz boosts for light-cone momenta are [14] the longitudinal boost, in the z direction, and a transverse boost, that leaves the plus component of momentum unchanged. For the longitudinal boost, of relative velocity $\vec{\beta} = \beta\hat{z}$, we have

$$p'^0 = \gamma(p^0 + \beta p^z), \;\; p'^z = \gamma(p^z + \beta p^0), \tag{2.8}$$

so that

$$p'^+ = \gamma(1+\beta)p^+, \;\; p'^- = \gamma(1-\beta)p^-, \;\; \vec{p}'_\perp = \vec{p}_\perp, \tag{2.9}$$

with $\gamma = 1/\sqrt{1-\beta^2}$. The light-cone transverse boost with relative velocity $\vec{\beta}_\perp$ is a combination of an ordinary transverse boost and a rotation, such that

$$p'^+ = p^+, \;\; p'^- = p^- + 2\vec{p}_\perp \cdot \vec{\beta}_\perp + \beta_\perp^2 p^+, \;\; \vec{p}'_\perp = \vec{p}_\perp + p^+ \vec{\beta}_\perp. \tag{2.10}$$

For a system of particles with momenta $\underline{p_i}$, the longitudinal momentum fractions $x_i = p_i^+/P^+$ and relative transverse momenta $\vec{k}_{i\perp} = \vec{p}_{i\perp} - x_i \vec{P}_\perp$ are invariant with respect to these boosts. This separates the internal momenta from the external momentum of the system.

The time variable is taken to be x^+, and time evolution of a system is then determined by $\mathcal{P}^-$, the operator associated with the momentum component conjugate to x^+. Usually one seeks stationary states obtained as eigenstates of $\mathcal{P}^-$. Frequently the eigenvalue problem is expressed in terms of a light-cone Hamiltonian [26]

$$H_{\rm LC} = \mathcal{P}^+\mathcal{P}^- \tag{2.11}$$

as

$$H_{\rm LC}|P\rangle = (M^2 + P_\perp^2)|P\rangle, \;\; \underline{\mathcal{P}}|P\rangle = \underline{P}|P\rangle, \tag{2.12}$$

where M is the mass of the state, and $\mathcal{P}^+$ and $\vec{\mathcal{P}}_\perp$ are light-cone momentum operators. Without loss of generality, we will limit the total transverse momentum $\vec{P}_\perp$ to zero.

The vacuum state is the zero-particle state $|0\rangle$. Fock states are created from the vacuum by the application of creation operators $b^\dagger_{is}(\underline{p})$, $d^\dagger_{is}(\underline{p})$, and $a^\dagger_{j\mu}(\underline{p})$ for electrons, positrons, and photons, respectively, with light-cone momentum $\underline{p}$. Here i and j are "flavor" indices that indicate a physical or PV type, s is a spin index for the fermions, and μ is a Lorentz index for the vector photon. The particles are said to be on the mass shell, meaning that $p^2 = p^\mu p_\mu = m^2$, the square of the rest mass. Therefore, we have $p^- = (m^2 + p_\perp^2)/p^+$.

The conjugate operators, $b_{is}(\underline{p})$, $d_{is}(\underline{p})$, and $a_{j\mu}(\underline{p})$, are the annihilation operators, because they obey the (anti)commutation relations

$$\{b_{is}(\underline{k}), b^\dagger_{i's'}(\underline{k}'\} \;\; = \;\; (-1)^i\delta_{ii'}\delta_{ss'}\delta(\underline{k} - \underline{k}'), \tag{2.13}$$

$$\{d_{is}(\underline{k}), d^\dagger_{i's'}(\underline{k}'\} \;\; = \;\; (-1)^i\delta_{ii'}\delta_{ss'}\delta(\underline{k} - \underline{k}'), \tag{2.14}$$

$$[a_{i\mu}(\underline{k}), a^\dagger_{i'\nu}(\underline{k}'] \;\; = \;\; (-1)^i\delta_{ii'}\epsilon^\mu\delta_{\mu\nu}\delta(\underline{k} - \underline{k}'). \tag{2.15}$$

Here $\epsilon^\mu = (-1, 1, 1, 1)$ is the metric signature for the photon field components in Gupta–Bleuler quantization [47, 48]. One of these operators acting on a Fock state

removes a matching particle with the same momentum, flavor, and spin, or, if no match is found, it acts directly on the vacuum state, yielding zero.

2.2. The Pauli–Villars-Regulated Hamiltonian

The Hamiltonian that defines the eigenvalue problem of interest comes from the Feynman-gauge QED Lagrangian, regulated with two PV photons and a PV fermion. This Lagrangian is

$$\begin{aligned}\mathcal{L} &= \sum_{i=0}^{2}(-1)^i\left[-\frac{1}{4}F_i^{\mu\nu}F_{i,\mu\nu}+\frac{1}{2}\mu_i^2A_i^\mu A_{i\mu}-\frac{1}{2}\left(\partial^\mu A_{i\mu}\right)^2\right] \\ &\quad+\sum_{i=0}^{1}(-1)^i\bar{\psi}_i(i\gamma^\mu\partial_\mu-m_i)\psi_i-e\bar{\psi}\gamma^\mu\psi A_\mu,\end{aligned} \tag{2.16}$$

where

$$A_\mu=\sum_{i=0}^{2}\sqrt{\xi_i}A_{i\mu},\quad \psi=\sum_{i=0}^{1}\psi_i,\quad F_{i\mu\nu}=\partial_\mu A_{i\nu}-\partial_\nu A_{i\mu}. \tag{2.17}$$

The subscript $i=0$ denotes a physical field and $i=1$ or 2 a PV field. Fields with odd index i are chosen to have a negative norm. In our approach, we can keep the mass μ_0 of the physical photon equal to zero [7], unlike perturbation theory where one would have infrared singularities.

The second PV photon $A_{2\mu}$ was not needed in the earlier work [7] and is not needed for ultraviolet regularization. It is, however, necessary for obtaining the correct chiral symmetry in the limit of a massless electron. The earlier work is recovered in the $\xi_2\to 0$ limit. This limit corresponds to the limit $\mu_2\to\infty$.

As is usually the case for PV regularization, the constants ξ_i satisfy constraints. In order that e be the charge of the physical electron, we must have $\xi_0=1$. Another constraint is to guarantee that summing over photon flavors, in an internal line of a Feynman graph, cancels the leading divergence associated with integration over the

momentum of that line. Since the ith flavor has norm $(-1)^i$ and couples to a charge $\sqrt{\xi_i}e$ at each end, the constraint is

$$\sum_{i=0}^{2}(-1)^i\xi_i = 0. \tag{2.18}$$

This also guarantees that A_μ in (2.17) is a zero-norm field. A third constraint will be imposed later; it will be chosen to obtain the correct chiral limit.

The dynamical fields are

$$\psi_{i+} = \frac{1}{\sqrt{16\pi^3}}\sum_s \int d\underline{k}\chi_s\left[b_{is}(\underline{k})e^{-i\underline{k}\cdot\underline{x}} + d^\dagger_{i,-s}(\underline{k})e^{i\underline{k}\cdot\underline{x}}\right], \tag{2.19}$$

$$A_{i\mu} = \frac{1}{\sqrt{16\pi^3}}\int \frac{d\underline{k}}{\sqrt{k^+}}\left[a_{i\mu}(\underline{k})e^{-i\underline{k}\cdot\underline{x}} + a^\dagger_{i\mu}(\underline{k})e^{i\underline{k}\cdot\underline{x}}\right], \tag{2.20}$$

with χ_s an eigenspinor of $\Lambda_+ = \gamma^0\gamma^+/2$ [46]. The creation and annihilation operators satisfy the (anti)commutation relations in (2.13). For the zero-norm photon field A_μ, we have $a_\mu = \sum_i \sqrt{\xi_i}a_{i\mu}$ and the commutator

$$[a_\mu(\underline{k}), a^\dagger_\nu(\underline{k}')] = \sum_i (-1)^i\xi_i\epsilon^\mu\delta_{\mu\nu}\delta(\underline{k}-\underline{k}') = 0. \tag{2.21}$$

An important consequence of the regularization method is that we are not limited to light-cone gauge. The coupling of the two zero-norm fields A_μ and ψ as the interaction term reduces the fermionic constraint equation to a solvable equation without forcing the gauge field $A_- = A^+$ to zero. The nondynamical components of the fermion fields satisfy the constraints ($i = 0, 1$)

$$\begin{aligned} i(-1)^i\partial_-\psi_{i-} + eA_-\sum_j \psi_{j-} &= (i\gamma^0\gamma^\perp)\left[(-1)^i\partial_\perp\psi_{i+} - ieA_\perp\sum_j\psi_{j+}\right] \\ &\quad -(-1)^i m_i\gamma^0\psi_{i+}. \end{aligned} \tag{2.22}$$

This comes from the Dirac equation for the full field ψ_i projected by $\Lambda_- \equiv \gamma^0\gamma^-/2 = 1 - \Lambda_+$, with $\psi_{i\pm} = \Lambda_\pm \psi_i$, and use of the identities [46]

$$\Lambda_\pm \beta = \beta \Lambda_\mp, \;\; \Lambda_\pm \vec{\alpha}_\perp = \vec{\alpha}_\perp \Lambda_\mp, \tag{2.23}$$

where $\beta = \gamma^0$ and $\vec{\alpha}_\perp = \gamma^0\gamma_\perp$.

It would appear that a nontrivial inversion of the covariant derivative is needed to solve the constraints for ψ_-, except when light-cone gauge ($A^+ = 0$) is used; however, for the null combination $\psi_0 + \psi_1$ that couples to A^+, the constraint reduces to

$$i\partial_-(\psi_{0-} + \psi_{1-}) = (i\gamma^0\gamma^\perp)\partial_\perp(\psi_{0+} + \psi_{1+}) - \gamma^0(m_0\psi_{0+} + m_1\psi_{1+}), \tag{2.24}$$

which is the same as the constraint for a free fermion. This constraint is then solved explicitly, and the nondynamical fermion fields are eliminated from the Lagrangian. The full Fermi field can then be written as

$$\psi_i = \frac{1}{\sqrt{16\pi^3}} \sum_s \int \frac{d\underline{k}}{\sqrt{k^+}} \left[b_{is}(\underline{k}) e^{-i\underline{k}\cdot\underline{x}} u_{is}(\underline{k}) + d^\dagger_{i,-s}(\underline{k}) e^{i\underline{k}\cdot\underline{x}} v_{is}(\underline{k}) \right], \tag{2.25}$$

with [46]

$$u_{is}(\underline{k}) = \frac{1}{\sqrt{k^+}}(k^+ + \vec{\alpha}_\perp \cdot \vec{k}_\perp + \beta m_i)\chi_s, \tag{2.26}$$

$$v_{is}(\underline{k}) = \frac{1}{\sqrt{k^+}}(k^+ + \vec{\alpha}_\perp \cdot \vec{k}_\perp - \beta m_i)\chi_{-s}, \tag{2.27}$$

and the light-cone Hamiltonian $\mathcal{P}^-$ can be constructed directly from the above Lagrangian.

The regularization scheme does have the disadvantage of breaking gauge invariance, through the presence of "flavor" changing currents where a physical fermion can be transformed to a PV fermion or vice-versa. However, the breaking effects disappear in the limit of large PV fermion mass [7], because the physical fermion cannot

make a transition to a state with infinite mass. At infinite PV fermion mass, gauge invariance is restored. This was seen explicitly in [7] for the case of a one-photon truncation; calculations done in Feynman gauge and light-cone gauge yielded consistent results. Here we will consider the two-photon truncation where the infinite-mass limit cannot be taken explicitly, but the PV fermion mass is kept large to minimize the effects of the breaking of gauge invariance.

The construction of the Hamiltonian requires formulas for spinor matrix elements that are more general than those given by Lepage and Brodsky [46], where the rules for light-cone perturbative calculations in QCD are given. The presence of the PV fields brings matrix elements that are off-diagonal in mass. These matrix elements are readily computed from the light-cone spinors in (2.26) and the Dirac gamma matrices. We obtain

$$
\begin{aligned}
\bar{u}_{is'}(p)\gamma^{+}u_{js}(q) &= 2\sqrt{p^{+}q^{+}}\delta_{s's}, \qquad (2.28)\\
\bar{u}_{is'}(p)\gamma^{-}u_{js}(q) &= \begin{cases} \frac{2}{\sqrt{p^{+}q^{+}}}[\vec{p}_{\perp}\cdot\vec{q}_{\perp} \pm i\vec{p}_{\perp}\times\vec{q}_{\perp} + m_i m_j], & s' = s = \pm \\ \mp\frac{2}{\sqrt{p^{+}q^{+}}}[m_j(p^1 \pm ip^2) - m_i(q^1 \pm iq^2)], & s' = -s = \mp, \end{cases}\\
\bar{u}_{is'}(p)\gamma_{\perp}^{l}u_{js}(q) &= \begin{cases} \frac{1}{\sqrt{p^{+}q^{+}}}[p^{+}(q^l \pm i\epsilon^{lk3}q^k) + q^{+}(p^l \mp i\epsilon^{lk3}p^k)], & s' = s = \pm \\ \mp\frac{1}{\sqrt{p^{+}q^{+}}}(m_i q^{+} - m_j p^{+})(\delta^{l1} \pm i\delta^{l2}), & s' = -s = \mp. \end{cases}
\end{aligned}
$$

Without antifermion terms, the result for the Hamiltonian is

$$
\begin{aligned}
\mathcal{P}^- = & \sum_{i,s} \int d\underline{p} \frac{m_i^2 + p_\perp^2}{p^+} (-1)^i b_{i,s}^\dagger(\underline{p}) b_{i,s}(\underline{p}) \\
& + \sum_{l,\mu} \int d\underline{k} \frac{\mu_l^2 + k_\perp^2}{k^+} (-1)^l \epsilon^\mu a_{l\mu}^\dagger(\underline{k}) a_{l\mu}(\underline{k}) \\
& + \sum_{i,j,l,s,\mu} \int d\underline{p} d\underline{q} \Big\{ b_{i,s}^\dagger(\underline{p}) \left[b_{j,s}(\underline{q}) V_{ij,2s}^\mu(\underline{p},\underline{q}) \right. \\
& \qquad \left. + b_{j,-s}(\underline{q}) U_{ij,-2s}^\mu(\underline{p},\underline{q}) \right] \sqrt{\xi_l} a_{l\mu}^\dagger(\underline{q}-\underline{p}) + H.c. \Big\} ,
\end{aligned}
\tag{2.29}
$$

which is a generalization to two PV photon flavors from the Hamiltonian in [7]. The vertex functions are

$$
\begin{aligned}
V_{ij\pm}^0(\underline{p},\underline{q}) &= \frac{e}{\sqrt{16\pi^3}} \frac{\vec{p}_\perp \cdot \vec{q}_\perp \pm i \vec{p}_\perp \times \vec{q}_\perp + m_i m_j + p^+ q^+}{p^+ q^+ \sqrt{q^+ - p^+}}, \\
V_{ij\pm}^3(\underline{p},\underline{q}) &= \frac{-e}{\sqrt{16\pi^3}} \frac{\vec{p}_\perp \cdot \vec{q}_\perp \pm i \vec{p}_\perp \times \vec{q}_\perp + m_i m_j - p^+ q^+}{p^+ q^+ \sqrt{q^+ - p^+}}, \\
V_{ij\pm}^1(\underline{p},\underline{q}) &= \frac{e}{\sqrt{16\pi^3}} \frac{p^+(q^1 \pm i q^2) + q^+(p^1 \mp i p^2)}{p^+ q^+ \sqrt{q^+ - p^+}}, \\
V_{ij\pm}^2(\underline{p},\underline{q}) &= \frac{e}{\sqrt{16\pi^3}} \frac{p^+(q^2 \mp i q^1) + q^+(p^2 \pm i p^1)}{p^+ q^+ \sqrt{q^+ - p^+}}, \\
U_{ij\pm}^0(\underline{p},\underline{q}) &= \frac{\mp e}{\sqrt{16\pi^3}} \frac{m_j(p^1 \pm i p^2) - m_i(q^1 \pm i q^2)}{p^+ q^+ \sqrt{q^+ - p^+}}, \\
U_{ij\pm}^3(\underline{p},\underline{q}) &= \frac{\pm e}{\sqrt{16\pi^3}} \frac{m_j(p^1 \pm i p^2) - m_i(q^1 \pm i q^2)}{p^+ q^+ \sqrt{q^+ - p^+}}, \\
U_{ij\pm}^1(\underline{p},\underline{q}) &= \frac{\pm e}{\sqrt{16\pi^3}} \frac{m_i q^+ - m_j p^+}{p^+ q^+ \sqrt{q^+ - p^+}}, \\
U_{ij\pm}^2(\underline{p},\underline{q}) &= \frac{ie}{\sqrt{16\pi^3}} \frac{m_i q^+ - m_j p^+}{p^+ q^+ \sqrt{q^+ - p^+}}.
\end{aligned}
\tag{2.30}
$$

As in Yukawa theory, the four-point vertices known as instantaneous fermion terms, which arise from eliminating the nondynamical Fermi field, do again cancel between physical and PV fields. The terms are independent of the fermion mass,

and the PV fermion terms have a sign opposite that of the physical fermion terms. This is another advantage of the regularization scheme, in that it produces a simpler Hamiltonian; matrix elements of four-point interactions require much more time to calculate and make the resulting matrix eigenvalue problem much less sparse.

For calculations with more than one photon in the Fock space, an helicity basis is convenient. The dependence of the vertex functions on azimuthal angle then becomes simple. This will allow us to take advantage of cylindrical symmetry in the integral equations, such that the azimuthal angle dependence can be handled analytically. There is then no need to discretize the angle in making the numerical approximation. To introduce the helicity basis, we define new annihilation operators for the photon fields

$$a_{l\pm} = \frac{1}{\sqrt{2}}(a_{l0} \pm a_{l3}) \,, \quad a_{l(\pm)} = \frac{1}{\sqrt{2}}(a_{l1} \pm i a_{l2}). \tag{2.31}$$

The Hamiltonian can then be rearranged to the form

$$\begin{aligned}
\mathcal{P}^- = & \sum_{i,s} \int d\underline{p} \frac{m_i^2 + p_\perp^2}{p^+} (-1)^i b_{i,s}^\dagger(\underline{p}) b_{i,s}(\underline{p}) \\
& + \sum_{l,\lambda} \int d\underline{k} \frac{\mu_l^2 + k_\perp^2}{k^+} (-1)^l \left[-a_{l\lambda}^\dagger(\underline{k}) a_{l,-\lambda}(\underline{k}) + a_{l(\lambda)}^\dagger(\underline{k}) a_{l(\lambda)}(\underline{k}) \right] \\
& + \sum_{i,j,l,s,\lambda} \int d\underline{p} d\underline{q} \sqrt{\xi_l} \Big\{ b_{i,s}^\dagger(\underline{p}) b_{j,s}(\underline{q}) \Big[V_{ij,2s}^\lambda(\underline{p},\underline{q}) a_{l\lambda}^\dagger(\underline{q}-\underline{p}) \\
& \qquad + V_{ij,2s}^{(\lambda)}(\underline{p},\underline{q}) a_{l(\lambda)} \dagger (\underline{q}-\underline{p}) \Big] \\
& \quad + b_{i,s}^\dagger(\underline{p}) b_{j,-s}(\underline{q}) \left[U_{ij,-2s}^\lambda(\underline{p},\underline{q}) a_{l\lambda}^\dagger(\underline{q}-\underline{p}) + U_{ij,-2s}^{(\lambda)} a_{l(\lambda)}^\dagger(\underline{q}-\underline{p}) \right] + H.c. \Big\} \,,
\end{aligned} \tag{2.32}$$

and the vertex functions become

$$
\begin{aligned}
V^{+}_{ij\pm}(\underline{p},\underline{q}) &= \frac{e}{\sqrt{8\pi^3(q^+-p^+)}}, \\
V^{-}_{ij\pm}(\underline{p},\underline{q}) &= \frac{e}{\sqrt{8\pi^3}}\frac{(p^1\mp ip^2)(q^1\pm iq^2)+m_im_j}{p^+q^+\sqrt{q^+-p^+}}, \\
V^{(\pm)}_{ij\pm}(\underline{p},\underline{q}) &= \frac{e}{\sqrt{8\pi^3}}\frac{q^1\pm iq^2}{q^+\sqrt{q^+-p^+}}, \\
V^{(\pm)}_{ij\mp}(\underline{p},\underline{q}) &= \frac{e}{\sqrt{8\pi^3}}\frac{p^1\pm ip^2}{p^+\sqrt{q^+-p^+}}, \\
U^{+}_{ij\pm}(\underline{p},\underline{q}) &= 0, \\
U^{-}_{ij\pm}(\underline{p},\underline{q}) &= \mp\frac{e}{\sqrt{8\pi^3}}\frac{m_j(p^1\pm ip^2)-m_i(q^1\pm iq^2)}{p^+q^+\sqrt{q^+-p^+}}, \\
U^{(\pm)}_{ij\pm}(\underline{p},\underline{q}) &= 0, \\
U^{(\pm)}_{ij\mp}(\underline{p},\underline{q}) &= \mp\frac{e}{\sqrt{8\pi^3}}\frac{m_iq^+-m_jp^+}{p^+q^+\sqrt{q^+-p^+}}.
\end{aligned}
\tag{2.33}
$$

The $a_{l\pm}$ operators are null, in the sense that $[a_{l\pm}(\underline{k}), a^\dagger_{l'\pm}(\underline{k}')] = 0$; however, we do have $[a_{l\pm}(\underline{k}), a^\dagger_{l'\mp}(\underline{k}')] = -\delta_{ll'}\delta(\underline{k}-\underline{k}')$.

2.3. Implementation of the Gauge Condition

Feynman gauge is a particular formulation of Lorentz gauge, for which the vector potential satisfies the gauge condition $\partial^\mu A_{i\mu} = 0$. In Gupta–Bleuler quantization [47, 48], this is implemented not as an operator condition but as a projection for the positive frequency part $\partial^\mu A^{(+)}_{i\mu}$, with physical states $|\psi\rangle$ restricted by

$$
\partial^\mu A^{(+)}_{i\mu}|\psi\rangle = \frac{1}{\sqrt{16\pi^3}}\int\frac{d\underline{k}}{\sqrt{k^+}}k^\mu a_{i\mu}(\underline{k})e^{-i\underline{k}\cdot\underline{x}}|\psi\rangle = 0. \tag{2.34}
$$

This restricts Fock-state expansions to physical polarizations in the following way [48, 45]. Let $e^{(\lambda)}_\mu(\underline{k})$, with $\lambda = 0, 1, 2, 3$, be polarization vectors for a photon with four-momentum k, with the properties

$$
e^{(\lambda)\mu}e^{(\lambda')}_\mu = -\epsilon^\lambda\delta_{\lambda\lambda'}, \tag{2.35}
$$

and

$$k^\mu e_\mu^{(\lambda)} = 0, \quad n^\mu e_\mu^{(\lambda)} = 0, \quad \lambda = 1, 2. \tag{2.36}$$

Here $\epsilon^\mu = (-1, 1, 1, 1)$ is the metric signature, as above, and n is the timelike four-vector that reduces to $(1, 0, 0, 0)$ in the frame where $\vec{k}_\perp = 0$. We express the annihilation operator $a_{i\mu}$ in terms of these polarizations as

$$a_{i\mu} = \sum_\lambda e_\mu^{(\lambda)} a_i^{(\lambda)}. \tag{2.37}$$

The polarizations $\lambda = 1, 2$ are the physical transverse polarizations. The scalar and longitudinal polarizations may be chosen to be [48]

$$e^{(0)} = n \ \text{ and } \ e^{(3)}(\underline{k}) = \frac{k - (k \cdot n)n}{k \cdot n}, \tag{2.38}$$

which satisfy the conditions (2.35). The dot product $k \cdot n$ is most readily computed in the $\vec{k}_\perp = 0$ frame, where

$$k \cdot n = k^0 = k^3 = \frac{1}{2} k^+; \tag{2.39}$$

this expression can still be used after a transverse boost (2.10) to non-zero $\vec{k}_\perp$, because the plus component is unchanged by such a boost.

From the choices for $e^{(0)}$ and $e^{(3)}$, we have

$$k^\mu e_\mu^{(0)} = k \cdot n, \quad k^\mu e_\mu^{(3)} = -k \cdot n, \tag{2.40}$$

and

$$k^\mu a_{i\mu} = k \cdot n (a_i^{(0)} - a_i^{(3)}). \tag{2.41}$$

Given this last result, it is convenient to define the linear combinations[1]

$$a_i^{(\pm)} = (a_i^{(0)} \pm a_i^{(3)})/\sqrt{2}. \tag{2.42}$$

[1]These linear combinations are distinct from those that appear in Eq. (2.31). They combine different polarizations, rather than the different Lorentz components used in (2.31).

They are both null and satisfy the commutation relations

$$[a_i^{(\pm)}(\underline{k}), a_i^{(\pm)\dagger}(\underline{k}')] = 0, \quad [a_i^{(\pm)}(\underline{k}), a_i^{(\mp)\dagger}(\underline{k}')] = -(-1)^i \delta(\underline{k} - \underline{k}'). \tag{2.43}$$

The restriction (2.34) on physical states then reduces to

$$a_i^{(-)}|\psi\rangle = 0. \tag{2.44}$$

Because $a_i^{(-)}$ commutes with all but $a_i^{(+)\dagger}$, the restriction (2.44) can be satisfied by removing from $|\psi\rangle$ all terms that contain $a_i^{(+)\dagger}$. This is accomplished by replacing all photon creation operators $a_{i\mu}^\dagger$ with the projected operator

$$\tilde{a}_{i\mu}^\dagger = \frac{1}{\sqrt{2}}(e_\mu^{(0)} - e_\mu^{(3)})a_i^{(-)\dagger} + \sum_{\lambda=1}^{2} e_\mu^{(\lambda)} a_i^{(\lambda)\dagger}. \tag{2.45}$$

Since the $a_i^{(-)\dagger}$ are null, only the physical polarizations contribute to expectation values of physical quantities.

The presence of photons created by $a_i^{(-)\dagger}$ corresponds to the residual gauge transformations [48] that satisfy $\partial^\mu A_{i\mu} = 0$, where $A_{i\mu} \to A_{i\mu} + \partial_\mu \Lambda_i$ with $\Box \Lambda_i = 0$. To see this, consider the expectation value [48] $\langle\psi|A_{i\mu}|\psi\rangle$, with $|\psi\rangle$ written as

$$|\psi\rangle = C_0|0\rangle + \int d\underline{q} C_1(\underline{q}) a_i^{(-)\dagger}(\underline{q})|0\rangle + \cdots, \tag{2.46}$$

and transverse polarizations absent. In the expectation value only the $a_i^{(+)}$ and $a_i^{(+)\dagger}$ terms of $A_{i\mu}$ can contribute, as follows from the commutators in Eq. (2.43), and these terms give

$$\langle\psi|A_{i\mu}|\psi\rangle = -(-1)^i C_0^* \int \frac{d\underline{q}}{\sqrt{16\pi^3 q^+}} C_1(\underline{q}) e^{-iq\cdot x} \frac{1}{\sqrt{2}}(e_\mu^{(0)}(\underline{q}) + e_\mu^{(3)}(\underline{q})) + \text{c.c.} \tag{2.47}$$

From (2.38) and (2.39), we have $e_\mu^{(0)}(\underline{q}) + e_\mu^{(3)}(\underline{q}) = q_\mu/q\cdot n = 2q_\mu/q^+$. The factor q_μ can be replaced by a partial derivative, leaving

$$\langle\psi|A_{i\mu}|\psi\rangle = \partial_\mu \Lambda_i(x), \tag{2.48}$$

with

$$\Lambda_i(x) = -i(-1)^i C_0^* \int \frac{d\underline{q}}{(2\pi q^+)^{3/2}} C_1(\underline{q}) e^{-iq\cdot x} + \text{c.c.} \tag{2.49}$$

Since q is null, $\Box\Lambda_i = 0$. Thus, the contribution from the unphysical polarizations is a pure gauge term consistent with the residual gauge symmetry. A choice of wave function for the minus polarization corresponds to a choice for the residual gauge.

For the calculations reported here, we do not make the gauge projection, because gauge invariance has been broken by both the truncation and the flavor-changing currents. The remaining negative norm of $a_{j0}^\dagger$ does not cause difficulties for our calculations; in particular, our solutions have positive norm.

Chapter 3

THE DRESSED-ELECTRON EIGENSTATE

We will study the state of the electron as an eigenstate of the light-cone Hamiltonian. It is dressed by photons and electron-positron pairs; however, we limit the calculation to photons and truncate the number of photons to two, at most. The eigenstate is then expanded in terms of Fock states, eigenstates of particle number and momentum, with wave functions as the coefficients. In order that the Fock expansion be an eigenstate of the light-cone Hamiltonian, the wave functions must satisfy coupled integral equations. The wave functions are also constrained by normalization of the state. The anomalous magnetic moment is then calculated from a spin-flip matrix element. In this chapter we collect the fundamental expressions for the Fock-state expansion, the coupled equations for the wave functions, the normalization of the wave functions, and the anomalous moment.

3.1. Fock-State Expansion

It is convenient to work in a Fock basis where $\mathcal{P}^+$ and $\vec{\mathcal{P}}_\perp$ are diagonal and the total transverse momentum $\vec{P}_\perp$ is zero. We expand the eigenfunction for the dressed-fermion state with total $J_z = \pm\frac{1}{2}$ in such a Fock basis as

$$|\psi^\pm(\underline{P})\rangle = \sum_i z_i b^\dagger_{i\pm}(\underline{P})|0\rangle + \sum_{ijs\mu}\int d\underline{k} C^{\mu\pm}_{ijs}(\underline{k}) b^\dagger_{is}(\underline{P}-\underline{k}) a^\dagger_{j\mu}(\underline{k})|0\rangle \tag{3.1}$$
$$+ \sum_{ijks\mu\nu}\int d\underline{k_1} d\underline{k_2} C^{\mu\nu\pm}_{ijks}(\underline{k_1},\underline{k_2}) \frac{1}{\sqrt{1+\delta_{jk}\delta_{\mu\nu}}} b^\dagger_{is}(\underline{P}-\underline{k_1}-\underline{k_2}) a^\dagger_{j\mu}(\underline{k_1}) a^\dagger_{k\nu}(\underline{k_2})|0\rangle,$$

where we have truncated the expansion to include at most two photons. The z_i are the amplitudes for the bare electron states, with $i = 0$ for the physical electron and $i = 1$ for the PV electron. The $C_{ijs}^{\mu\pm}$ are the two-body wave functions for Fock states with an electron of flavor i and spin component s and a photon of flavor $j = 0$, 1 or 2 and field component μ, expressed as functions of the photon momentum. The upper index of $\pm$ refers to the J_z value of $\pm\frac{1}{2}$ for the eigenstate. Similarly, the $C_{ijks}^{\mu\nu\pm}$ are the three-body wave functions for the states with one electron and two photons, with flavors j and k and field components μ and ν.

Careful interpretation of the eigenstate is required to obtain physically meaningful answers. In particular, there needs to be a physical state with positive norm. We apply the same approach as was used in Yukawa theory [6]. A projection onto the physical subspace is accomplished by expressing Fock states in terms of positively normed creation operators $a_{0\mu}^\dagger$, $a_{2\mu}^\dagger$, and $b_{0s}^\dagger$ and the null combinations $a_\mu^\dagger = \sum_i \sqrt{\xi_i} a_{i\mu}^\dagger$ and $b_s^\dagger = b_{0s}^\dagger + b_{1s}^\dagger$. The $b_s^\dagger$ particles are annihilated by the generalized electromagnetic current $\bar{\psi}\gamma^\mu\psi$; thus, $b_s^\dagger$ creates unphysical contributions to be dropped, and, by analogy, we also drop contributions created by $a_\mu^\dagger$. The projected dressed-fermion state is

$$
\begin{aligned}
|\psi^\pm(\underline{P})\rangle_{\rm phys} \;=\; & \sum_i (-1)^i z_i b_{0\pm}^\dagger(\underline{P})|0\rangle \qquad (3.2)\\
& + \sum_{s\mu} \int d\underline{k} \sum_{i=0}^{1} \sum_{j=0,2} \sqrt{\xi_j} \sum_{k=j/2}^{j/2+1} \frac{(-1)^{i+k}}{\sqrt{\xi_k}} C_{iks}^{\mu\pm}(\underline{k}) b_{0s}^\dagger(\underline{P}-\underline{k}) a_{j\mu}^\dagger(\underline{k})|0\rangle \\
& + \sum_{s\mu\nu} \int d\underline{k_1} d\underline{k_2} \sum_{i=0}^{1} \sum_{j,k=0,2} \sqrt{\xi_j \xi_k} \sum_{l=j/2}^{j/2+1} \sum_{m=k/2}^{k/2+1} \frac{(-1)^{i+l+m}}{\sqrt{\xi_l \xi_m}} \frac{C_{ilms}^{\mu\nu\pm}(\underline{k_1},\underline{k_2})}{\sqrt{1+\delta_{lm}\delta_{\mu\nu}}} \\
& \qquad \times b_{0s}^\dagger(\underline{P}-\underline{k_1}-\underline{k_2}) a_{j\mu}^\dagger(\underline{k_1}) a_{k\nu}^\dagger(\underline{k_2})|0\rangle.
\end{aligned}
$$

This projection is to be used to compute the anomalous moment.

Before using these states, it is important to consider the renormalization of the external coupling to the charge [49, 45]. We exclude fermion-antifermion states, and, therefore, there is no vacuum polarization. Thus, if the vertex and wave function renormalizations cancel, there will be no renormalization of the external coupling. As shown in [45] and Appendix A, this is what happens, but only for the plus component of the current. Our calculations of the anomalous moment are therefore based on matrix elements of the plus component and do not require additional renormalization.

3.2. Coupled Integral Equations

The bare amplitudes z_i and wave functions $C^{\mu\pm}_{ijs}$ and $C^{\mu\nu\pm}_{ijks}$ that define the eigenstate must satisfy the coupled system of equations that results from the field-theoretic mass-squared eigenvalue problem (2.12). We work in a frame where the total transverse momentum is zero and require that this state be an eigenstate of P^- with eigenvalue M^2/P^+. The form of P^- is given in Eq. (2.32). The wave functions then satisfy the following coupled integral equations:

$$\begin{aligned}[M^2-m_i^2]z_i \;&=\; \int d\underline{q}\sum_{j,l,\mu}\sqrt{\xi_l}(-1)^{j+l}\epsilon^\mu P^+\left[V^{\mu *}_{ji\pm}(\underline{P}-\underline{q},\underline{P})C^{\mu\pm}_{jl\pm}(\underline{q})\right. \\ &\qquad\left.+U^{\mu *}_{ji\pm}(\underline{P}-\underline{q},\underline{P})C^{\mu\pm}_{jl\mp}(\underline{q})\right],\end{aligned} \tag{3.3}$$

$$\begin{aligned}&\left[M^2-\frac{m_i^2+q_\perp^2}{(1-y)}-\frac{\mu_l^2+q_\perp^2}{y}\right]C^{\mu\pm}_{ils}(\underline{q}) \\ &\;=\; \sqrt{\xi_l}\sum_j(-1)^j z_j P^+\left[\delta_{s,\pm 1/2}V^\mu_{ijs}(\underline{P}-\underline{q},\underline{P})+\delta_{s,\mp 1/2}U^\mu_{ij,-s}(\underline{P}-\underline{q},\underline{P})\right] \\ &\quad+\sum_{ab\nu}(-1)^{a+b}\epsilon^\nu\int d\underline{q}'\frac{2\sqrt{\xi_b}}{\sqrt{1+\delta_{bl}\delta^{\mu\nu}}}\left[V^{\nu *}_{ais}(\underline{P}-\underline{q}'-\underline{q},\underline{P}-\underline{q}')C^{\nu\mu\pm}_{abls}(\underline{q}',\underline{q})\right. \\ &\qquad\left.+U^{\nu *}_{ais}(\underline{P}-\underline{q}'-\underline{q},\underline{P}-\underline{q}')C^{\nu\mu\pm}_{abl,-s}(\underline{q}',\underline{q})\right],\end{aligned} \tag{3.4}$$

$$\left[M^2 - \frac{m_i^2 + (\vec{q}_{1\perp} + \vec{q}_{2\perp})^2}{(1-y_1-y_2)} - \frac{\mu_j^2 + q_{1\perp}^2}{y_1} - \frac{\mu_l^2 + q_{2\perp}^2}{y_2}\right] C_{ijls}^{\mu\nu\pm}(\underline{q}_1, \underline{q}_2) \tag{3.5}$$

$$= \frac{\sqrt{1+\delta_{jl}\delta^{\mu\nu}}}{2} \sum_a (-1)^a \Big\{ \sqrt{\xi_j} \Big[V_{ias}^{\mu}(\underline{P} - \underline{q}_1 - \underline{q}_2, \underline{P} - \underline{q}_2) C_{als}^{\nu\pm}(\underline{q}_2) + U_{ia,-s}^{\mu}(\underline{P} - \underline{q}_1 - \underline{q}_2, \underline{P} - \underline{q}_2) C_{al,-s}^{\nu\pm}(\underline{q}_2) \Big] + \sqrt{\xi_l} \Big[V_{ias}^{\nu}(\underline{P} - \underline{q}_1 - \underline{q}_2, \underline{P} - \underline{q}_1) C_{ajs}^{\mu\pm}(\underline{q}_1) + U_{ia,-s}^{\nu}(\underline{P} - \underline{q}_1 - \underline{q}_2, \underline{P} - \underline{q}_1) C_{aj,-s}^{\mu\pm}(\underline{q}_1) \Big] \Big\}.$$

A diagrammatic representation is given in Fig. 3.1. The first of these equations

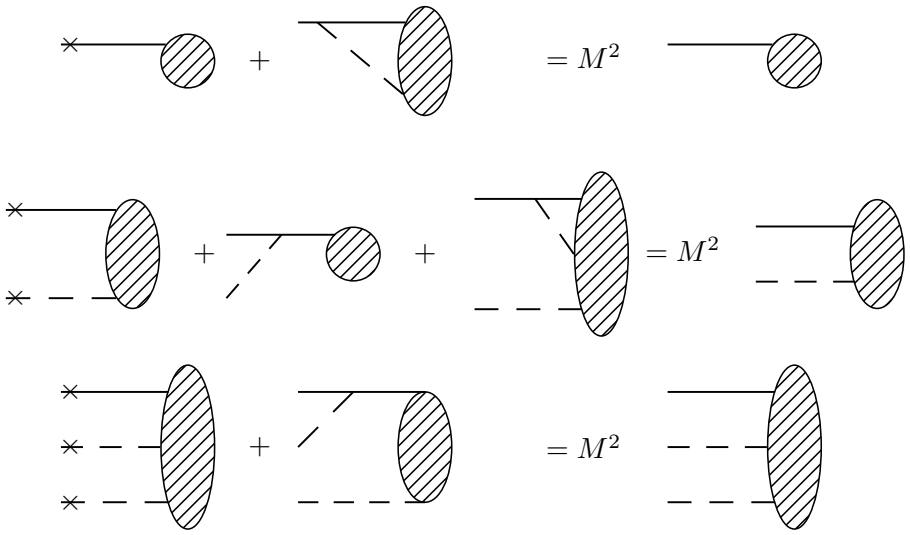

Figure 3.1. Diagrammatic representation of the coupled equations (3.3), (3.4), and (3.5) of the text. The filled circles and ovals represent wave functions for Fock states; the solid lines represent fermions; and the dashed lines represent photons. The crosses on lines represent the light-cone kinetic energy contributions, which are summed over all particles in the Fock state.

couples the bare amplitudes z_i to the two-body wave functions, $C^{\mu\pm}_{ijs}$. The second couples the $C^{\mu\pm}_{ijs}$ to the z_i and to the three-body wave functions, $C^{\mu\nu\pm}_{ijks}$. The third is truncated, with no four-body terms, and simply couples $C^{\mu\nu\pm}_{ijks}$ to $C^{\mu\pm}_{ijs}$ algebraically. From the structure of the equations, one can show that the two-body wave functions for the $J_z = -1/2$ eigenstate are related to the $J_z = +1/2$ wave functions by

$$C^{\mu-}_{ij+} = -C^{\mu+*}_{ij-}, \;\; C^{\mu-}_{ij-} = C^{\mu+*}_{ij+}. \tag{3.6}$$

This will be useful in computing the spin-flip matrix element needed for the anomalous moment.

3.3. Normalization and Anomalous Moment

The projected Fock expansion (3.2) is normalized according to

$$\langle \psi^{\sigma'}(\underline{P}')|\psi^{\sigma}(\underline{P})\rangle_{\rm phys} = \delta(\underline{P}' - \underline{P})\delta_{\sigma'\sigma}. \tag{3.7}$$

In terms of the wave functions, this becomes

$$\begin{aligned} 1 \;\; = \;\; & |\sum_i (-1)^i z_i|^2 + \sum_{s\mu}\int d\underline{k}\epsilon^\mu \sum_{j=0,2}\xi_j \left| \sum_{i=0}^{1}\sum_{k=j/2}^{j/2+1} \frac{(-1)^{i+k}}{\sqrt{\xi_k}} C^{\mu+}_{iks}(\underline{k}) \right|^2 \\ & + \sum_{s\mu\nu}\int d\underline{k_1}d\underline{k_2} \sum_{j,k=0,2}\xi_j\xi_k \left| \sum_{i=0}^{1}\sum_{l=j/2}^{j/2+1}\sum_{m=k/2}^{k/2+1} \frac{(-1)^{i+l+m}}{\sqrt{\xi_l\xi_m}} \frac{\sqrt{2}C^{\mu\nu\pm}_{ilms}(\underline{k_1},\underline{k_2})}{\sqrt{1+\delta_{lm}\delta_{\mu\nu}}} \right|^2 . \end{aligned} \tag{3.8}$$

Using the coupled equations, we can express all the wave functions $C^{\mu\pm}_{ijs}$ and $C^{\mu\nu\pm}_{ijks}$ and the amplitude z_1 through the bare-electron amplitude z_0. The normalization condition then determines z_0. For the two-photon truncation, where the wave functions are computed numerically, the integrals for the normalization must also be done numerically, using quadrature schemes discussed in Appendix D.

The anomalous moment a_e can be computed from the spin-flip matrix element of the electromagnetic current J^+ [50]

$$-\left(\frac{Q_x - iQ_y}{2M}\right) F_2(Q^2) = \pm\frac{1}{2}\langle\psi^{\pm}(\underline{P}+\underline{Q})|\frac{J^+(0)}{P^+}|\psi^{\mp}(\underline{P})\rangle_{\rm phys}, \tag{3.9}$$

where Q is the momentum of the absorbed photon, F_2 is the Pauli form factor, and we work in a frame where Q^+ is zero. At zero momentum transfer, we have $a_e = F_2(0)$ and

$$\begin{aligned} a_e &= m_e \sum_{s\mu}\int d\underline{k}\epsilon^{\mu}\sum_{j=0,2}\xi_j\left(\sum_{i'=0}^{1}\sum_{k'=j/2}^{j/2+1}\frac{(-1)^{i'+k'}}{\sqrt{\xi_{k'}}}C^{\mu+}_{i'k's}(\underline{k})\right)^* \\ &\quad \times y\left(\frac{\partial}{\partial k_x}+i\frac{\partial}{\partial k_y}\right)\left(\sum_{i=0}^{1}\sum_{k=j/2}^{j/2+1}\frac{(-1)^{i+k}}{\sqrt{\xi_k}}C^{\mu-}_{iks}(\underline{k})\right) \\ &\quad + m_e\sum_{s\mu\nu}\int d\underline{k_1}d\underline{k_2}\sum_{j,k=0,2}\xi_j\xi_k \\ &\qquad\qquad \times\left(\sum_{i'=0}^{1}\sum_{l'=j/2}^{j/2+1}\sum_{m'=k/2}^{k/2+1}\frac{(-1)^{i'+l'+m'}}{\sqrt{\xi_{l'}\xi_{m'}}}\frac{\sqrt{2}C^{\mu\nu+}_{i'l'm's}(\underline{k_1},\underline{k_2})}{\sqrt{1+\delta_{l'm'}\delta_{\mu\nu}}}\right)^* \\ &\quad \times\sum_a\left[y_a\left(\frac{\partial}{\partial k_{ax}}+i\frac{\partial}{\partial k_{ay}}\right)\right]\left(\sum_{i=0}^{1}\sum_{l=j/2}^{j/2+1}\sum_{m=k/2}^{k/2+1}\frac{(-1)^{i+l+m}}{\sqrt{\xi_l\xi_m}}\frac{\sqrt{2}C^{\mu\nu-}_{ilms}(\underline{k_1},\underline{k_2})}{\sqrt{1+\delta_{lm}\delta_{\mu\nu}}}\right). \end{aligned} \tag{3.10}$$

In general, these integrals must also be computed numerically.

The terms that depend on the three-body wave functions $C^{\mu\nu\pm}_{ilms}$ are higher order in α than the leading two-body terms. This is because (3.5) determines $C^{\mu\nu\pm}_{ilms}$ as being of order $\sqrt{\alpha}$ or e times the two-body wave functions, the vertex functions being proportional to the coupling, e. Given the numerical errors in the leading terms, these three-body contributions are not significant and are not evaluated. The important three-body contributions come from the couplings of the three-body wave functions that will enter the calculation of the two-body wave functions.

Chapter 4

ONE-PHOTON TRUNCATION

The dressed-electron problem in QED has been solved analytically for a one-photon/one-electron truncation [7] in the limit of an infinite PV electron mass. Our goal is to be able to calculate an approximation to the anomalous moment in the two-photon truncation. In this truncation we cannot take the infinite-mass limit for the PV electron, but must instead work at large but finite values. For purposes of comparison, we then need results for the one-photon truncation at finite PV electron mass.

What we discover in doing so is that a single PV photon flavor is not enough for an accurate calculation [45]. Without a second flavor, the chiral symmetry of the massless-electron limit is broken, and the calculation displays a strong dependence on the PV masses.

One other check of the formalism is to show that the one-loop electron self-energy agrees with the standard result from covariant Feynman theory. This is done in [45] and Appendix B.

4.1. Analytic Reduction

The Fock-state expansion (3.1) for the $J_z = \pm\frac{1}{2}$ eigenstate is truncated at one photon, which leaves

$$|\psi^{\pm}(\underline{P})\rangle = \sum_i z_i b^{\dagger}_{i,\pm}(\underline{P})|0\rangle + \sum_{i,l,s,\mu} \int d\underline{k} C^{\mu\pm}_{ils}(\underline{k}) b^{\dagger}_{is}(\underline{P}-\underline{k}) a^{\dagger}_{l\mu}(\underline{k})|0\rangle, \qquad (4.1)$$

with the total transverse momentum of the state set to zero. The amplitudes satisfy the coupled equations (3.3) and (3.4), with the three-body terms removed. The second equation then becomes

$$\left[M^2 - \frac{m_i^2+k_\perp^2}{(1-y)} - \frac{\mu_l^2+k_\perp^2}{y}\right] C^{\mu\pm}_{il\pm}(\underline{k}) = \sqrt{\xi_l}\sum_j (-1)^j z_j P^+ V^\mu_{ij\pm}(\underline{P}-\underline{k},\underline{P}), \quad (4.2)$$

$$\left[M^2 - \frac{m_i^2+k_\perp^2}{(1-y)} - \frac{\mu_l^2+k_\perp^2}{y}\right] C^{\mu\pm}_{il\mp}(\underline{k}) = \sqrt{\xi_l}\sum_j (-1)^j z_j P^+ U^\mu_{ij\pm}(\underline{P}-\underline{k},\underline{P}). \quad (4.3)$$

The wave functions $C^{\mu\pm}_{ils}$ are obtained directly as

$$C^{\mu\pm}_{il\pm}(\underline{k}) = \sqrt{\xi_l}\frac{\sum_j (-1)^j z_j P^+ V^\mu_{ij\pm}(\underline{P}-\underline{k},\underline{P})}{M^2 - \frac{m_i^2+k_\perp^2}{1-y} - \frac{\mu_l^2+k_\perp^2}{y}}, \quad (4.4)$$

$$C^{\mu\pm}_{il\mp}(\underline{k}) = \sqrt{\xi_l}\frac{\sum_j (-1)^j z_j P^+ U^\mu_{ij\pm}(\underline{P}-\underline{k},\underline{P})}{M^2 - \frac{m_i^2+k_\perp^2}{1-y} - \frac{\mu_l^2+k_\perp^2}{y}}. \quad (4.5)$$

These can be eliminated from the first of the coupled equations to yield a 2×2 eigenvalue problem for the amplitudes z_i,

$$(M^2-m_i^2)z_i = \int dy\, d^2k_\perp \sum_{\mu,i',j,l} (-1)^{i'+j+l}\xi_l z_j (P^+)^3 \epsilon^\mu \times \frac{V^{\mu *}_{i'i\pm}(\underline{P}-\underline{k},\underline{P})V^\mu_{i'j\pm}(\underline{P}-\underline{k},\underline{P}) + U^{\mu *}_{i'i\pm}(\underline{P}-\underline{k},\underline{P})U^\mu_{i'j\pm}(\underline{P}-\underline{k},\underline{P})}{M^2 - \frac{m_{i'}^2+k_\perp^2}{1-y} - \frac{\mu_l^2+k_\perp^2}{y}}, \quad (4.6)$$

which, on use of the definitions (2.30) of the vertex functions, can be written more usefully as

$$(M^2-m_i^2)z_i = 2e^2\sum_j (-1)^j z_j \left[m_i m_j \bar{I}_0 - 2(m_i+m_j)\bar{I}_1 + \bar{J}\right], \quad (4.7)$$

in terms of the following important integrals:

$$\bar{I}_n(M^2) = \int \frac{dydk_\perp^2}{16\pi^2} \sum_{jl} \frac{(-1)^{j+l}\xi_l}{M^2 - \frac{m_j^2+k_\perp^2}{1-y} - \frac{\mu_l^2+k_\perp^2}{y}} \frac{m_j^n}{y(1-y)^n}\,, \tag{4.8}$$

$$\bar{J}(M^2) = \int \frac{dydk_\perp^2}{16\pi^2} \sum_{jl} \frac{(-1)^{j+l}\xi_l}{M^2 - \frac{m_j^2+k_\perp^2}{1-y} - \frac{\mu_l^2+k_\perp^2}{y}} \frac{m_j^2+k_\perp^2}{y(1-y)^2}. \tag{4.9}$$

The singular behavior of the integrands is characteristic of the integral equations in general and provides a useful testing ground for quadratures and discretizations. The integrals $\bar{I}_0$ and $\bar{J}$ satisfy the identity $\bar{J}(M^2) = M^2\bar{I}_0(M^2)$. A proof is given in [45] and in Appendix C.

4.2. Solution of the Eigenvalue Problem

The form of the eigenvalue equation (4.7) matches that of the equivalent eigenvalue problem in Yukawa theory [6], with the replacements $g^2 \to 2e^2$, $\mu_0 I_1 \to -2\bar{I}_1$, and $\mu_0^2 J \to \bar{J}$. Therefore, the solution can be taken directly from [6] with these minor substitutions; it is

$$\alpha_\pm = \frac{(M \pm m_0)(M \pm m_1)}{8\pi(m_1 - m_0)(2\bar{I}_1 \pm M\bar{I}_0)}, \quad z_1 = \frac{M \pm m_0}{M \pm m_1} z_0, \tag{4.10}$$

with z_0 determined by normalization. The simplicity of this result is due in part to the algebraic simplification of (4.7) that comes from the identity $\bar{J} = M^2\bar{I}_0$.

The value of m_0 is determined by requiring $\alpha_\pm$ to be equal to the physical value of $\alpha = e^2/4\pi$ when the eigenmass M is equal to the physical mass of the electron m_e. For small values of the PV masses there may be no such solution; however, for reasonable values we do find at least one solution for each branch.

The plot in Fig. 4.1 shows $\alpha_\pm/\alpha$ as functions of m_0. The α_- branch is the physical choice, because the no-interaction limit ($\alpha_- = 0$) corresponds to the bare mass m_0

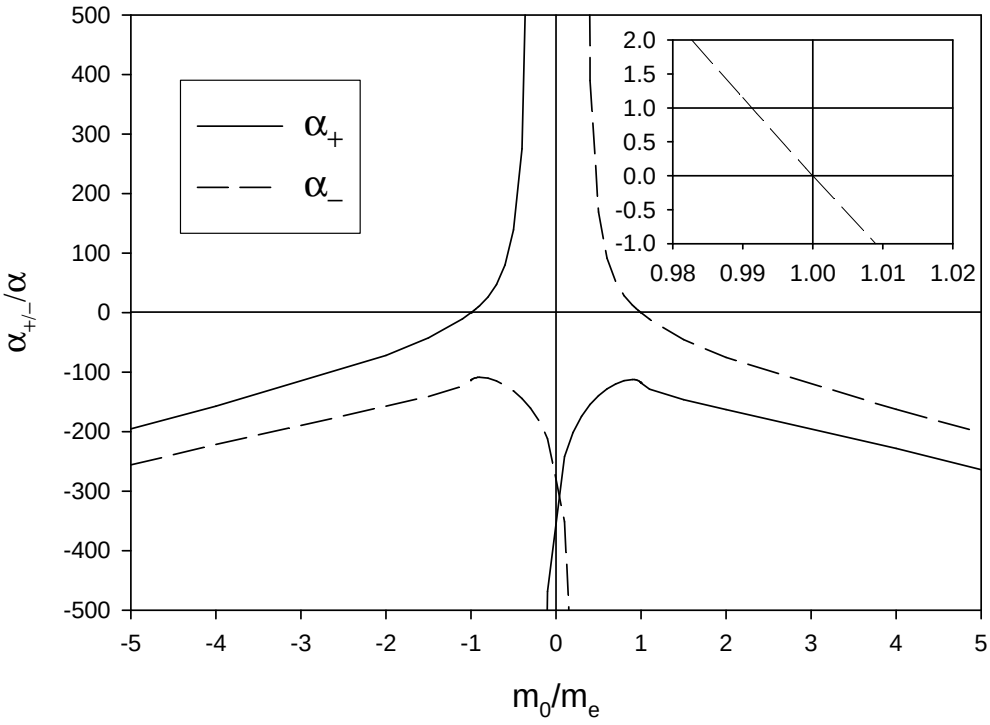

Figure 4.1. The two solutions of the one-photon eigenvalue problem, for PV masses $m_1 = 1000m_e$, $\mu_1 = 10m_e$, and $\mu_2 = \infty$. The horizontal line shows where $\alpha_\pm = \alpha$; the inset shows the detail near the intersection with α_-, with horizontal lines at zero and one and a vertical line at $m_0 = m_e$. The α_- branch corresponds to the physical choice, but with m_0 less than m_e.

becoming equal to the physical electron mass. If the PV electron has a sufficiently large mass, as used in Fig. 4.1, the value of m_0 that yields $\alpha_- = \alpha$ is less than m_e. In this case, the integrals $\bar{I}_n$ and $\bar{J}$ contain poles for $j = l = 0$ and are defined by a principal-value prescription [7].

The presence of the poles can then admit an additional delta-function term to the two-body wave function:

$$C^{\mu\sigma}_{00s}(\underline{k}) \to C^{\mu\sigma}_{00s}(\underline{k}) + c^{\mu\sigma}_s \delta(\underline{k} - \underline{k}_0), \tag{4.11}$$

where $\underline{k}_0$ is such that $M^2 = \frac{m_0^2+k_{0\perp}^2}{1-y_0} + \frac{\mu_0^2+k_{0\perp}^2}{y_0}$. This remains a solution to (4.2), but there will be additional terms in (4.7) proportional to $c_s^{\mu\sigma}$. We do not explore this possibility, because we have found that when we include self-energy corrections from a two-photon truncation, the poles in these wave functions disappear.

4.3. Normalization

The normalization of the wave functions is determined by Eq. (3.8) with no more than the two-body terms kept. For the given wave functions, after some tedious calculations, this becomes

$$\begin{aligned}\frac{1}{z_0^2} &= (1-\zeta_1)^2 \\ &+\frac{\alpha}{2\pi}\int y dy dk_\perp^2 \sum_{l,l'}(-1)^{l+l'}\zeta_l\zeta_{l'}\sum_{i'i}(-1)^{i'+i}\sum_{j=0,2}\xi_j\sum_{k'=j/2}^{j/2+1}\sum_{k=j/2}^{j/2+1}(-1)^{k'+k} \\ &\times\frac{m_{i'}m_i-(m_i+m_{i'})(m_l+m_{l'})(1-y)+m_lm_{l'}(1-y)^2+k_\perp^2}{[ym_{i'}^2+(1-y)\mu_{k'}^2+k_\perp^2-m_e^2y(1-y)][ym_i^2+(1-y)\mu_k^2+k_\perp^2-m_e^2y(1-y)]},\end{aligned} \tag{4.12}$$

where $\zeta_l = z_l/z_0$.

For terms with $i = k = 0$ or $i' = k' = 0$, there are simple poles defined by a principal-value prescription. For the terms where all four of these indices are zero, there is a double pole, defined by the prescription [7]

$$\int dx\frac{f(x)}{(x-a)^2} \equiv \lim_{\eta\to 0}\frac{1}{2\eta}\left[\mathcal{P}\int dx\frac{f(x)}{x-a-\eta} - \mathcal{P}\int dx\frac{f(x)}{x-a+\eta}\right]. \tag{4.13}$$

One could instead compute the norm by taking the zero-momentum limit of the Dirac form factor, F_1; however, this would correspond to a more complicated point splitting. Our prescription splits only with respect to the magnitude of the momentum, rather than the magnitude and angle. With the prescription (4.13) for double poles, the transverse integrals that appear in the normalization integrals are

$$\int_0^\infty \frac{dx}{(x \pm a)^2} = \pm\frac{1}{a}, \tag{4.14}$$

$$\int_0^\infty \frac{dx}{(x \pm a)(x + b)} = \frac{\ln(b/a)}{b \pm a}, \tag{4.15}$$

$$\int_0^\infty \frac{xdx}{(x \pm a)^2} = \begin{cases} -1 - \ln(a), & \text{upper sign} \\ -1, & \text{lower sign,} \end{cases} \tag{4.16}$$

$$\int_0^\infty \frac{xdx}{(x \pm a)(x + b)} = \frac{\ln(b/a)}{1 \pm b/a} - \ln(b), \tag{4.17}$$

with a and b positive. These same integrals appear in the expression below for the anomalous moment.

4.4. Anomalous Moment

From the normalized wave functions, we can compute the anomalous magnetic moment. We consider both one and two PV photon flavors and, in the second case, derive a constraint on the second PV photon flavor that restores the correct chiral limit.

4.4.1. Basic Expressions

We evaluate the expression given in Eq. (3.10), keeping only the two-body contributions. The presence of the derivative of the wave functions, given in Eqs. (4.4) and (4.5), implies that we may face a triple pole; however, these terms cancel, and the expression for the anomalous moment simplifies to

$$a_e = \frac{\alpha}{\pi} m_e \int y^2(1-y)dydk_\perp^2 \sum_{l,l'} (-1)^{l+l'} z_l z_{l'} m_l \sum_{j=0,2} \xi_j \times \left(\sum_{i=0}^{1} \sum_{k=j/2}^{j/2+1} \frac{(-1)^{i+k}}{ym_i^2 + (1-y)\mu_k^2 + k_\perp^2 - m_e^2 y(1-y)} \right)^2 . \tag{4.18}$$

The double pole is handled in the same way as for the normalization integrals, discussed in Sec. 4.3. The integrals can be done analytically.

In the limit where the PV electron mass m_1 is infinite, the bare-electron amplitude ratio z_1/z_0 is zero but the limit of the product $m_1 z_1/z_0$ is $m_0 - m_e$. Thus, the limit of the expression for the anomalous moment is

$$a_e = \frac{\alpha}{\pi} m_e^2 z_0^2 \int y^2(1-y)dydk_\perp^2 \sum_{j=0,2} \xi_j \left(\sum_{k=j/2}^{j/2+1} \frac{(-1)^k}{ym_0^2 + (1-y)\mu_k^2 + k_\perp^2 - m_e^2 y(1-y)} \right)^2 . \tag{4.19}$$

This differs slightly from the expression given in Eq. (70) of [7], where only one PV photon was included, the projection onto physical states was not taken, and $m_1 z_1$ was assumed to be zero; however, the difference in values is negligible when μ_1 and μ_2 are sufficiently large.

4.4.2. One PV Photon Flavor

If the second PV photon is not included, the results for the anomalous moment have a very strong dependence on the PV masses m_1 and μ_1 [45], as can be seen in Fig. 4.2. A slowly varying behavior with respect to the PV photon mass μ_1 is obtained only if the PV electron mass m_1 is (nearly) infinite. The PV electron mass needs to be quite large, on the order of $10^7\, m_e$, before results for the one-photon truncation approach the infinite-mass limit. Thus, we would estimate that the PV electron mass must be at least this large for the two-photon truncation, if only one

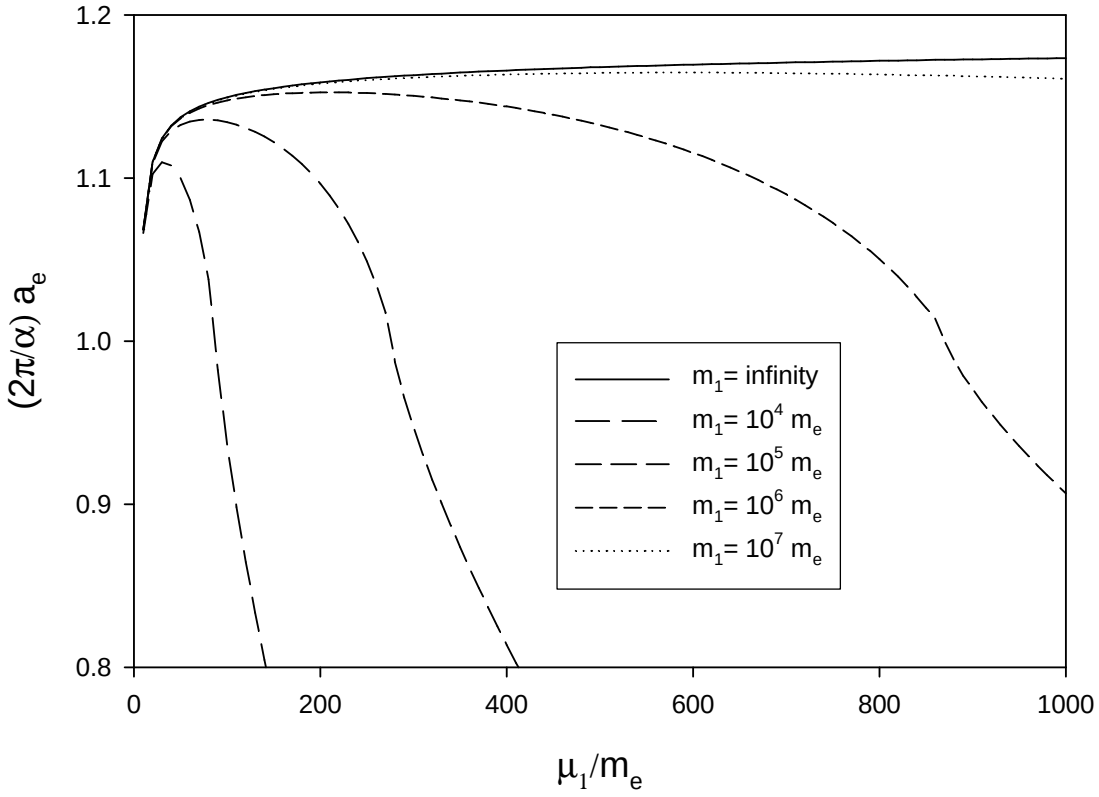

Figure 4.2. The anomalous moment of the electron in units of the Schwinger term $(\alpha/2\pi)$ plotted versus the PV photon mass, μ_1, for a few values of the PV electron mass, m_1. The second PV photon is absent, and the chiral symmetry of the massless limit is broken.

PV photon flavor is included. Unfortunately, such large mass values make numerical calculations difficult, because of contributions to integrals at momentum fractions of order $(m_e/m_1)^2 \simeq 10^{-14}$, which are then subject to large round-off errors.

The strong variation with μ_1 occurs because the anomalous moment is very sensitive to the masses of the constituents [20]. The mass m_0 of the bare electron is determined by the eigenvalue solution (4.10), which contains the integral $\bar{I}_1$, and this integral has a strong dependence on PV masses, much stronger than a $(\mu_1/m_1)^2$

dependence that one might naively expect. Relative to the integral's value $\bar{I}_{1\infty}$ at infinite m_1, we have, with $M = m_e$,

$$\bar{I}_1 = \bar{I}_{1\infty} + \int \frac{dydk_\perp^2}{16\pi^2} \sum_j \frac{(-1)^j \xi_j m_1}{k_\perp^2 + y m_1^2 + (1-y)\mu_j^2 - m_e^2 y(1-y)}. \tag{4.20}$$

When m_e is neglected compared to m_1, the second term becomes equal to $\bar{I}_1(0)$, and this introduces a correction to the bare-electron mass of the form $\frac{\mu_1^2 \ln(\mu_1/m_1)}{8\pi^2 m_e m_1 (1-\mu^2/m_1^2)}$. This correction injects a very strong dependence on μ_1 and m_1 into the behavior of the bare mass m_0 and thus into the behavior of the anomalous moment.

4.4.3. Two PV Photon Flavors

What is the origin of this strong dependence on PV mass? It is in the breaking of chiral symmetry in the limit of a massless electron. The expression (B.1) for the one-loop electron self-energy, given in Appendix B, does not have the correct massless limit of zero, and chiral symmetry is broken [45]. From (B.1) and the identity $\bar{J} = M^2 \bar{I}_0$, we have

$$\delta m = 16\pi^2 \frac{\alpha}{2\pi} \left[m_0 \bar{I}_0(m_0^2) - 2\bar{I}_1(m_0^2) \right]. \tag{4.21}$$

In the chiral limit, $m_0 \to 0$, we obtain

$$\delta m = -32\pi^2 \frac{\alpha}{2\pi} \bar{I}_1(0), \tag{4.22}$$

with

$$\bar{I}_1(0) = \frac{m_1}{16\pi^2} \sum_l (-1)^l \xi_l \int dy d^2k_\perp \frac{1}{k_\perp^2 + m_1^2 y + \mu_l^2 (1-y)}. \tag{4.23}$$

The integrals in $\bar{I}_1(0)$ can be easily done, to find

$$\delta m = -\frac{\alpha}{\pi} m_1 \sum_l (-1)^l \xi_l \frac{\mu_l^2/m_1^2}{1-\mu_l^2/m_1^2} \ln(\mu_l^2/m_1^2). \tag{4.24}$$

Clearly, this is zero only if m_1 is infinite or the ξ_l and masses μ_l satisfy the constraint

$$\sum_l (-1)^l \xi_l \frac{\mu_l^2/m_1^2}{1-\mu_l^2/m_1^2} \ln(\mu_l^2/m_1^2) = 0. \tag{4.25}$$

This cannot be satisfied without the introduction of a second PV photon. With the constraint satisfied, the leading correction to the eigenvalue problem, which was shown in the previous subsection to be also proportional to $\bar{I}_1(0)$, will disappear.

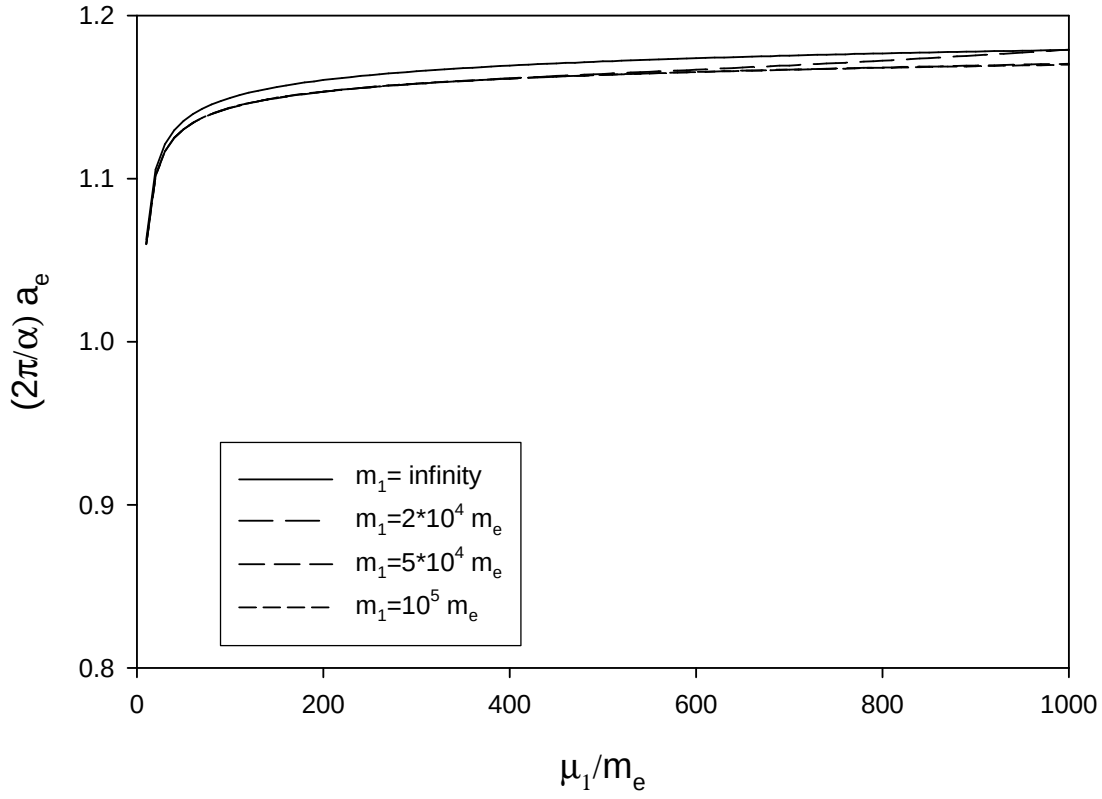

Figure 4.3. Same as Fig. 4.2, but with the second PV photon included, with a mass $\mu_2 = \sqrt{2}\mu_1$, and the chiral symmetry restored. The mass ratio is held fixed as μ_1 and μ_2 are varied.

When the PV electron mass is sufficiently large, the chiral-limit constraint can be approximated by

$$\sum_l (-1)^l \xi_l \mu_l^2 \ln(\mu_l/m_1) = 0. \tag{4.26}$$

This constraint is of the same general form as the constraint obtained earlier for Yukawa theory with three PV bosons [30, 2]. The solution to the set of constraints,

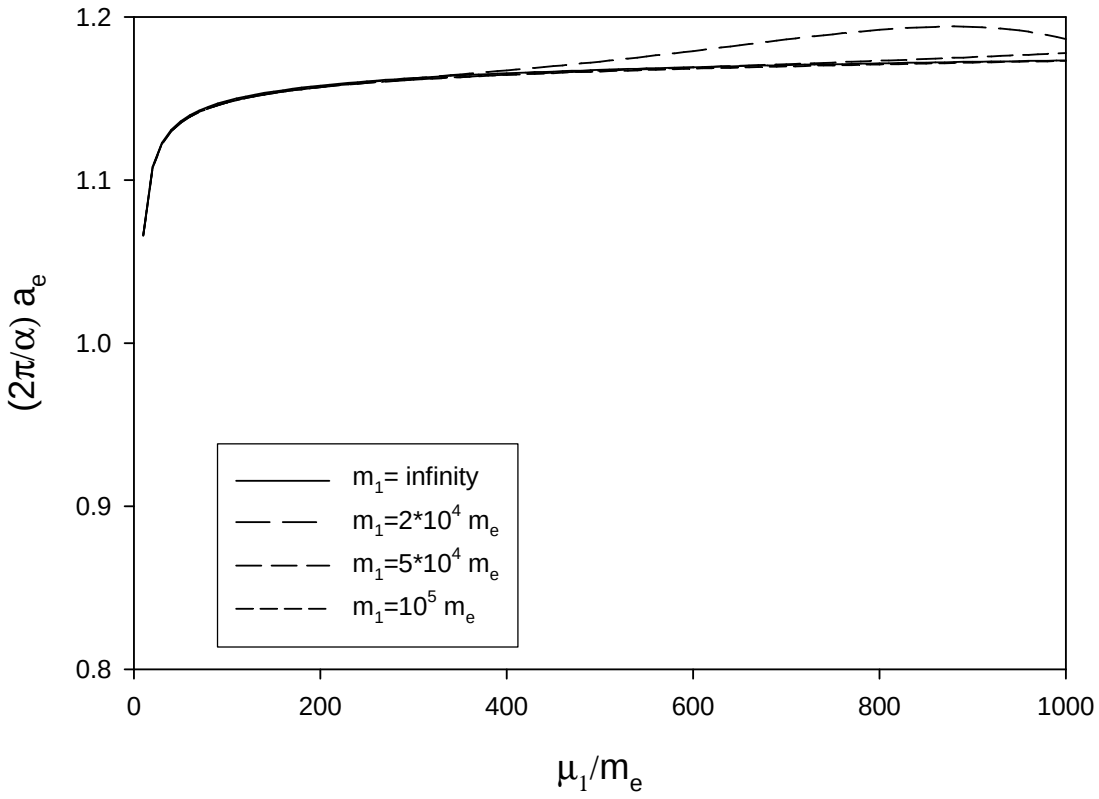

Figure 4.4. Same as Fig. 4.3, but for $\mu_2 = 4\mu_1$.

Eq. (2.18) and (4.26) along with $\xi_0 = 1$ and $\mu_0 = 0$, is

$$\xi_1 = 1 + \xi_2 \text{ and } \xi_2 = \frac{\mu_1^2 \ln(\mu_1/m_1)}{\mu_2^2 \ln(\mu_2/m_1) - \mu_1^2 \ln(\mu_1/m_1)}. \tag{4.27}$$

Without loss of generality, we require $\mu_2 > \mu_1$, so that ξ_2 is positive.

For less severe truncations, where more photons are allowed in Fock states, the number of PV photon flavors does not need to increase [35]. However, the chiral constraint will be more complicated. We might expect that, since the corrections are higher order in α, they will be small enough to be neglected. As will be seen in Chap. 6, this is not the case.

With the second PV photon flavor included, the dependence on PV masses is much reduced, as can be seen in Figs. 4.3 and 4.4. In Fig. 4.4, the strong variation with μ_1 that occurs for $m_1 = 2 \cdot 10^4 m_e$ is the result of $\mu_2 (= 4\mu_1)$ becoming comparable in magnitude to m_1.

From the plots in Figs. 4.3 and 4.4, we can conclude that useful calculations can be done with $m_1 = 2 \cdot 10^4 m_e$ and $\mu_2 = \sqrt{2}\mu_1$, and we will use these values for comparison with the two-photon truncation in later chapters.

The value obtained for the anomalous moment differs from the leading-order Schwinger result $\alpha/2\pi$ [33], and thus from the physical value, by 17%. It will be much improved by the inclusion of the two-photon self-energy contributions.

Chapter 5

SELF-ENERGY CONTRIBUTION

Before solving the full two-photon truncation problem, we consider the effects of the electron self-energy contribution alone. This yields an eigenvalue problem that is similar to the one-photon truncation problem and can be solved almost analytically; only some integrals require numerical treatment. The effect of including the self-energy is to bring the anomalous moment into complete agreement with experiment, to within numerical error.

5.1. The Eigenvalue Problem

The Fock-state expansion for the $J_z = \pm\frac{1}{2}$ eigenstate is given in (3.1). The wave functions satisfy the coupled integral equations (3.3), (3.4), and (3.5). The third equation can be solved for the one-electron/two-photon wave functions, in terms of the one-electron/one-photon wave functions, as

$$\begin{aligned} C^{\mu\nu\pm}_{ijls}(\underline{q}_1,\underline{q}_2) \;=\; & \frac{1}{M^2 - \frac{m_i^2+(\vec{q}_{1\perp}+\vec{q}_{2\perp})^2}{(1-y_1-y_2)} - \frac{\mu_j^2+q_{1\perp}^2}{y_1} - \frac{\mu_l^2+q_{2\perp}^2}{y_2}} \frac{\sqrt{1+\delta_{jl}\delta^{\mu\nu}}}{2} \\ & \times \sum_a (-1)^a \Big\{ \sqrt{\xi_j} \Big[V^{\mu}_{ias}(\underline{P}-\underline{q}_1-\underline{q}_2, \underline{P}-\underline{q}_2) C^{\nu\pm}_{als}(\underline{q}_2) \\ & \qquad + U^{\mu}_{ia,-s}(\underline{P}-\underline{q}_1-\underline{q}_2, \underline{P}-\underline{q}_2) C^{\nu\pm}_{al,-s}(\underline{q}_2) \Big] \\ & + \sqrt{\xi_l} \Big[V^{\nu}_{ias}(\underline{P}-\underline{q}_1-\underline{q}_2, \underline{P}-\underline{q}_1) C^{\mu\pm}_{ajs}(\underline{q}_1) \\ & \qquad + U^{\nu}_{ia,-s}(\underline{P}-\underline{q}_1-\underline{q}_2, \underline{P}-\underline{q}_1) C^{\mu\pm}_{aj,-s}(\underline{q}_1) \Big] \Big\} . \end{aligned} \tag{5.1}$$

Substitution of this solution into the second coupled equation eliminates the three-body wave functions from the problem. For our present purpose, we retain only the self-energy contributions, where the emitted photon is immediately reabsorbed by the electron, and omit the remaining two-photon contributions, where one photon is emitted and the other absorbed. The second equation (3.4) then becomes

$$\begin{aligned}
&\left[M^2 - \frac{m_i^2+q_\perp^2}{(1-y)} - \frac{\mu_l^2+q_\perp^2}{y}\right] C_{ils}^{\mu\pm}(\underline{q}) \qquad (5.2)\\
&= \sqrt{\xi_l}\sum_j (-1)^j z_j P^+ \left[\delta_{s,\pm 1/2} V_{ijs}^{\mu}(\underline{P}-\underline{q},\underline{P}) + \delta_{s,\mp 1/2} U_{ij,-s}^{\mu}(\underline{P}-\underline{q},\underline{P})\right]\\
&\quad + \sum_{abi'\nu}\int \frac{(-1)^{a+b+i'}\xi_b \epsilon^\nu d\underline{q}'}{M^2 - \frac{m_a^2+(\vec{q}_\perp'+\vec{q}_\perp)^2}{(1-y-y')} - \frac{\mu_b^2+q_\perp'^2}{y'} - \frac{\mu_l^2+q_\perp^2}{y}}\\
&\qquad \times \left[V_{ais}^{\nu *}(\underline{P}-\underline{q}'-\underline{q},\underline{P}-\underline{q}')V_{ai's}^{\nu}(\underline{P}-\underline{q}'-\underline{q},\underline{P}-\underline{q})\right.\\
&\qquad\quad \left. + U_{ais}^{\nu *}(\underline{P}-\underline{q}'-\underline{q},\underline{P}-\underline{q}')U_{ai's}^{\nu}(\underline{P}-\underline{q}'-\underline{q},\underline{P}-\underline{q})\right] C_{i'ls}^{\mu\pm}(\underline{q}).
\end{aligned}$$

The second term on the right-hand side is the self-energy contribution. Notice that it includes a flavor changing self-energy, where the index i' need not be the same as the index i; this is a result of the flavor changing currents used in the interaction Lagrangian (2.16). A diagrammatic representation is given in Fig. 5.1.

To simplify the expressions, we define

$$S_{ils}^{\mu\pm} = \sqrt{\xi_l}\sum_j (-1)^j z_j P^+ [\delta_{s,\pm 1/2} V_{ijs}^{\mu}(\underline{P}-\underline{q},\underline{P}) + \delta_{s,\mp 1/2} U_{ij,-s}^{\mu}(\underline{P}-\underline{q},\underline{P})], \qquad (5.3)$$

and

$$\begin{aligned}
I_{ili'}(y,q_\perp) &= (1-y)\frac{2\pi}{\alpha}\sum_{ab\nu}\int \frac{(-1)^{a+b+i'}\xi_b \epsilon^\nu d\underline{q}'}{M^2 - \frac{m_a^2+(\vec{q}_\perp'+\vec{q}_\perp)^2}{(1-y-y')} - \frac{\mu_b^2+q_\perp'^2}{y'} - \frac{\mu_l^2+q_\perp^2}{y}} \qquad (5.4)\\
&\quad \times \left[V_{ais}^{\nu *}(\underline{P}-\underline{q}'-\underline{q},\underline{P}-\underline{q}')V_{ai's}^{\nu}(\underline{P}-\underline{q}'-\underline{q},\underline{P}-\underline{q})\right.\\
&\quad\quad \left. + U_{ais}^{\nu *}(\underline{P}-\underline{q}'-\underline{q},\underline{P}-\underline{q}')U_{ai's}^{\nu}(\underline{P}-\underline{q}'-\underline{q},\underline{P}-\underline{q})\right].
\end{aligned}$$

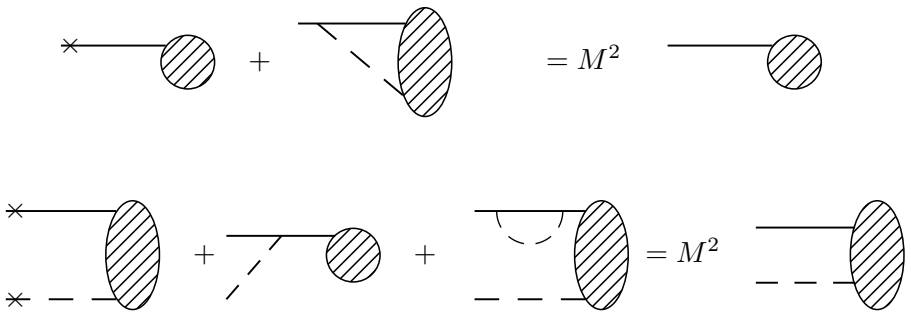

Figure 5.1. Diagrammatic representation of the coupled equations (3.3) and (5.2) of the text. The conventions for the diagrams are the same as in Fig. 3.1.

The integral equations for the two-body wave functions then take the form

$$\left[M^2 - \frac{m_i^2 + q_\perp^2}{1-y} - \frac{\mu_j^2 + q_\perp^2}{y}\right] C_{ijs}^{\mu\pm}(y, q_\perp) = S_{ijs}^{\mu\pm} + \frac{\alpha}{2\pi} \sum_{i'} \frac{I_{iji'}(y, q_\perp)}{1-y} C_{i'js}^{\mu\pm}(y, q_\perp), \quad (5.5)$$

with $i = 0, 1$ and $j = 0, 1, 2$. This, combined with the coupled equation (3.3) for the one-body amplitude, constitutes the eigenvalue problem when only the self-energy contributions of the two-photon states are included.

5.2. Two-Body Wave Functions

The self-energy term contributes to the denominators of the wave functions. Define

$$A_{ij} = \frac{m_i^2 + q_\perp^2}{1-y} + \frac{\mu_j^2 + q_\perp^2}{y} + \frac{\alpha}{2\pi} \frac{I_{iji}}{1-y} - M^2, \quad (5.6)$$

and

$$B_j = \frac{\alpha}{2\pi} \frac{I_{1j0}}{1-y} = -\frac{\alpha}{2\pi} \frac{I_{0j1}}{1-y}. \quad (5.7)$$

The eigenvalue problem can then be expressed compactly as

$$
\begin{aligned}
A_{0j}C^{\mu\pm}_{0js} - B_j C^{\mu\pm}_{1js} &= -S^{\mu\pm}_{0js} \\
B_j C^{\mu\pm}_{0js} + A_{1j} C^{\mu\pm}_{1js} &= -S^{\mu\pm}_{1js}.
\end{aligned} \tag{5.8}
$$

We solve this 2×2 system for the two-body wave functions

$$
C^{\mu\pm}_{ijs} = -\frac{A_{1-i,j}S^{\mu\pm}_{ijs} + (-1)^i B_j S^{\mu\pm}_{1-i,js}}{A_{0j}A_{1j} + B_j^2}. \tag{5.9}
$$

The denominators now contain self-energy contributions.

On use of the form of the vertex functions (2.30), the expression (5.4) for the self-energy contribution reduces to

$$
\begin{aligned}
I_{iji'}(y,q_\perp) &= \sum_{a,b}(-1)^{i'+a+b}\xi_b(1-y)\int_0^{1-y}\frac{dy'}{y'}\frac{d\phi'}{2\pi}dq'^2_\perp\frac{-1}{D_{ajb}+F\cos\phi'} \\
&\quad\times\left[\frac{m_a^2}{(1-y-y')^2} - 2\frac{(m_i+m_{i'})m_a}{(1-y)(1-y-y')} + \frac{m_i m_{i'}}{(1-y)^2}\right. \\
&\quad\left.+\frac{1}{(1-y-y')^2}\left(\frac{y'^2q_\perp^2}{(1-y)^2} + q'^2_\perp + \frac{2y'q_\perp q'_\perp\cos\phi'}{(1-y)}\right)\right],
\end{aligned} \tag{5.10}
$$

with

$$
\begin{aligned}
D_{ajb}(q_\perp,q'_\perp) &= \frac{m_a^2+q_\perp^2+q'^2_\perp}{1-y-y'} + \frac{\mu_j^2+q_\perp^2}{y} + \frac{\mu_b^2+q'^2_\perp}{y'} - M^2, \\
F(q_\perp,q'_\perp) &= \frac{2q_\perp q'_\perp}{1-y-y'}.
\end{aligned} \tag{5.11}
$$

The self-energy contribution can be evaluated analytically, in the same way as for Yukawa theory [8]. The change of variables $x = q'^+/q^+ = y'/(1-y)$ and $\vec{k}_\perp = \vec{q}'_\perp + x\vec{q}_\perp$ yields

$$
\begin{aligned}
I_{iji'}(y,q_\perp) &= \sum_{a,b}(-1)^{i'+a+b}\xi_b \int_0^1 \frac{dx}{x}\frac{d^2k_\perp}{\pi}\frac{m_i m_{i'} - 2\frac{m_i+m_{i'}}{1-x}m_a + \frac{m_a^2+k_\perp^2}{(1-x)^2}}{\Lambda_j - \frac{m_a^2+k_\perp^2}{1-x} - \frac{\mu_b^2+k_\perp^2}{x}} \qquad (5.12)\\
&= 16\pi^2(-1)^{i'}\left[m_i m_{i'}\bar{I}_0(\Lambda_j) - 2(m_i+m_{i'})\bar{I}_1(\Lambda_j) + \bar{J}(\Lambda_j)\right],
\end{aligned}
$$

with

$$
\Lambda_j \equiv \mu_j^2 + (1-y)M^2 - \frac{\mu_j^2+q_\perp^2}{y}, \qquad (5.13)
$$

and $\bar{I}_0$, $\bar{I}_1$, and $\bar{J}$ defined in Eqs. (4.8) and (4.9). For $\bar{J}$ we still have the identity $\bar{J}(\Lambda_j) = \Lambda_j \bar{I}_0(\Lambda_j)$. However, unlike the case for Yukawa theory, Λ_j can be positive. For either sign of Λ_j the integrals can be evaluated analytically, but, for extreme values of the momentum, such as momentum fractions on the order of $(m_0/m_1)^2 \sim 10^{-10}$, evaluation of the analytic form suffers from round-off error due to the finite precision available in floating-point calculations. The self-energy is then best computed by numerical evaluation of the longitudinal integrals, as discussed in Appendix D.

Without the self-energy contributions, we have $B_j = 0$, and the wave functions reduce to the forms given in (4.4) and (4.5), with their line of poles whenever $m_0 < m_e$, as discussed in Sec. 4.2. Here, however, the self-energy contributions make the denominators more complicated. For values of m_0 that are smaller than m_e by an amount of order α, there need not be a line of poles. In fact, we find that, for the solution with self-energy contributions, there is no pole in this two-body Fock sector.

5.3. Semi-Analytic Solution

To solve the eigenvalue problem, we substitute the expressions (5.9) for the two-body wave functions into the one-body equation, Eq. (3.3). On use of the expressions

(2.30) for the vertex functions, this yields

$$[M^2 - m_i^2]z_i = 2e^2 \sum_l (-1)^l z_l [m_i m_l \tilde{I}_0 - 2(m_i + m_l)\tilde{I}_1 + \tilde{J}], \tag{5.14}$$

where

$$\begin{aligned}
\tilde{I}_0 &= \int \frac{dydq_\perp^2}{16\pi^2} \sum_j (-1)^j \xi_j \frac{A_{0j} - A_{1j} - 2B_j}{y[A_{0j}A_{1j} + B_j^2]}, \\
\tilde{I}_1 &= \int \frac{dydq_\perp^2}{16\pi^2} \sum_j (-1)^j \xi_j \frac{m_1 A_{0j} - m_0 A_{1j} - (m_0 + m_1)B_j}{y(1-y)[A_{0j}A_{1j} + B_j^2]}, \\
\tilde{J} &= \int \frac{dydq_\perp^2}{16\pi^2} \sum_j (-1)^j \xi_j \frac{(m_1^2 + q_\perp^2)A_{0j} - (m_0^2 + q_\perp^2)A_{1j} - 2(m_0 m_1 + q_\perp^2)B_j}{y(1-y)^2[A_{0j}A_{1j} + B_j^2]}.
\end{aligned} \tag{5.15}$$

When the self-energy contributions are neglected, these return to the previous expressions Eq. (4.8) and (4.9) for $\bar{I}_0$, $\bar{I}_1$, and $\bar{J}$ in the one-photon truncation. What is more, the eigenvalue equation for z_i has nearly the same form as the eigenvalue equation (4.7) in the one-photon case. The only difference in finding the analytic solution is that $\tilde{I}_0$ and $\tilde{J}$ are not connected by any known identity.

Therefore, we proceed by simply solving the 2×2 matrix problem that (5.14) represents. First, write it in standard matrix form

$$G\vec{z} = \frac{1}{2e^2}\vec{z}, \tag{5.16}$$

with

$$\vec{z} = \begin{pmatrix} z_0 \\ z_1 \end{pmatrix}, \quad G = \begin{pmatrix} G_{00} & G_{01} \\ G_{10} & G_{11} \end{pmatrix}, \tag{5.17}$$

and

$$G_{il} = \frac{(-1)^l}{M^2 - m_i^2}[m_i m_l \tilde{I}_0 - 2(m_i + m_l)\tilde{I}_1 + \tilde{J}]. \tag{5.18}$$

Then use the standard solution to obtain

$$\alpha_\pm = \frac{G_{00} + G_{11} \pm \sqrt{(G_{00} - G_{11})^2 - 4G_{10}G_{01}}}{16\pi[G_{00}G_{11} - G_{10}G_{01}]}, \tag{5.19}$$

$$\frac{z_1}{z_0} = \frac{[G_{11} - G_{00}]/2 \mp \sqrt{(G_{00} - G_{11})^2 - 4G_{10}G_{01}}}{G_{01}}. \tag{5.20}$$

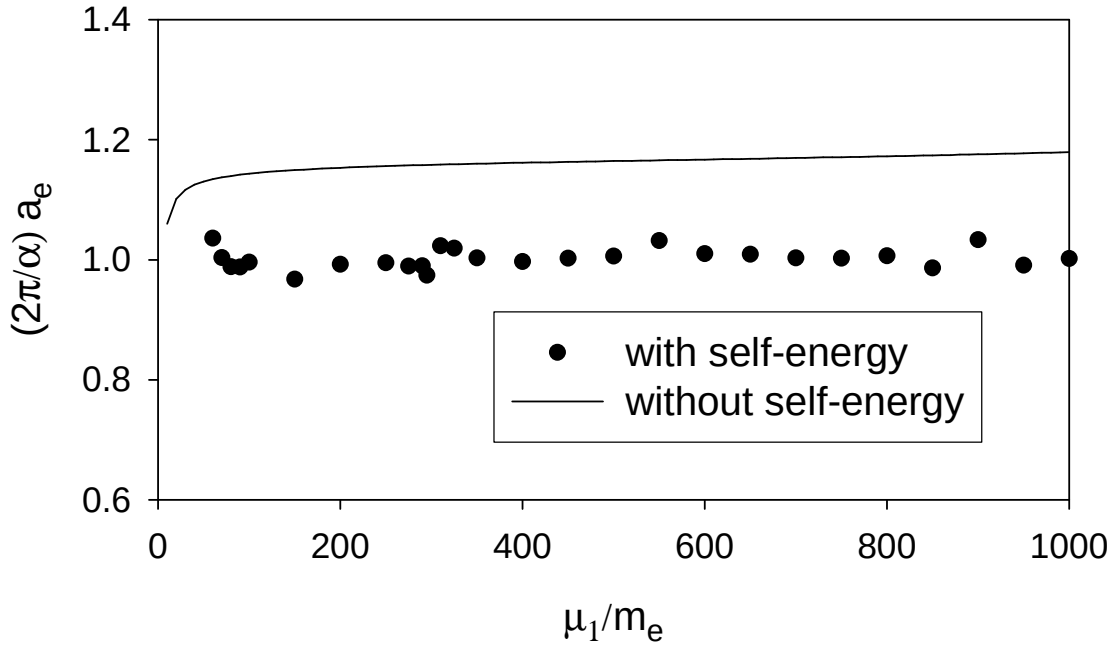

Figure 5.2. The anomalous moment of the electron in units of the Schwinger term $(\alpha/2\pi)$ plotted versus the PV photon mass, μ_1, with the second PV photon mass, μ_2, set to $\sqrt{2}\mu_1$ and the PV electron mass m_1 equal to $2 \cdot 10^4\, m_e$. The plot compares results with and without the two-photon self-energy corrections.

As before, this yields α as a function of m_0 and the PV masses. We then find m_0 such that α takes the standard physical value. The search for the correct value of m_0 is done numerically, by an iteration algorithm due to Müller [51] and described

in Appendix E. Although the form of the solution for α is analytic, the integrals involved, the $\tilde{I}_n$ and $\tilde{J}$, must be computed numerically, using quadratures described in Appendix D.

The wave functions $C_{ijs}^{\mu\pm}$ are constructed from (5.9) and used in the one-photon truncation of (3.10) to compute the anomalous moment. The results for the anomalous moment are shown in Fig. 5.2. As discussed in Chap. 4, the value of the PV electron mass m_1 is chosen to be $2 \cdot 10^4\, m_e$, which was found in the case of the one-photon truncation to be sufficiently large. The ratio of PV photon masses μ_2/μ_1 is held fixed at $\sqrt{2}$, and μ_1 is varied. The results are consistent with perturbative QED, showing only variations expected from numerical errors of order 1% in calculating the underlying integrals $\tilde{I}_n$ and $\tilde{J}$.

That the self-energy contribution brings the result so close to the leading Schwinger contribution can be understood. The dominant contribution to the expression (3.10) for the anomalous moment is the $j = 0$, $i = i' = 0$, and $k = k' = 0$ contribution to the first term; the other terms are suppressed by the large PV masses that appear in the denominators of the wave functions $C_{iks}^{\mu\pm}(\underline{k})$. For the dominant term, the denominator, as determined by (5.9) and (5.6), is essentially the square of

$$A_{00} = \frac{m_0^2 + \frac{\alpha}{2\pi} I_{000} + q_\perp^2}{1-y} + \frac{\mu_0^2 + q_\perp^2}{y} - m_e^2, \tag{5.21}$$

with

$$I_{000} = 16\pi^2[(m_0^2 + \Lambda_0)\bar{I}_0(\Lambda_0) - 4m_0\bar{I}_1(\Lambda_0)] \tag{5.22}$$

and

$$\Lambda_0 = \mu_0^2 + (1-y)m_e^2 - \frac{\mu_0^2 + q_\perp^2}{y} \tag{5.23}$$

from the expressions in (5.12) and (5.13). For the physical photon, $\mu_0 = 0$ and the two-body wave function is peaked at $q_\perp = 0$ and $y = 0$, so that we can approximate

Λ_0 as m_e^2. We then have

$$A_{00} \simeq \frac{m_0^2 + 8\pi\alpha[(m_0^2 + m_e^2)\bar{I}_0(m_e^2) - 4m_0\bar{I}_1(m_e^2)] + q_\perp^2}{1-y} + \frac{q_\perp^2}{y} - m_e^2 \tag{5.24}$$

From the mass shift given in (B.1), we also have, to leading order in α,

$$m_0^2 = m_e^2 - 8\pi\alpha[(m_0^2 + m_e^2)\bar{I}_0(m_e^2) - 4m_0\bar{I}_1(m_e^2)]. \tag{5.25}$$

Therefore, the denominator reduces to the square of

$$A_{00} = \frac{m_e^2 + q_\perp^2}{1-y} + \frac{q_\perp^2}{y} - m_e^2 + \mathcal{O}(\alpha^2), \tag{5.26}$$

which matches the denominator of the integral that yields the Schwinger contribution, written as [50]

$$a_e = \frac{\alpha}{\pi} m_e^2 \int \frac{dy dq_\perp^2/(1-y)}{\left[\frac{m_e^2+q_\perp^2}{1-y} + \frac{q_\perp^2}{y} - m_e^2\right]^2}. \tag{5.27}$$

Thus, the dominant contribution with the self-energy included is very close in form to the integral that yields the Schwinger result.

Chapter 6

TWO-PHOTON TRUNCATION

We now construct the dressed-electron problem in the two-photon truncation. This will define an eigenvalue problem in the form of an integral equation for the one-electron/one-photon wave function. From these wave functions the bare-electron amplitudes and the one-electron/two-photon wave functions can be computed. We then compute the overall normalization and the anomalous moment. As in the case of the one-photon truncation, these matrix elements are computed from a physical projection of the eigenstate that maintains positivity of probability distributions. Solution of this problem and computation of the matrix elements require numerical techniques, which are discussed in Appendices D through G.

6.1. Integral Equations for Two-Body Wave Functions

The Fock-state expansion for the $J_z = \pm\frac{1}{2}$ eigenstate is given in (3.1). The coupled integral equations for the wave functions are given in Eqs. (3.3), (3.4), and (3.5). The first and third equations can be solved for the bare-electron amplitudes and one-electron/two-photon wave functions, respectively, in terms of the one-electron/one-photon wave functions. From (3.3), we have

$$z_i = \frac{1}{M^2 - m_i^2} \int d\underline{q} \sum_{j,l,\mu} \sqrt{\xi_l}(-1)^{j+l} \epsilon^\mu \left[P^+ V^{\mu *}_{ji\pm}(\underline{P} - \underline{q}, \underline{P}) C^{\mu\pm}_{jl\pm}(\underline{q}) + P^+ U^{\mu *}_{ji\pm}(\underline{P} - \underline{q}, \underline{P}) C^{\mu\pm}_{jl\mp}(\underline{q}) \right]. \tag{6.1}$$

The three-body wave functions are already obtained, in (5.1).

Substitution of these solutions into the second integral equation (3.4) yields a reduced integral eigenvalue problem in the one-electron/one-photon sector. To isolate the dependence on the azimuthal angles, we use $q_i^1 \pm iq_i^2 = q_{i\perp}e^{\pm i\phi_i}$ and $q_i^+ = y_i P^+$, and write the vertex functions (2.33) as

$$
\begin{aligned}
V^+_{ia\pm}(\underline{P}-\underline{q}_1-\underline{q}_2,\underline{P}-\underline{q}_2) &= \frac{1}{(P^+)^{1/2}}\frac{e}{\sqrt{8\pi^3 y_2}}, \qquad (6.2)\\
V^-_{ia\pm}(\underline{P}-\underline{q}_1-\underline{q}_2,\underline{P}-\underline{q}_2) &= \frac{1}{(P^+)^{5/2}}\frac{e}{\sqrt{8\pi^3 y_2}}\frac{(q_{1\perp}e^{\mp i(\phi_1-\phi_2)}+q_{2\perp})q_{2\perp}+m_i m_a}{(1-y_2)(1-y_1-y_2)},\\
V^{(\pm)}_{ia\pm}(\underline{P}-\underline{q}_1-\underline{q}_2,\underline{P}-\underline{q}_2) &= -\frac{e^{\pm i\phi_2}}{(P^+)^{3/2}}\frac{e}{\sqrt{8\pi^3 y_2}}\frac{q_{2\perp}}{1-y_2},\\
V^{(\pm)}_{ia\mp}(\underline{P}-\underline{q}_1-\underline{q}_2,\underline{P}-\underline{q}_2) &= -\frac{e^{\pm i\phi_2}}{(P^+)^{3/2}}\frac{e}{\sqrt{8\pi^3 y_2}}\frac{q_{1\perp}e^{\pm i(\phi_1-\phi_2)}+q_{2\perp}}{1-y_1-y_2},\\
U^+_{ia\pm}(\underline{P}-\underline{q}_1-\underline{q}_2,\underline{P}-\underline{q}_2) &= 0,\\
U^-_{ia\pm}(\underline{P}-\underline{q}_1-\underline{q}_2,\underline{P}-\underline{q}_2) &= \pm\frac{e^{\pm i\phi_2}}{(P^+)^{5/2}}\frac{e}{\sqrt{8\pi^3 y_2}}\frac{m_a(q_{1\perp}e^{\pm i(\phi_1-\phi_2)}+q_{2\perp})-m_i q_{2\perp}}{(1-y_2)(1-y_1-y_2)},\\
U^{(\pm)}_{ia\pm}(\underline{P}-\underline{q}_1-\underline{q}_2,\underline{P}-\underline{q}_2) &= 0,\\
U^{(\pm)}_{ia\mp}(\underline{P}-\underline{q}_1-\underline{q}_2,\underline{P}-\underline{q}_2) &= \mp\frac{1}{(P^+)^{3/2}}\frac{e}{\sqrt{8\pi^3 y_2}}\frac{m_i(1-y_2)-m_a(1-y_1-y_2)}{(1-y_2)(1-y_1-y_2)}.
\end{aligned}
$$

The angular dependence of the wave functions is determined by the sum of J_z contributions for each Fock state. For example, in the case of $C^{(+)+}_{ij-}$, the photon is created by $a^\dagger_{j(+)} = \frac{1}{\sqrt{2}}(a^\dagger_{j1} - ia^\dagger_{j2})$, which contributes $J_z = -1$ to the state, and the constituent electron contributes $J_z = -\frac{1}{2}$; therefore, to have a total J_z of $+\frac{1}{2}$, the wave function must contribute $J_z = 2$, which corresponds to a factor of $e^{2i\phi}$. For the full set of $J_z = +\frac{1}{2}$ wave functions, we find

$$
\begin{aligned}
C^{++}_{ij+}(\underline{q}) &= \sqrt{P^+}C^{++}_{ij+}(y,q_\perp),\;\; C^{-+}_{ij+}(\underline{q}) = \frac{1}{P^{+3/2}}C^{-+}_{ij+}(y,q_\perp), \qquad (6.3)\\
C^{(\pm)+}_{ij+}(\underline{q}) &= \frac{e^{\pm i\phi}}{\sqrt{P^+}}C^{(\pm)+}_{ij+}(y,q_\perp),\\
C^{++}_{ij-}(\underline{q}) &= \sqrt{P^+}e^{i\phi}C^{++}_{ij-}(y,q_\perp),\;\; C^{-+}_{ij-}(\underline{q}) = \frac{e^{i\phi}}{P^{+3/2}}C^{-+}_{ij-}(y,q_\perp), \qquad (6.4)\\
C^{(+)+}_{ij-}(\underline{q}) &= \frac{e^{2i\phi}}{\sqrt{P^+}}C^{(+)+}_{ij-}(y,q_\perp),\;\; C^{(-)+}_{ij-}(\underline{q}) = \frac{1}{\sqrt{P^+}}C^{(-)+}_{ij-}(y,q_\perp).
\end{aligned}
$$

The factors of total light-cone momentum P^+ are introduced to cancel corresponding factors in subsequent expressions. The energy denominator of the three-body wave function can be written as

$$
\begin{aligned}
&M^2 - \frac{m_i^2 + (\vec{q}_{1\perp}+\vec{q}_{2\perp})^2}{(1-y_1-y_2)} - \frac{\mu_j^2+q_{1\perp}^2}{y_1} - \frac{\mu_l^2+q_{2\perp}^2}{y_2} \qquad (6.5)\\
&\quad = M^2 - \frac{m_i^2 + q_{1\perp}^2 + q_{2\perp}^2 + 2q_{1\perp}q_{2\perp}\cos(\phi_1-\phi_2)}{(1-y_1-y_2)} - \frac{\mu_j^2+q_{1\perp}^2}{y_1} - \frac{\mu_l^2+q_{2\perp}^2}{y_2}.
\end{aligned}
$$

The light-cone volume element $d\underline{q}'$ becomes $\frac{1}{2}P^+dy'd\phi'dq_\perp'^2$. All the angular dependence can then be gathered into integrals of the form

$$
\mathcal{I}_n = \int_0^{2\pi}\frac{d\phi'}{2\pi}\frac{e^{in(\phi-\phi')}}{D_{ajb}(q_{1\perp},q_{2\perp}) + F(q_{1\perp},q_{2\perp})\cos(\phi-\phi')}, \qquad (6.6)
$$

with $|n| = 0,1,2,3$ and D_{ajb} and F defined in (5.11). The integral equations for the two-body wave functions then take the form

$$
\begin{aligned}
\left[M^2 - \frac{m_i^2+q_\perp^2}{1-y} - \frac{\mu_j^2+q_\perp^2}{y}\right] C^{\mu\pm}_{ijs}(y,q_\perp) &= \frac{\alpha}{2\pi}\sum_{i'}\frac{I_{iji'}(y,q_\perp)}{1-y}C^{\mu\pm}_{i'js}(y,q_\perp) \qquad (6.7)\\
&+ \frac{\alpha}{2\pi}\sum_{i'j's'\nu}\epsilon^\nu\int_0^1 dy'dq_\perp'^2 J^{(0)\mu\nu}_{ijs,i'j's'}(y,q_\perp;y',q_\perp')C^{\nu\pm}_{i'j's'}(y',q_\perp')\\
&+ \frac{\alpha}{2\pi}\sum_{i'j's'\nu}\epsilon^\nu\int_0^{1-y} dy'dq_\perp'^2 J^{(2)\mu\nu}_{ijs,i'j's'}(y,q_\perp;y',q_\perp')C^{\nu\pm}_{i'j's'}(y',q_\perp').
\end{aligned}
$$

There is a total of 48 coupled equations, with $i = 0, 1$; $j = 0, 1, 2$; $s = \pm\frac{1}{2}$; and $\mu = \pm, (\pm)$. A diagrammatic representation is given in Fig. 6.1.

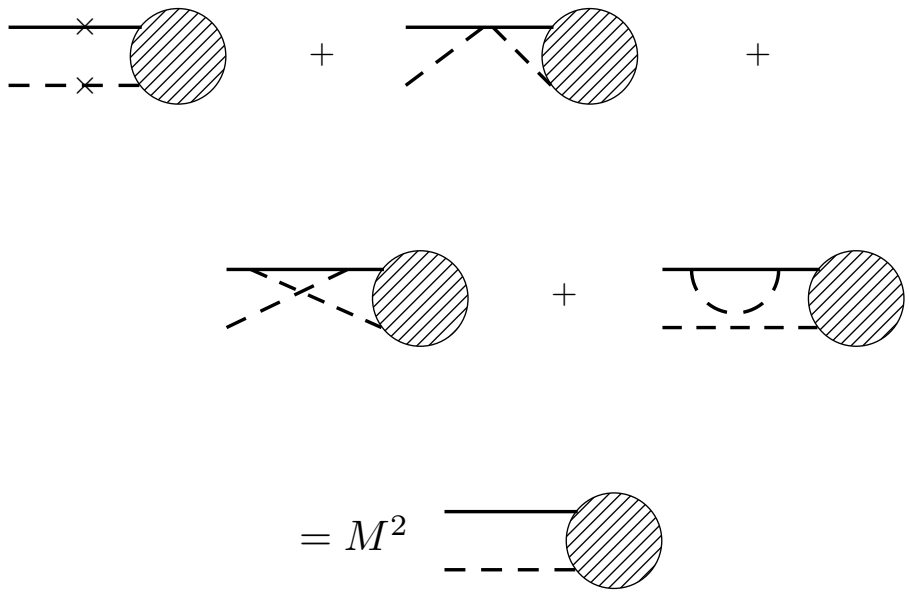

Figure 6.1. Diagrammatic representation of Eq. (6.7) of the text. The conventions for the diagrams are the same as in Fig. 3.1.

The first term on the right-hand side of (6.7) is the self-energy contribution, already discussed in Chap. 5. The kernels $J^{(0)}$ and $J^{(2)}$ in the second and third terms correspond to interactions with zero or two photons in intermediate states. The zero-photon kernel factorizes as

$$J^{(0)\mu\nu}_{ijs,i'j's'}(y, q_\perp; y', q'_\perp) = \sum_a V^{(0)\mu}_{ijas}(y, q_\perp) \frac{(-1)^a}{M^2 - m_a^2} V^{(0)\nu *}_{i'j'as'}(y', q'_\perp), \tag{6.8}$$

with

$$V^{(0)+}_{ija+} = \sqrt{\xi_j}\frac{1}{\sqrt{y}}, \;\; V^{(0)-}_{ija+} = \sqrt{\xi_j}\frac{m_i m_a}{(1-y)\sqrt{y}}, \;\; V^{(0)(+)}_{ija+} = 0, \;\; V^{(0)(-)}_{ija+} = \sqrt{\xi_j}\frac{q_\perp}{(1-y)\sqrt{y}}, \tag{6.9}$$

and

$$V^{(0)+}_{ija-}=0,\;\; V^{(0)-}_{ija-}=\sqrt{\xi_j}\frac{m_a q_\perp}{(1-y)\sqrt{y}},\;\; V^{(0)(+)}_{ija-}=0,\;\; V^{(0)(-)}_{ija-}=\sqrt{\xi_j}\frac{m_a(1-y)-m_i}{(1-y)\sqrt{y}}. \tag{6.10}$$

The two-photon kernels are considerably more involved and are therefore listed in Appendix H. The angular integrals $\mathcal{I}_n$ are worked out in detail in Appendix I.

6.2. Fermion Flavor Mixing

The presence of the flavor changing self-energies leads naturally to a fermion flavor mixing of the two-body wave functions. The integral equations for these functions have the structure

$$\begin{aligned} A_{0j}C^{\mu\pm}_{0js}-B_jC^{\mu\pm}_{1js} &= -\frac{\alpha}{2\pi}J^{\mu\pm}_{0js}, \\ B_jC^{\mu\pm}_{0js}+A_{1j}C^{\mu\pm}_{1js} &= -\frac{\alpha}{2\pi}J^{\mu\pm}_{1js}, \end{aligned} \tag{6.11}$$

where A_{ij} and B_j are defined in (5.6) and (5.7), and $J^{\mu\pm}_{ijs}$ is given by

$$\begin{aligned} J^{\mu\pm}_{ijs} &= \sum_{i'j's'\nu}\epsilon^\nu\int_0^1 dy'dq'^2_\perp J^{(0)\mu\nu}_{ijs,i'j's'}(y,q_\perp;y',q'_\perp)C^{\nu\pm}_{i'j's'}(y',q'_\perp) \\ &\quad+\sum_{i'j's'\nu}\epsilon^\nu\int_0^{1-y}dy'dq'^2_\perp J^{(2)\mu\nu}_{ijs,i'j's'}(y,q_\perp;y',q'_\perp)C^{\nu\pm}_{i'j's'}(y',q'_\perp). \end{aligned} \tag{6.12}$$

The structure of (6.11) is similar to that of (5.8); however, in the case of (6.11), the one-body amplitudes have been eliminated from the right-hand side and all the two-photon terms have been kept.

The wave functions that diagonalize the left-hand side of (6.11), and mix the physical ($i = 0$) and PV ($i = 1$) fermion flavors, are

$$\tilde{f}^{\mu\pm}_{ijs} = A_{ij} C^{\mu\pm}_{ijs} + (-1)^i B_j C^{\mu\pm}_{1-i,js}. \tag{6.13}$$

In terms of these functions, the eigenvalue problem (6.11) can be written as

$$J^{\mu\pm}_{ijs}[\tilde{f}] = -\frac{2\pi}{\alpha} \tilde{f}^{\mu\pm}_{ijs}. \tag{6.14}$$

Here $J^{\mu\pm}_{ijs}$, the contribution of the zero-photon and two-photon kernels, is implicitly a functional of these new wave functions. The factors of α that appear in A_{ij} and B_j are assigned the physical value and not treated as eigenvalues. The original wave functions are recovered as

$$C^{\mu\pm}_{ijs} = \frac{A_{1-i,js} \tilde{f}^{\mu\pm}_{ijs} + (-1)^i B_j \tilde{f}^{\mu\pm}_{1-i,js}}{A_{0j} A_{1j} + B_j^2}. \tag{6.15}$$

As in Chap. 5, self-energy contributions appear in the denominators of the wave functions.

To express the eigenvalue problem explicitly in terms of the $\tilde{f}^{\mu\pm}_{ijs}$, we first write the definition (6.12) of $J^{\mu\pm}_{ijs}$ in a simpler form

$$J^{\mu\pm}_{ijs} = \int dy' dq'^2_\perp \sum_{i'j's'\nu} (-1)^{i'+j'} \epsilon^\nu J^{\mu\nu}_{ijs,i'j's'}(y, q_\perp; y', q'_\perp) C^{\nu\pm}_{i'j's'}(y', q'_\perp), \tag{6.16}$$

where $J^{\mu\nu}_{ijs,i'j's'} = J^{(0)\mu\nu}_{ijs,i'j's'} + J^{(2)\mu\nu}_{ijs,i'j's'}$. Substitution of (6.15) then yields, in matrix form,

$$\begin{pmatrix} J^{\mu\pm}_{0js} \\ J^{\mu\pm}_{1js} \end{pmatrix} = \int dy' dq'^2_\perp \sum_{j's'\nu} (-1)^{j'} \epsilon^\nu \begin{pmatrix} J^{\mu\nu}_{0js,0j's'} & J^{\mu\nu}_{0js,1j's'} \\ J^{\mu\nu}_{1js,0j's'} & J^{\mu\nu}_{1js,1j's'} \end{pmatrix} \times \begin{pmatrix} A_{1j'} & B_{j'} \\ B_{j'} & -A_{0j'} \end{pmatrix} \begin{pmatrix} \tilde{f}^{\nu\pm}_{0j's'} \\ \tilde{f}^{\nu\pm}_{1j's'} \end{pmatrix} \tag{6.17}$$

The sum over ν can also be written in matrix form for the helicity components $\nu = \pm, (\pm)$ by the introduction of

$$\lambda = \begin{pmatrix} 0 & -1 & 0 & 0 \\ -1 & 0 & 0 & 0 \\ 0 & 0 & 1 & 0 \\ 0 & 0 & 0 & 1 \end{pmatrix}, \tag{6.18}$$

so that

$$\sum_{\nu} \epsilon^{\nu} J^{\mu\nu} \tilde{f}^{\nu\pm} = \sum_{\alpha,\beta} J^{\mu\alpha} \lambda_{\alpha\beta} \tilde{f}^{\beta\pm}. \tag{6.19}$$

Finally, we define

$$\eta_{j',\alpha\beta} = (-1)^{j'} \lambda_{\alpha\beta} \begin{pmatrix} A_{1j'} & B_{j'} \\ B_{j'} & -A_{0j'} \end{pmatrix} \tag{6.20}$$

as a tensor product of simpler matrices. The eigenvalue problem then becomes

$$\int dy' dq'^2_{\perp} \sum_{i'j's'\alpha\beta i''} J^{\mu\alpha}_{ijs,i'j's'}(y, q_{\perp}; y', q'_{\perp}) \eta_{j',\alpha\beta,i'i''} \tilde{f}^{\beta\pm}_{i''j's'} = -\frac{2\pi}{\alpha} \tilde{f}^{\mu\pm}_{ijs}. \tag{6.21}$$

Once again, this yields α as a function of m_0 and the PV masses. We then find m_0 such that, for chosen values of the PV masses, α takes the standard physical value $e^2/4\pi$. The eigenproblem solution also yields the functions $\tilde{f}^{\mu\pm}_{ijs}$ which determine the wave functions $C^{\mu\pm}_{ijs}$. From these wave functions we can compute physical quantities as expectation values with respect to the projection (3.2) of the eigenstate onto the physical subspace.

6.3. Solution of the Eigenvalue Problem

Before presenting the results for the two-photon truncation in Sec. 6.3.3, we discuss the numerical methods used and the convergence properties of the calculations. Additional detail for the numerical methods can be found in the Appendices.

6.3.1. Numerical Methods

The integral equations (6.21) for the wave functions of the electron require numerical techniques for their solution. They are converted to a matrix eigenvalue problem by a discrete approximation to the integrals, as discussed in Appendix D. These approximations involve variable transformations and Gauss–Legendre quadrature; the transformations are done to minimize the number of quadrature points required, in order to keep the matrix problem from becoming too large, and to reduce the infinite transverse momentum range to a finite interval. The resolution of the numerical approximation is measured by two parameters, K and $N_\perp$, that control the number of quadrature points in the longitudinal and transverse directions.

The integrals for the normalization and anomalous moment, (3.8) and (3.10) respectively, are also done numerically, but are summed over different quadrature points. These points take into account the different shape of the integrand that comes from the square of the wave functions. The values of the wave functions at these other points are found by cubic-spline interpolation, described in Appendix G. Regions of integration near the line of poles associated with the energy denominator require special treatment, if the poles exist, through quadrature formulas that take the poles into account explicitly.

The matrix eigenvalue problem is solved for the lowest physical state via the Lanczos diagonalization algorithm [9, 10]. The matrix is too large for standard methods; it is typically of order 80,000×80,000 and not sparse, requiring approximately 55 gigabytes of storage for the matrix alone and 95 gigabytes total for the computer code. The Lanczos algorithm is an iterative method, summarized in Appendix F, that uses only matrix multiplication and dot products to generate a tridiagonal approximation to the original matrix. After a sufficient number of Lanczos iterations, the extreme eigenvalues of the tridiagonal matrix are good approximations to those of the original

matrix; the associated eigenvectors can also be constructed. The usual Lanczos algorithm does require a Hermitian matrix, which is not available here due to the negative metric of the PV fields. However, the Lanczos algorithm developed for PV-regulated Yukawa theory [4] can be generalized to the present case.

The renormalization requires finding the value of the bare mass that corresponds to the physical value of the coupling. This defines a nonlinear equation for the bare mass, which is solved with use of the Müller algorithm [51]. Finding the poles in the two-body wave function also requires solution of nonlinear equations, and again the Müller algorithm is used. The algorithm is described in Appendix E.

The calculation of the anomalous moment requires computation of a transverse derivative of the wave functions. Because the quadrature points used for integration are not uniformly spaced, they are not convenient for estimating the derivative directly. Instead, the wave functions are first approximated by cubic splines; the derivatives are then obtained from the splines, as discussed in Appendix G. For the largest matrices considered by the Lanczos method, the total time required, for a calculation of the anomalous moment at a fixed set of PV mass values, is four to eight cpu-days on a Sun Fire X4600; most of this time is spent on the Lanczos iterations, which are a part of finding the value of the bare mass m_0 that yields the physical value for α.

The computing facilities immediately available limit the Lanczos-based calculation to resolutions no more than $K = 26$ and $N_\perp = 20$. At such resolutions, the Lanczos approach was found to be unstable with respect to extraction of the desired eigenstate from among states with negative norm. This is at least partly due to the small magnitude of the two-photon contribution relative to the numerical error in the discrete representation of the integral equations. The successful Yukawa-theory calculations [8] were done at stronger coupling, where the two-boson contribution was

not so small.

To isolate the two-photon contributions, we treat them explicitly, but still non-perturbatively, as corrections to the one-photon truncation with self-energy, solved in the previous chapter. We solve the coupled system

$$(M^2 - m_a^2) z_a / z_0 = \sqrt{\frac{\alpha}{2}} \sum_{i'j's'\alpha\beta i''} \int dy' dq_\perp'^2 V^{(0)\alpha *}_{i'j'as'} \eta_{j',\alpha\beta,i'i''} \tilde{f}^{\beta\pm}_{i''j's'} / z_0, \tag{6.22}$$

$$\begin{aligned} \tilde{f}^{\mu\pm}_{ijs} / z_0 &= -\sqrt{\frac{\alpha}{2\pi^2}} \sum_a (-1)^a V^{(0)\mu}_{ijas} z_a / z_0 \\ &\quad - \frac{\alpha}{2\pi} \int dy' dq_\perp'^2 \sum_{i'j's'\alpha\beta i''} J^{(2)\mu\alpha}_{ijs,i'j's'} \eta_{j',\alpha\beta,i'i''} \tilde{f}^{\beta\pm}_{i''j's'} / z_0, \end{aligned} \tag{6.23}$$

which can be obtained from (6.1) and (6.21), with use of the factorization (6.8) for $J^{(0)}$ and the connection (6.15) between the original and flavor-mixed two-body wave functions.

The solution is obtained by iteration. When the index a in (6.22) is equal to zero, we obtain an equation for m_0,

$$m_0 = + \sqrt{M^2 - \sqrt{\frac{\alpha}{2}} \sum_{i'j's'\alpha\beta i''} \int dy' dq_\perp'^2 V^{(0)\alpha *}_{i'j'0s'} \eta_{j',\alpha\beta,i'i''} \tilde{f}^{\beta\pm}_{i''j's'} / z_0}, \tag{6.24}$$

and when a is equal to 1, we obtain an equation for z_1,

$$z_1 / z_0 = \frac{1}{M^2 - m_1^2} \sqrt{\frac{\alpha}{2}} \sum_{i'j's'\alpha\beta i''} \int dy' dq_\perp'^2 V^{(0)\alpha *}_{i'j'1s'} \eta_{j',\alpha\beta,i'i''} \tilde{f}^{\beta\pm}_{i''j's'} / z_0. \tag{6.25}$$

These provide the updates of m_0 and z_1/z_0, and (6.23) is solved by Jacobi iteration [51] of the linear system that comes from the discretization of the rearrangement

$$\begin{aligned} \tilde{f}^{\mu\pm}_{ijs} / z_0 &+ \frac{\alpha}{2\pi} \int dy' dq_\perp'^2 \sum_{i'j's'\alpha\beta i''} J^{(2)\mu\alpha}_{ijs,i'j's'} \eta_{j',\alpha\beta,i'i''} \tilde{f}^{\beta\pm}_{i''j's'} / z_0 \\ &= -\sqrt{\frac{\alpha}{2\pi^2}} \sum_a (-1)^a V^{(0)\mu}_{ijas} z_a / z_0. \end{aligned} \tag{6.26}$$

Only a few Jacobi iterations are performed per update of m_0 and z_1/z_0; further inner iteration is unnecessary, due to the subsequent changes in m_0 and z_1/z_0. The outer iterations of the full system of equations is terminated when the changes in m_0, z_1/z_0, and the two-body wave function are all of order 10^{-6} or less. The bare amplitude z_0 is obtained at the end by normalization. The coupling α is held fixed at the physical value; hence, this iterative method yields not only the two-body wave functions and one-body amplitudes but also the bare mass, m_0. The anomalous moment can then be calculated as before.

The number of wave-function updates is small enough that the matrix representing the discretization of the integral equations can be computed at each iteration without making the time for calculation too large. Thus, the matrix need not be stored, which allows much larger resolutions. We find that reasonable results are not obtained until the longitudinal resolution K is at least 50 and that there is still considerable sensitivity to the longitudinal resolution. There is much less sensitivity to the transverse resolution, for which $N_\perp = 20$ is found sufficient. The dependence on longitudinal resolution is discussed at the end of the next subsection.

6.3.2. Numerical Convergence

The primary constraint on numerical accuracy is the error in the estimation of the integrals in the integral equations for the wave functions and in the expressions for the normalization and the anomalous moment. This accuracy is determined by the choice of quadrature scheme, discussed in Appendix D, and the resolution, controlled by the longitudinal parameter K and transverse parameter $N_\perp$. The other numerical parts of the calculation, the Lanczos diagonalization and the solution of nonlinear equations, are iterated to what is effectively exact convergence, with remaining uncertainties much smaller than the errors in the numerical quadratures.

Table 6.1. Dependence on longitudinal resolution K of the integrals $\bar{I}_0$, $\bar{I}_1$, and $\bar{J}$, defined in (4.8) and (4.9) of the text and computed according to the quadrature scheme described in Appendix D. The bare-electron mass is $m_0 = 0.98m_e$. The PV masses are $m_1 = 2 \cdot 10^4 m_e$, $\mu_1 = 200m_e$, and $\mu_2 = \sqrt{2}\mu_1$. The transverse resolution is $N_\perp = 40$.

K	$\bar{I}_0(m_e^2)$	$\bar{I}_1(m_e^2)/m_e$	$\bar{J}(m_e^2)/m_e^2$
5	-7.113	-13.530	-11606.
10	-6.2586	-10.6182	932.3
15	-6.2641	-10.7354	-26.487
20	-6.2645	-10.7327	-6.7126
25	-6.2645	-10.7328	-6.3982
30	-6.2645	-10.7328	-6.4401
exact	-6.2645	-10.7328	-6.2645

For the one-photon truncation, discussed in Chap. 4, all the integrals can be done analytically. This makes the one-photon problem a convenient first test for numerical convergence. The key integrals are $\bar{I}_0$, $\bar{I}_1$, and $\bar{J}$, defined in (4.8) and (4.9). Tables 6.1 and 6.2 and Figs. 6.2 and 6.3 summarize results for numerical calculation of these integrals. They show that $\bar{I}_0$ and $\bar{I}_1$ are well approximated for a wide range of resolutions, but $\bar{J}$ is particularly sensitive to the longitudinal resolution K and requires that both K and $N_\perp$ be on the order of 20 or larger. At these resolutions, $\bar{J}$ is approximated with an accuracy of about 4%, and this then becomes a minimal estimate of the accuracy of any of the results.

As expected, the results for the one-photon truncation, if computed numerically, converge to better than 1% at the same resolution, of $K = 20$ and $N_\perp = 20$, as can be seen in Tables 6.3 and 6.4 and Figs. 6.4 and 6.5. However, the results with the self-energy contribution, shown in the same tables and figures, require $K \simeq 25$ before nearing convergence. Although the exact answer is not known in this case, $K = 20$ is

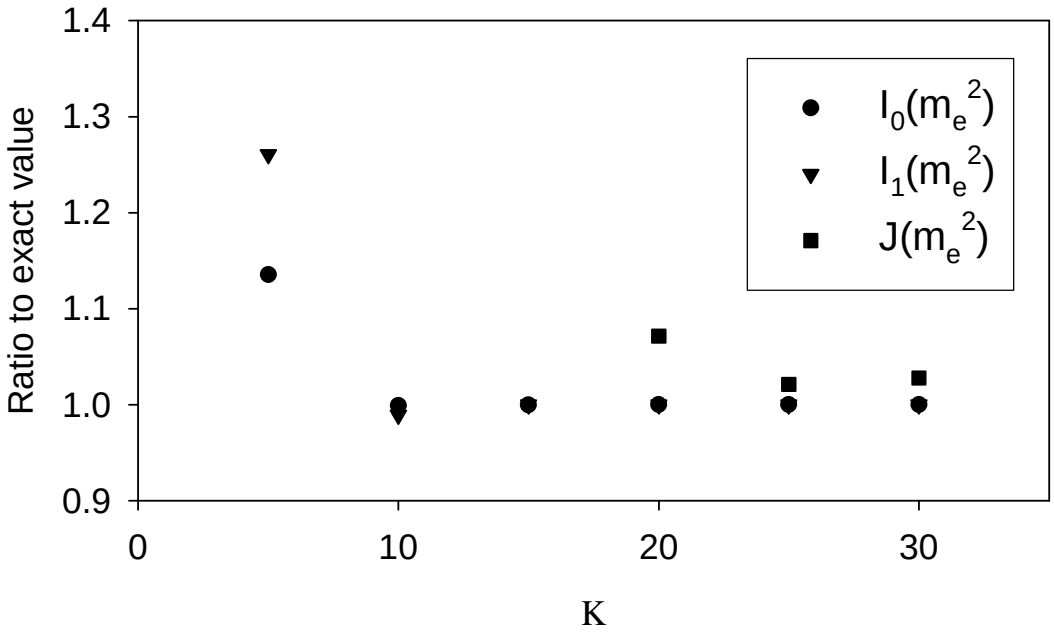

Figure 6.2. Dependence on longitudinal resolution K of the integrals I_0, I_1, and J, defined in (4.8) and (4.9) of the text and computed according to the quadrature scheme described in Appendix D. The values plotted are ratios to the exact values, listed in Table 6.1. The bare-electron mass is $m_0 = 0.98m_e$. The PV masses are $m_1 = 2 \cdot 10^4 m_e$, $\mu_1 = 200m_e$, and $\mu_2 = \sqrt{2}\mu_1$. The transverse resolution is $N_\perp = 40$.

clearly insufficient, but $K \gg 25$ yields a reasonable result with an error on the order of 1%.

The two-photon truncation incorporates numerical approximations to the integrals $\bar{I}_0$, $\bar{I}_1$, and $\bar{J}$ through the action of the zero-photon kernel $J^{(0)}$, in Eq. (6.7), and approximations to the self-energy contribution, also in Eq. (6.7). Thus, the minimum resolution for the two-photon calculation would appear to be approximately $K = 25$ and $N_\perp = 20$. We extrapolate from the one-photon and self-energy calculations to estimate an error of 5-10% for the two-photon truncation.

Table 6.2. Same as Table 6.1, but for the dependence on transverse resolution $N_\perp$. The longitudinal resolution is $K = 30$.

$N_\perp$	$\bar{I}_0(m_e^2)$	$\bar{I}_1(m_e^2)/m_e$	$\bar{J}(m_e^2)/m_e^2$
10	-6.2646	-10.7324	-2.9845
15	-6.2645	-10.7327	-7.5428
20	-6.2645	-10.7327	-6.9137
25	-6.2645	-10.7328	-6.6961
30	-6.2645	-10.7328	-6.5712
35	-6.2645	-10.7328	-6.4922
40	-6.2645	-10.7328	-6.4401
exact	-6.2645	-10.7328	-6.2645

For the two-photon truncation, there is a significant dependence on longitudinal resolution at the reasonably attainable resolutions. This is shown in Fig. 6.6 for three different values of the PV mass μ_1. Each case is extrapolated to infinite resolution in a quadratic fit. A linear fit changes the extrapolation only slightly, relative to the error estimate of 10%. Values of the bare mass are extrapolated in the same way.

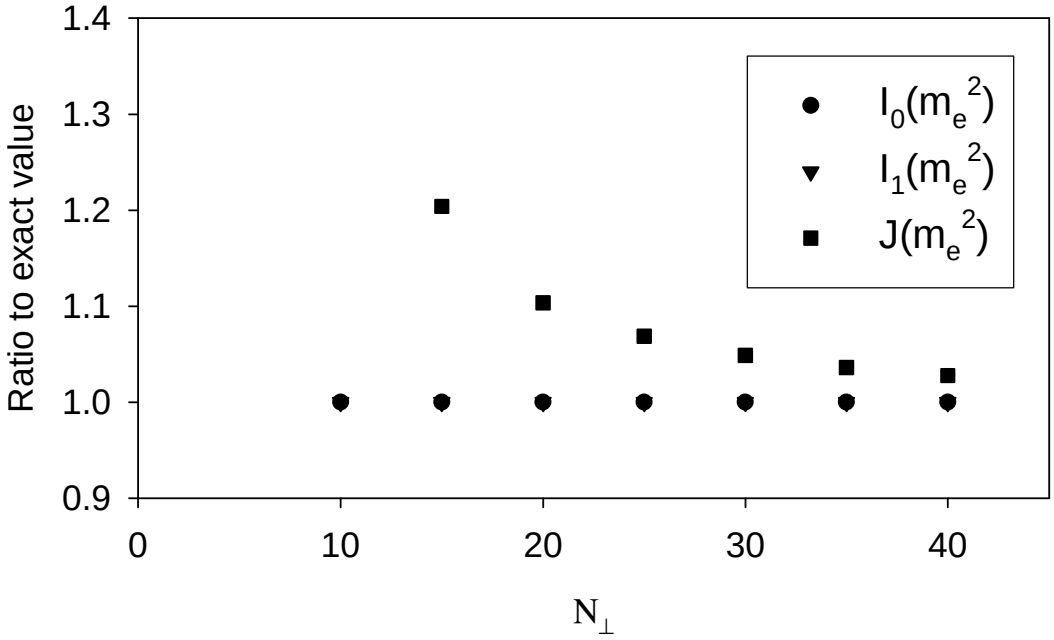

Figure 6.3. Same as Fig. 6.2, but for the dependence on transverse resolution $N_\perp$. The longitudinal resolution is $K = 30$. For these resolutions, the values for $\bar{I}_0$ and $\bar{I}_1$ are nearly exact, and the plotted points for the ratios to the exact values are at the same places; only J shows variation.

Table 6.3. Dependence on longitudinal resolution K of the bare mass m_0 and anomalous moment a_e of the electron in units of the physical mass m_e and the Schwinger term $(\alpha/2\pi)$, respectively, for both the one-photon truncation, when solved numerically, and the case with the self-energy included. The value of the bare mass is obtained as the value that yields a physical value of the coupling constant α; for $K = 15$, two solutions are found. The PV masses are $m_1 = 2 \cdot 10^4 m_e$, $\mu_1 = 200 m_e$, and $\mu_2 = \sqrt{2}\mu_1$. The transverse resolution is $N_\perp = 40$.

	one-photon		with self-energy	
K	m_0/m_e	$2\pi a_e/\alpha$	m_0/m_e	$2\pi a_e/\alpha$
5	4.4849	0.09921	4.4845	0.09444
10	1.7445	0.22992	1.7106	0.22620
15	1.07487	0.64482	1.07481	0.59092
15	0.98906	1.12763	0.97537	1.07444
20	0.98223	1.15430	0.99028	0.90337
25	0.98240	1.15382	0.98295	0.99242
30	0.98241	1.15567	0.98245	1.00612

Table 6.4. Same as Table 6.3, but for the dependence on transverse resolution $N_\perp$. The longitudinal resolution is $K = 30$.

	one-photon		with self-energy	
$N_\perp$	m_0/m_e	$2\pi a_e/\alpha$	m_0/m_e	$2\pi a_e/\alpha$
10	0.98023	1.16121	0.97918	—
15	0.98297	1.15317	0.98307	0.99071
20	0.98268	1.15380	0.98275	0.99776
25	0.98256	1.15484	0.98261	1.00130
30	0.98248	1.15399	0.98253	1.00348
35	0.98244	1.15404	0.98248	1.00501
40	0.98241	1.15567	0.98245	1.00612

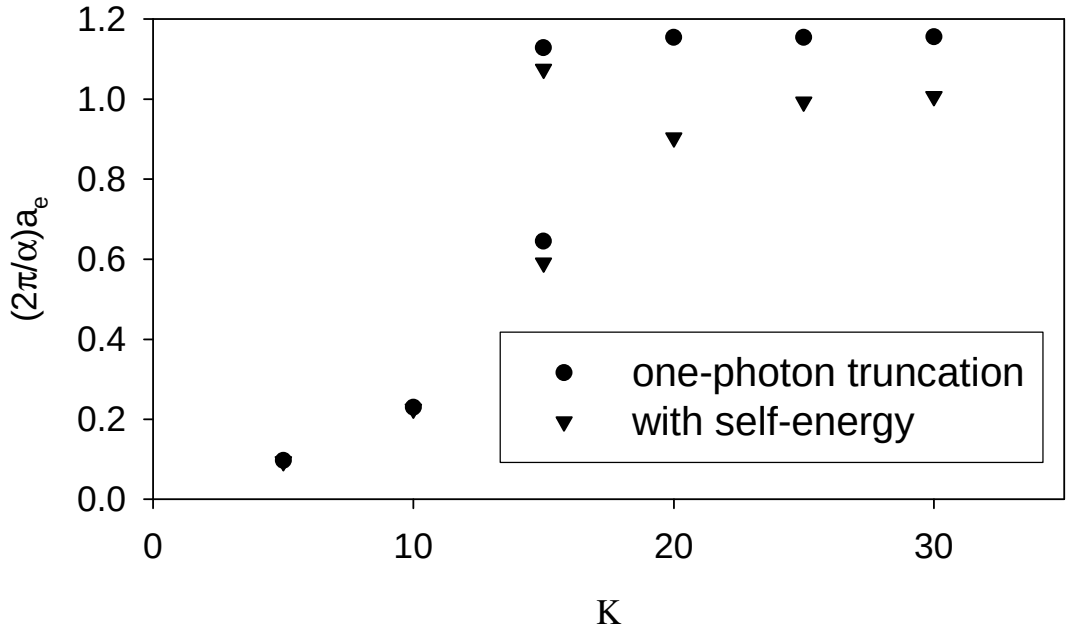

Figure 6.4. Dependence on longitudinal resolution K of the anomalous moment a_e of the electron in units of the the Schwinger term $(\alpha/2\pi)$ for both the one-photon truncation, when solved numerically, and the case with the self-energy included. The PV masses are $m_1 = 2{\cdot}10^4 m_e$, $\mu_1 = 200 m_e$, and $\mu_2 = \sqrt{2}\mu_1$. The transverse resolution is $N_\perp = 40$.

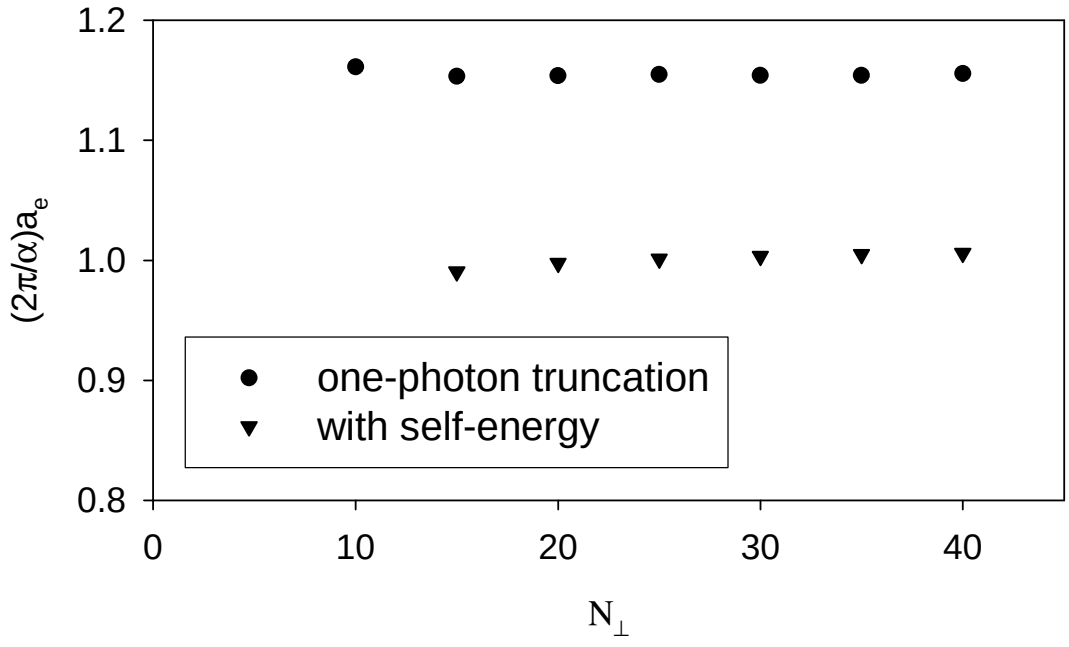

Figure 6.5. Same as Fig. 6.4, but for the dependence on transverse resolution $N_\perp$. The longitudinal resolution is $K = 30$.

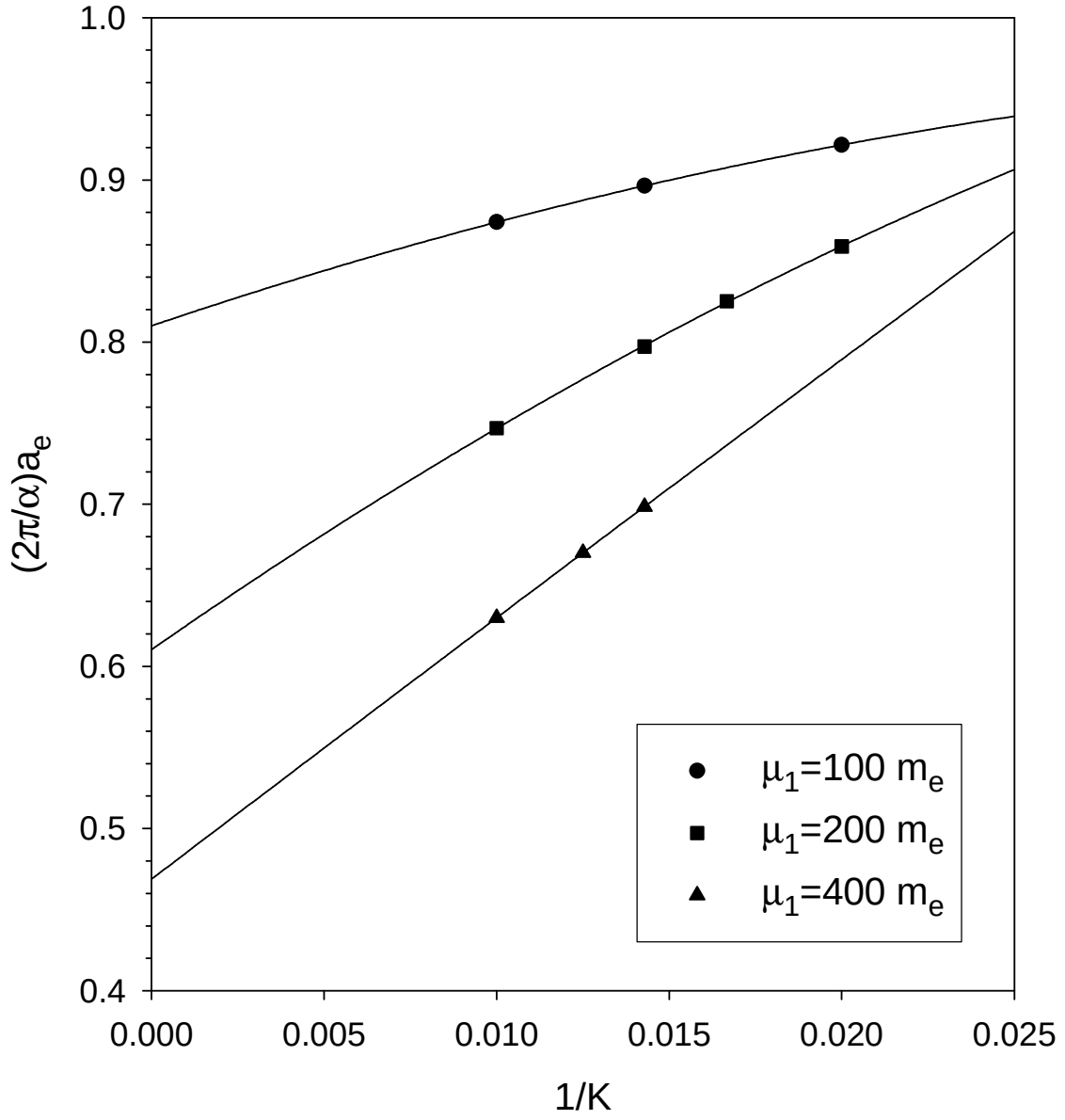

Figure 6.6. Dependence on longitudinal resolution K of the anomalous moment a_e of the electron in units of the the Schwinger term $(\alpha/2\pi)$ for the two-photon truncation. The PV masses are $m_1 = 2 \cdot 10^4 m_e$; $\mu_1 = 100m_e$, $200m_e$, and $400m_e$; and $\mu_2 = \sqrt{2}\mu_1$. The transverse resolution is $N_\perp = 20$.

6.3.3. Results

A summary of the results is given in Table 6.5 and Fig. 6.7. The variation in the results for the one-photon truncation plus self-energy contributions gives another measure of the numerical error and is consistent with an estimate of $< 5\%$. The results for the two-photon truncation are shown with error bars that reflect a conservative estimate of a 10% error.

Table 6.5. The bare mass m_0 and anomalous moment a_e of the electron in units of the physical mass m_e and the Schwinger term $(\alpha/2\pi)$, respectively, as functions of the PV photon mass, μ_1, with the second PV photon mass, μ_2, set to $\sqrt{2}\mu_1$ and the PV electron mass m_1 equal to $2 \cdot 10^4\, m_e$. The resolutions used for the two-photon results are $K = 50$ to 100, combined with extrapolation to $K = \infty$, and $N_\perp = 20$.

	one-photon		with self-energy		two-photon	
μ_1/m_e	m_0/m_e	$2\pi a_e/\alpha$	m_0/m_e	$2\pi a_e/\alpha$	m_0/m_e	$2\pi a_e/\alpha$
100	0.98469	1.1437	0.98516	0.996	1.01	0.81±0.08
200	0.98240	1.1536	0.98295	0.992	1.06	0.61±0.06
400	0.98004	1.1625	0.98031	0.997	1.22	0.47±0.05
600	0.97826	1.1687	0.97804	1.010		
800	0.97624	1.1745	0.97617	1.007		
1000	0.97329	1.1817	0.97282	1.002		

The results for the two-photon truncation show a very strong dependence on the PV photon mass μ_1. This is a pattern already seen in Fig. 4.2 for the one-photon truncation, where a similar decrease occurred until the correct chiral limit was restored, as discussed in Sec. 4.4.3. In the present case, it is therefore likely that the correct chiral limit has again been lost. The constraint used in determining the parameters of the second PV photon flavor was determined only to one-loop order, with the two-loop and higher contributions being of higher powers in $\alpha/2\pi$ and therefore expected to be small. However, estimates of the two-loop contribution,

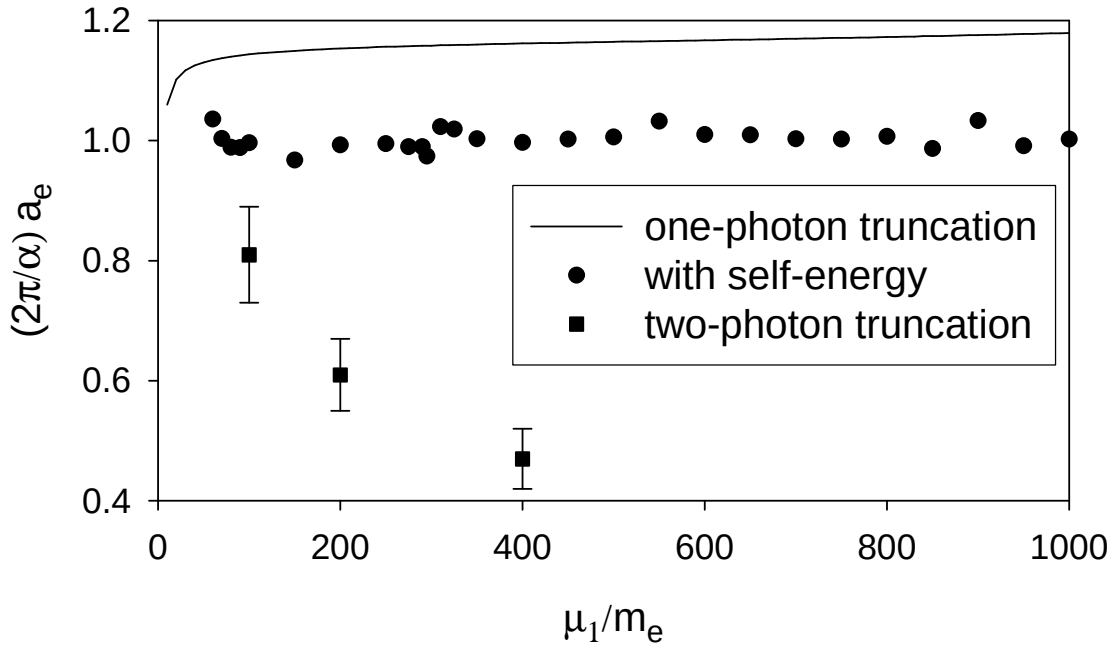

Figure 6.7. The anomalous moment of the electron in units of the Schwinger term $(\alpha/2\pi)$ plotted versus the PV photon mass, μ_1, with the second PV photon mass, μ_2, set to $\sqrt{2}\mu_1$ and the PV electron mass m_1 equal to $2 \cdot 10^4\, m_e$. The plot compares results with and without the two-photon contributions. The resolutions used for the two-photon results are $K = 50$ to 100, combined with extrapolation to $K = \infty$, and $N_\perp = 20$.

extracted from the iteration of the coupled system (6.22) and (6.23), show that the contribution is actually comparable to the one-loop contribution. Thus, for a better calculation of the anomalous moment, the chiral constraint (4.26) should be modified to include higher-order contributions. The parameter ξ_2 will need to be recalculated to include two-loop contributions to the shift in the electron mass, such that the shift will be zero when the bare mass is zero. This will be a numerical calculation because, unlike the derivation of (4.26), the integrals involved cannot be done analytically. An alternative is to increase the value of the PV electron mass m_1, but this causes

difficulties for the numerical integrations.

Once the two-loop chiral constraint is implemented, the values calculated for the anomalous moment in the two-photon truncation may still be shifted away from the experimental value, in analogy to the 17% shift found in the case of the one-photon truncation, until self-energy contributions are included. One might expect the shift in the two-photon case to be small because the two-loop contribution higher order in $\alpha/2\pi$, but again the two-loop contributions may be comparable to the one-loop contribution. The cure should be the analog of what happened for the one-photon result, that the two-photon truncation will require a three-photon self-energy contribution before coming into agreement with experiment.

Chapter 7

SUMMARY AND CONCLUSIONS

The quantitative results of this work are summarized in Fig. 6.7 and Table 6.5. The calculated anomalous magnetic moment of the electron is given for the particular approximations considered, that is, the one-photon truncation, without and with two-photon self-energy contributions, and the full two-photon truncation. The calculations of each case are described in Chaps. 4, 5, and 6. The two-photon results should include enough physics to bring the calculated value of the anomalous moment into agreement with the experimental result to within the numerical errors of the calculation. However, the correct chiral limit has not been maintained, as a consequence of unexpectedly large two-loop contributions to the bare mass, and the anomalous moment has developed a strong dependence on the PV masses. The one-photon results with the two-photon self-energy contributions are in complete agreement with experiment.

To obtain these results required several new developments, some already published [45], as well as incorporation of what was already known from previous work [7, 8]. The new developments include extension of the light-front QED Hamiltonian $\mathcal{P}^-$ (2.29) to include a second PV photon flavor; derivation of the helicity form of the light-front Hamiltonian (2.32) and the associated vertex functions (2.33); a new proof of the integral identity $\bar{J} = M^2 \bar{I}_0$, in Appendix C; construction of the kernels $J^{(0)}$ and $J^{(2)}$ of the integral equations for the two-body wave functions, in (6.8) and Appendix H; and evaluation of the angular integrals $\mathcal{I}_n$ (6.6), in Appendix I. The numerical solution of the eigenvalue problem and the numerical calculation of the anomalous moment

from the wave functions required new discretizations and quadrature schemes (Appendix D), particularly those that take into account the simple and double poles in energy denominators; extension of the Lanczos diagonalization algorithm to a non-diagonal indefinite metric (Appendix F); a new iterative algorithm, described at the end of Sec. 6.3.1, to allow higher resolutions; and alternate forms of the two-photon kernels, to minimize round-off error in their evaluation (Appendix H).

In addition to the progress made with respect to solving a nonperturbative light-front problem, there was also significant progress in understanding the regularization method itself in the context of a gauge theory [45]. The restoration of the correct chiral limit, by including a second PV photon flavor as discussed in Sec. 4.4.3, was critical to the success of the numerical calculation as well as an important fundamental correction to the regularization. The checks of charge renormalization, in Appendix A, and of the one-loop equivalence with covariant theory, in Appendix B, provide nontrivial confirmation that the method is consistent.

Despite the progress made, open questions for light-front QED certainly remain. In the analysis of the dressed-electron state, the extension of the chiral constraint to include two-loop effects is needed to control the PV mass dependence. More generally, the inclusion of Fock states with an electron-positron pair would be very interesting; the renormalization of the electron charge would need to be re-examined, both because of vacuum polarization contributions and because covariance of the current may be restored, at least partially. True bound states, such as positronium [52], would also be interesting as further tests of the method. Of course, in none of these cases is the nonperturbative analysis likely to produce results competitive with high-order perturbation theory; the numerical errors are large compared to the tiny perturbative corrections in a weakly coupled theory such as QED.

In a strongly coupled theory, such as QCD, the method may be more quantitative. For QCD, the PV-regulated formulation by Paston *et al.* [35] could be a starting point. The analog of the dressed-electron problem does not exist, of course, and the minimum truncation that would include non-Abelian effects would be to include at least two gluons. The smallest calculation would then be in the glueball sector. In the meson sector, the minimum truncation would be a quark-antiquark pair plus two gluons, which as a four-body problem would require discretization techniques beyond what are discussed here, since the coupled integral equations for the wave functions cannot be analytically reduced to a single Fock sector. Instead, one would discretize the coupled integral equations directly, in analogy with the original method of DLCQ [14], and diagonalize a very large but very sparse matrix. As an intermediate step, one can select a less ambitious yet very interesting challenge of modeling the meson sector with effective interactions, particularly with an interaction to break chiral symmetry [36].

Appendix A

CHARGE RENORMALIZATION

That the wave function renormalization constant Z_2 is equal to the vertex renormalization Z_1, order by order in covariant perturbation theory, is a consequence of the Ward identity [53]. As discussed in [49] and [45], this equality holds true more generally for nonperturbative bound-state calculations. However, a Fock-space truncation can have the effect of destroying covariance of the electromagnetic current, so that some components of the current require renormalization despite the absence of vacuum polarization. In the particular case here, only couplings to the plus component are not renormalized. The lack of fermion-antifermion vertices destroys covariance.

To show that $Z_1 = Z_2$ holds for the plus component, we repeat the discussion in [45]. Define a bare state $|\psi\rangle_{\rm bare}$ of the electron as a Fock-state expansion in which the one-electron state has amplitude 1. It is then related to the physical electron state by

$$|\psi\rangle_{\rm phys} = \sqrt{Z_2}|\psi\rangle_{\rm bare}. \tag{A.1}$$

The normalization of the physical state $\langle\psi(p')|\psi(p)\rangle_{\rm phys} = \delta(\underline{p}' - \underline{p})$ implies

$$\langle\psi(p')|\psi(p)\rangle_{\rm bare} = Z_2^{-1}\delta(\underline{p}' - \underline{p}). \tag{A.2}$$

Matrix elements of the current J^μ define Z_1 by

$$\langle\psi(p)|J^\mu(0)|\psi(p)\rangle_{\rm bare} = Z_1^{-1}\bar{u}(p)\gamma^\mu u(p). \tag{A.3}$$

For the plus component, this matrix element can also be calculated as [50]

$$\langle\psi(p')|J^+(0)|\psi(p)\rangle_{\rm bare} = 2p^+ F_{1\rm bare}(-(p'-p)^2). \tag{A.4}$$

Because [46] $\bar{u}(p)\gamma^+u(p) = 2p^+$ and $F_{1\text{bare}}(0) = Z_2^{-1}$, we find that the matrix element $\langle\psi(p)|J^+(0)|\psi(p)\rangle_{\text{bare}}$ is equal to both $2p^+Z_2^{-1}$ and $2p^+Z_1^{-1}$, and therefore we have $Z_1 = Z_2$.

Appendix B

PERTURBATIVE EQUIVALENCE WITH COVARIANT THEORY

As a check, we discuss the comparison [45] of the result for the one-loop electron self-energy with the standard result from covariant Feynman theory. This is done indirectly, by first comparing with the infinite-momentum-frame result of Brodsky, Roskies, and Suaya [49], which they show to be consistent with Feynman theory.

In our formulation, the perturbative one-loop electron self-energy can be read from Eq. (4.7) for $i = 0$, with $z_1 = 0$, $M^2 = m_0^2 + \delta m^2$ on the left, and $M^2 = m_0^2$ on the right. This yields

$$\delta m^2 = 2e^2 \left[m_0^2 \bar{I}_0(m_0^2) - 4m_0 \bar{I}_1(m_0^2) + \bar{J}(m_0^2) \right]. \tag{B.1}$$

When $\delta m = \delta m^2/2m_0$ is written explicitly in terms of $\alpha = e^2/4\pi$ and the integrals (4.8) and (4.9), we have

$$\delta m = \frac{\alpha}{4\pi} \sum_{jl} (-1)^{j+l} \frac{\xi_l}{m_0} \int \frac{dy}{y} \frac{d^2k_\perp}{\pi} \frac{m_0^2 - \frac{4m_0 m_j}{1-y} + \frac{m_j^2 + k_\perp^2}{(1-y)^2}}{m_0^2 - \frac{m_0^2 + k_\perp^2}{1-y} - \frac{\mu_l^2 + k_\perp^2}{y}}. \tag{B.2}$$

To compare with [49], where the self-energy is regulated with only one PV photon, we restrict the sum over l to two terms, $l = 0$ and $l = 1$. In this case, the $j = 0$ term matches the form of δm_a in Eq. (3.40) of [49], which we quote here

$$\begin{aligned} \delta m_a &= \frac{e^2}{16\pi^2 m_0} \int d^2k_\perp \int \frac{dx}{1-x} \left[\frac{m_0^2(2-2x-x^2) - k_\perp^2}{\lambda^2(1-x) + k_\perp^2 + m_0^2 x^2} \right. \\ &\qquad \left. - \frac{m_0^2(2-2x-x^2) - k_\perp^2}{\Lambda^2(1-x) + k_\perp^2 + m_0^2 x^2} \right]. \end{aligned} \tag{B.3}$$

The $j = 0$ term of (B.2) takes this form after setting $y = 1 - x$, $\mu_0 = \lambda$, and $\mu_1 = \Lambda$, and making some algebraic rearrangements.

Also, the $j = 1$ term reduces to δm_b in Eq. (3.41) of [49] in the limit $m_1 \to \infty$. In general, it is in this limit that the instantaneous fermion contributions return to the theory, and the source of δm_b is just this type of graph. Here we do not take this limit, and the $j = 1$ term remains as written and yields a different form for δm_b. However, if Brodsky *et al.* [49] had used our regularization, they would also obtain this different form.

Thus, our regularization produces a one-loop self-energy correction which is consistent with [49] when the same regularization is used, namely one PV electron and two PV photons, since the subtractions of contributions from the PV particles have exactly the same forms. This, in turn, is consistent with the Feynman result.

Appendix C

PROOF OF AN INTEGRAL IDENTITY

The integrals $\bar{I}_0$ and $\bar{J}$ satisfy the identity $\bar{J}(M^2) = M^2\bar{I}_0(M^2)$. This can be shown [45] in the following steps.

We write the integrals in terms of their individual Fock-sector contributions as

$$\begin{aligned} \bar{I}_0 &= -\frac{1}{16\pi^2}\sum_{jl}(-1)^{j+l}\xi_l I_{0jl}, \\ \bar{J} &= -\frac{1}{16\pi^2}\sum_{jl}(-1)^{j+l}\xi_l J_{jl}, \end{aligned} \tag{C.1}$$

with

$$\begin{aligned} I_{0jl} &\equiv \int \frac{dydk_\perp^2}{y}\frac{1}{\frac{m_j^2+k_\perp^2}{1-y}+\frac{\mu_l^2+k_\perp^2}{y}-M^2}, \\ J_{jl} &\equiv \int \frac{dydk_\perp^2}{y(1-y)^2}\frac{m_j^2+k_\perp^2}{\frac{m_j^2+k_\perp^2}{1-y}+\frac{\mu_l^2+k_\perp^2}{y}-M^2}. \end{aligned} \tag{C.2}$$

For the J integral, we replace y with a new variable x defined by

$$x = (1-y)\frac{\mu_l^2+k_\perp^2}{m_j^2 y+\mu_l^2(1-y)+k_\perp^2}. \tag{C.3}$$

It also ranges between 0 and 1, though in the reverse order, and has the remarkable property that

$$\frac{m_j^2+k_\perp^2}{1-y}+\frac{\mu_l^2+k_\perp^2}{y} = \frac{m_j^2+k_\perp^2}{1-x}+\frac{\mu_l^2+k_\perp^2}{x}, \tag{C.4}$$

even though x and y are clearly not equal and are not even linearly related. With this change of variable, the J integral becomes

$$J_{jl} = \int \frac{dxdk_\perp^2}{x} \frac{m_j^2 x + \mu_l^2(1-x) + k_\perp^2}{x(1-x)} \frac{1}{\frac{m_j^2+k_\perp^2}{1-x} + \frac{\mu_l^2+k_\perp^2}{x} - M^2}. \tag{C.5}$$

The middle factor can be written as

$$\frac{m_j^2 x + \mu_l^2(1-x) + k_\perp^2}{x(1-x)} = \frac{m_j^2 + k_\perp^2}{1-x} + \frac{\mu_l^2 + k_\perp^2}{x} - M^2 + M^2, \tag{C.6}$$

so that the J integral becomes

$$J_{jl} = \int \frac{dxdk_\perp^2}{x} + \int \frac{dxdk_\perp^2}{x} \frac{M^2}{\frac{m_j^2+k_\perp^2}{1-x} + \frac{\mu_l^2+k_\perp^2}{x} - M^2}. \tag{C.7}$$

This result shows that J_{jl} is just $M^2 I_{0jl}$ plus an (infinite) constant. Since the constant cancels in the sum over PV particles, we have the desired identity of $\bar{J} = M^2 \bar{I}_0$.

Appendix D

DISCRETIZATIONS AND QUADRATURES

The integral equations involve integration over the longitudinal momentum fraction and the square of the transverse momentum. The normalization, anomalous moment, and self-energy contributions also require integrals of this form. In each case there can be a line of poles $q^2_{\rm pole}$ in the integrand for a range of values of the longitudinal momentum fraction y. The location of the line is determined by the energy denominator that appears in each integrand. For simple poles, the transverse momentum integral is defined as the principal value. For those values of longitudinal momentum y for which the pole exists, the $q^2_\perp$ integration is subdivided into two parts, one from zero to $2q^2_{\rm pole}$ and the other from there to infinity. If the pole does not exist, transverse integration is not subdivided. When self-energy effects are included, the location of the pole, if it still exists, must be found by solving a nonlinear equation numerically, as discussed in Appendix E.

For the interval that contains a simple pole, the integral is approximated by an open Newton–Cotes formula that uses a few equally-spaced points placed symmetrically about the pole at $q^2_i = (2i-1)q^2_{\rm pole}/N$ with $i = 1, \ldots, N$ and N even. This particular Newton–Cotes formula uses a rectangular approximation to the integrand, with the height equal to the integrand value at the midpoint of an interval of width $2q^2_{\rm pole}/N$. An integral is then approximated by

$$\int_0^{2q^2_{\rm pole}} dq^2_\perp f(q^2_\perp) \simeq \frac{2q^2_{\rm pole}}{N} \sum_{i=1}^{N} f(q^2_i). \tag{D.1}$$

The equally spaced points provide an approximation to the principal value.

This form avoids use of $q_\perp^2 = 0$ as a quadrature point. Such a choice is important for evaluating terms with two-photon kernels, where there is another pole associated with the three-particle energy denominator. By keeping $q_\perp^2$ nonzero, this pole can be handled analytically as a principal value in the angular integration.

For the infinite intervals, $q_\perp^2$ is mapped to a new variable v by the transformation

$$q_\perp^2 = a^2 \frac{1 - (b^2/a^2)^v}{(b^2/a^2)^{v-1} - 1}, \tag{D.2}$$

with v in the range 0 to 1. (If the pole exists, this transformation is shifted by $2q_{\text{pole}}^2$.) The PV contributions make the integrals finite; therefore, no transverse cutoff is needed. Only the positive Gauss–Legendre quadrature points of an even order $2N_\perp$ are used for v between -1 and 1, so that $v = 0$, and therefore $q'_\perp = 0$ (or $2q_{\text{pole}}^2$), is never a quadrature point. The points in the negative half of the range, which would be used for representing $q_\perp^2 \in [-\infty, 0]$, are discarded. One could map $q_\perp^2 \in [0, \infty]$ to $[-1, 1]$ and not discard any part of the Gauss–Legendre range; however, the quadrature would then place points focused on some finite $q_\perp^2$ value, rather than on the natural integrand peak at $q_\perp^2 = 0$. The total number of quadrature points in the transverse direction is $N_\perp + N$, with $N = 0$ when there is no pole and $N_\perp$ typically of order 20.

This transformation was used in [8] and was selected to obtain an exact result for the integral $\int [1/(a^2 + q^2) - 1/(b^2 + q^2)] dq^2$. In the present work, the scales a^2 and b^2 are chosen to be the smallest and largest scales in the problem, i.e. $a^2 = |q_{\text{pole}}^2|$ and $b^2 = m_1^2 y + \mu_1^2(1 - y) - M^2 y(1 - y)$. Here q_{pole}^2 is the location of the root of the nonlinear equation for the pole. If q_{pole}^2 is negative, a pole does not exist; however, $|q_{\text{pole}}^2|$ is still a natural scale for the integrand.

For the normalization and anomalous moment integrals, the transverse quadrature scheme is based on a different transformation

$$q_\perp^2 = a^2 \frac{v}{1-v}, \tag{D.3}$$

where, again, if the pole exists, the transformation is shifted by $2q_{\rm pole}^2$. Cubic-spline interpolation, discussed in Appendix G, is then used to compute the values of the wave functions at the new quadrature points. This transformation is selected to yield an exact result for the integral of $1/(a^2+q^2)^2$, which is the form of the dominant contribution to the normalization and anomalous moment.

The longitudinal integration is subdivided into three parts when the line of poles is present. Two parts are symmetrically placed about the logarithmic singularity at $y_{\rm pole}$ that arises where the line of poles reaches $q_\perp^2 = 0$. When self-energy effects are not included in the energy denominator, this occurs at $y_{\rm pole} = 1 - m_0^2/M^2$; when self-energy effects are present, the location must be found by solving a nonlinear equation. The third part of the integration covers the remainder of the unit interval. Specifically, these intervals are $[0, y_{\rm pole}]$, $[y_{\rm pole}, 2y_{\rm pole}]$, and $[2y_{\rm pole}, 1]$. This structure is designed to maintain a left-right symmetry around the logarithmic singularity, because in the normalization and anomalous moment integrals (which use the same longitudinal quadrature points) the singularity becomes a simple pole defined by a principal-value prescription. The left-right symmetry then assures the necessary cancellations from opposite sides of the pole. When no pole is present, the longitudinal integration is not subdivided.

The intervals are each mapped linearly to $\tilde{y} \in [0,1]$ and then altered by the transformations [8]

$$\tilde{y}(t) = t^3(1+dt)/[1+d-(3+4d)t+(3+6d)t^2-4dt^3+2dt^4] \tag{D.4}$$

and

$$t(u) = (u+1)/2. \tag{D.5}$$

The new variable u ranges between -1 and 1, and standard Gauss–Legendre quadrature is applied. The transformation from $\tilde{y}$ to t is constructed to concentrate many points near the end-points of each interval, where integrands are rapidly varying. The parameter d is chosen such that $\tilde{y} \simeq 0.01t^3$ for small t. The transformation was found empirically [8], beginning with a transformation constructed to compute the integral $\int_0^1 [\ln(y+\epsilon_0) - \ln(y+\epsilon_1)]dy$ exactly, with ϵ_0 and ϵ_1 small. The symmetry with respect to the replacements $t \to (1-t)$ and $\tilde{y} \to (1-\tilde{y})$ is not necessary but is the simplest choice for restricting the coefficients in the denominator of (D.4).

The need for a concentration of longitudinal quadrature points near 0 and 1 is particularly true for the integral $\bar{J}$, defined in (4.9). Although this integral can be done analytically for the case of the one-photon truncation discussed in Chap. 4, the integral is only implicit in the integral equations for the two-body wave functions discussed in Chap. 6 and must therefore be well represented by any discretization of the integral equations. After the transverse integration is performed, the integrand is sharply peaked near $y = 0$ and $y = 1$, at distances of order $m_0/m_1 \sim 10^{-10}$ from these end-points, and needs to be sampled on both sides of the peaks.

The number of points in each of the three intervals is denoted by K, which becomes the measure of the resolution analogous to the harmonic resolution of DLCQ [26]. Thus the total number of quadrature points in the longitudinal direction is $3K$, with K typically of order 20.

For those longitudinal integrals with an upper limit less than 1, the integrand is transformed as above and given a value of zero for the points beyond the original integration range.

For the normalization and anomalous moment integrals, the pole in the transverse integral (when it exists) is a double pole, defined by the limit [7]

$$\begin{aligned}
&\int dy\, dq_\perp^2\, \frac{f(y,q_\perp^2)}{[m^2y+\mu_0^2(1-y)-M^2y(1-y)+q_\perp^2]^2} \\
&\equiv \lim_{\epsilon\to 0}\frac{1}{2}\epsilon\int dy\int dq_\perp^2 f(y,k_\perp^2)\Bigg[\frac{1}{[m^2y+\mu_0^2(1-y)-M^2y(1-y)+q_\perp^2-\epsilon]} \\
&-\frac{1}{[m^2y+\mu_0^2(1-y)-M^2y(1-y)+q_\perp^2+\epsilon]}\Bigg].
\end{aligned} \tag{D.6}$$

The simple poles that remain are prescribed as principal values. Of course, the limit must be taken after the integral is performed.

This limiting process is taken into account numerically by using a quadrature formula that is specific to this double-pole form. On the interval $[0, 2q_{\rm pole}^2]$, the quadrature points are chosen to be the same as those used for the integral equations, which are $q_i^2 = (2i-1)q_{\rm pole}^2/N$ with $i = 1,\ldots,N$, as given above. The interval is divided into $N/2$ subintervals $[\frac{4m}{N}q_{\rm pole}^2, \frac{4(m+1)}{N}q_{\rm pole}^2]$, with $m = 0, 1, \ldots, (N-2)/2$, each containing two of the quadrature points. The quadrature formula for such a subinterval is taken to be

$$\int_{\frac{4m}{N}q_{\rm pole}^2}^{\frac{4(m+1)}{N}q_{\rm pole}^2} dq_\perp^2\frac{f(q_\perp^2)}{(q_\perp^2-q_{\rm pole}^2)^2} \simeq w_{2m+1}f(\frac{(4m+1)}{N}q_{\rm pole}^2)+w_{2m+2}f(\frac{(4m+3)}{N}q_{\rm pole}^2), \tag{D.7}$$

where the integral on the left is *defined* by the limit formula in (D.6) when the pole is in the subinterval. The weights w_i are chosen to make the formula exact for $f = 1$ and $f = q_\perp^2$ on each individual $q_\perp^2$ subinterval. For these numerator functions, the limit in (D.6) can be taken explicitly. The weights are then found to be $w_{N/2} = w_{N/2+1} = -N/2q_{\rm pole}^2$, for the quadrature points on either side of the pole. For all other points, the weights are given by

$$
\begin{aligned}
w_{2m+1} &= -\frac{N}{2q_{\rm pole}^2}\left[\ln\left|\frac{4m+4-N}{4m-N}\right| + \frac{4(N-4m-3)}{(4m-N)(4m+4-N)}\right], \qquad \text{(D.8)}\\
w_{2m+2} &= \frac{N}{2q_{\rm pole}^2}\left[\ln\left|\frac{4m+4-N}{4m-N}\right| + \frac{4(N-4m-1)}{(4m-N)(4m+4-N)}\right].
\end{aligned}
$$

The integral from 0 to $2q_{\rm pole}^2$ is obtained by summing over the individual subintervals.

For the self-energy contribution (5.12), which is expressed in terms of the integrals $\bar{I}_0$, $\bar{I}_1$, and $\bar{J} = M^2\bar{I}_0$ given in (4.8) and (4.9), the transverse integral is done analytically. Only the longitudinal integral is done numerically, by the scheme discussed above with resolution $K = 30$.

Appendix E

SOLUTION OF NONLINEAR EQUATIONS

The renormalization condition that determines the bare mass m_0 is the requirement that the eigenvalue of the matrix be consistent with the physical value of α. This can be stated as a nonlinear equation of the form $g(m_0) = 0$. Of course, calculation of the function g is quite complicated, since it involves construction of the Hamiltonian matrix for the given value of m_0 and many iterations of the Lanczos algorithm to determine the eigenvalue. Nevertheless, the process does define a function for which the root can be sought.

Another nonlinear problem that also requires solution is location of the poles in the two-body wave function when the self-energy contribution is included. The corresponding functions g are simpler to compute in this case, but the idea is the same. The nonlinear problem is formulated as $g(x) = 0$, and we need to find a root of g.

The algorithm used for this root finding is the iterative Müller algorithm [51]. The iterations begin with two guesses for the solution, x_0 and x_1; the root need not be between them. The function values $g_i = g(x_i)$ are computed at these points, and a third guess x_2 is computed from the interpolation

$$x_2 = x_1 - g_1(x_1 - x_0)/(g_1 - g_0). \tag{E.1}$$

With the function value $g_2 = g(x_2)$ computed also for this guess, the iteration can begin.

The next guess is computed from a quadratic fit of $ax^2 + bx + c$ to the three most recent points. The coefficients of the fit are

$$
\begin{aligned}
a &= \frac{(x_{n-1}-x_n)(g_{n-2}-g_n)-(x_{n-2}-x_n)(g_{n-1}-g_n)}{(x_{n-2}-x_{n-1})(x_{n-2}-x_n)(x_{n-1}-x_n)}, \\
b &= \frac{(g_{n-1}-g_n)(x_{n-2}-x_n)^2-(g_{n-2}-g_n)(x_{n-1}-x_n)^2}{(x_{n-2}-x_{n-1})(x_{n-2}-x_n)(x_{n-1}-x_n)}, \\
c &= g_n,
\end{aligned}
\tag{E.2}
$$

and the next guess is given by

$$
x_{n+1} = x_n + \Delta x, \tag{E.3}
$$

where

$$
\Delta x = -\frac{2\mathrm{sgn}(b)c}{|b|+\sqrt{d}} \tag{E.4}
$$

and

$$
d = \max(b^2 - 4ac, 0). \tag{E.5}
$$

The function value $g_{n+1} = g(x_{n+1})$ is then computed, to be ready for the next iteration. The iterations are terminated when g_{n+1} and Δx are less than chosen tolerances.

Appendix F

MATRIX DIAGONALIZATION

The quadrature schemes discussed in Appendix D convert the integral equations into a large matrix eigenvalue problem. Because the original coupled integral equations have been reduced to the two-particle Fock sector, the matrix is not particularly sparse. However, the size of the matrix makes ordinary diagonalization methods impractical; there can also be stability issues, as found in recent work on Yukawa theory [8].

The alternative to more standard methods is an iterative method, such as the Lanczos algorithm [9, 10], which requires only matrix multiplication rather than extensive transformation of the matrix. The basic Lanczos algorithm does not apply here, because the negative metric of the PV fields cause the matrix to be not Hermitian, but a modified form of the algorithm, developed for Yukawa theory [4], can be extended to the present case.

The matrix *is* self-adjoint with respect to an indefinite norm [54]. Let η be the matrix that represents the structure of the norm, so that numerical dot products are written $\vec{\phi}'^{*} \cdot \eta\vec{\phi}$. In [4] η was a diagonal matrix determined by the metric signatures; here it again depends on the metric signatures but also has off-diagonal terms that take into account the mixing of the longitudinal helicity components and of the fermion flavors. It is symmetric, real, and block diagonal, with the blocks determined by the definition of $\eta_{j',\alpha\beta}$ in (6.20) and by the quadrature weights associated with the integrals in (6.21). The matrix $H = J\eta$ that defines the discrete form of the eigenvalue problem (6.21) is constructed to be self-adjoint with respect to this norm:

$$\eta^{-1}H^\dagger\eta = \eta^{-1}(J\eta)^\dagger\eta = \eta^{-1}\eta J\eta = J\eta = H. \tag{F.1}$$

Given such a self-adjoint matrix, a Lanczos algorithm for its diagonalization is [4]

$$\begin{aligned} \alpha_j &= \nu_j\vec{q}_j^{\,*}\cdot\eta H\vec{q}_j\,,\ \ \vec{r}_j = H\vec{q}_j - \gamma_{j-1}\vec{q}_{j-1} - \alpha_j\vec{q}_j\,,\ \ \beta_j = +\sqrt{|\vec{r}_j^{\,*}\cdot\eta\vec{r}_j|}\,, \\ \vec{q}_{j+1} &= \vec{r}_j/\beta_j\,,\ \ \nu_{j+1} = \mathrm{sgn}(\vec{r}_j^{\,*}\cdot\eta\vec{r}_j)\,,\ \ \nu_1 = \mathrm{sgn}(\vec{q}_1^{\,*}\cdot\eta\vec{q}_1)\,,\ \ \gamma_j = \nu_{j+1}\nu_j\beta_j. \end{aligned} \tag{F.2}$$

The vector $\vec{q}_1$ is the (normalized) initial guess and γ_0 is defined to be zero. This algorithm produces a real tridiagonal matrix

$$H \to T \equiv \begin{pmatrix} \alpha_1 & \beta_1 & 0 & 0 & 0 & \dots \\ \gamma_1 & \alpha_2 & \beta_2 & 0 & 0 & \dots \\ 0 & \gamma_2 & \alpha_3 & \beta_3 & 0 & \dots \\ 0 & 0 & \gamma_3 & . & . & \dots \\ 0 & 0 & 0 & . & . & \dots \\ . & . & . & . & . & \dots \end{pmatrix}. \tag{F.3}$$

It represents H with respect to the basis $\{\vec{q}_j\}$ and can be easily diagonalized by standard means; the Lapack routine DGEEV is used.

This new matrix is self-adjoint with respect to an induced metric ν, which is a diagonal matrix with elements $\nu_1, \nu_2, \dots$. The extreme eigenvalues are good approximations to those of H, and the approximate associated eigenvectors of H are constructed from the right eigenvectors $\vec{c}_i$ of T as $\vec{\phi}_i = \sum_k (c_i)_k\vec{q}_k$, with $(c_i)_k$ the kth component of $\vec{c}_i$.

Some of the eigenvalues of T can be spurious, due to round-off error. These can be detected [10] by comparing the eigenvalues of the matrix obtained from T by deleting the first row and first column. Any eigenvalue that appears in both lists is spurious.

The desired eigenvalue is chosen from the eigenvalues of T as the largest real negative eigenvalue that is not spurious. The value of α is proportional to the negative reciprocal of this eigenvalue and is then the smallest such, so that the eigenstate is the lowest state associated with this value of the coupling.

Convergence is monitored by measuring directly the convergence of the desired eigenvalue and by checking an estimate of the error in the eigenvalue, given by [10] $|\beta_n(c_i)_n|$, where n is the number of Lanczos iterations and i is the index of the desired eigenvalue of T. If the error estimate begins to grow, the iterations are restarted from the last best approximation to the eigenvector.

The initial vector is chosen to be the solution to the problem with only self-energy effects included. The Lanczos algorithm is then run twice; once for the eigenvalue without saving the intermediate vectors and a second time for the eigenvector, accumulating this vector as the iterations proceed. This double iteration approach eliminates the need to store the intermediate Lanczos vectors, which saves considerable space and disk access time.

Appendix G

INTERPOLATION AND DIFFERENTIATION

The computation of the anomalous moment requires differentiation of the wave functions with respect to transverse momentum. Since the wave functions are known only at the discrete quadrature points, the differentiation must be done numerically. Standard finite difference approximations for the derivative work best with equally spaced points, which is not the case here. Instead, we use cubic-spline interpolation [51] to obtain a smooth approximation to the wave function, and then differentiate the spline. The spline is also used to interpolate the wave functions themselves, in order to use quadrature points in the transverse direction for the anomalous moment calculation that are different from the points used to solve the integral equations.

To optimize the interpolation, the spline is fit to functions obtained from the wave functions rather than to the wave functions directly. The primary dependence on the transverse momentum $q_\perp$ is through the standard denominator factor $A_{0j}A_{1j} + B_j^2$, with A_{ij} and B_j defined in (5.6) and (5.7). Therefore, we multiply by this factor to remove this nonpolynomial dependence. In addition, if the wave function is for a Fock-state component where the constituent fermion has a spin opposite that of the dressed electron, the wave function is divided by $q_\perp$. This is to remove a factor $(q_x \pm iq_y) = q_\perp e^{\pm i\phi}$ associated with orbital angular momentum. The remaining functions depend on $q_\perp^2$ and are readily fit by polynomials in $q_\perp^2$. For the one-photon truncation, the new functions are independent of $q_\perp^2$; in general, there will be some $q_\perp^2$ dependence, of order α.

On the interval $[q_j^2, q_{j+1}^2]$, a cubic spline s_j takes the form $s_j = a_j + b_j(q^2 - q_j^2) + c_j(q^2 - q_j^2)^2 + d_j(q^2 - q_j^2)^3$. The coefficients are determined by requiring continuity of the s_j and their first two derivatives at the endpoints of the intervals. For the first and last points we assume that the second derivative is zero. One can then solve for the coefficients in terms of the values of the approximated function $f(q^2)$

$$\begin{aligned} a_j &= f(q_j^2), \\ b_j &= \frac{a_{j+1} - a_j}{h_j} - \frac{h_j}{3}(2c_j + c_{j+1}), \\ d_j &= (c_{j+1} - c_j)/(3h_j), \end{aligned} \tag{G.1}$$

with $h_j \equiv q_{j+1}^2 - q_j^2$ and c_j determined by a tridiagonal linear system

$$h_{j-1}c_{j-1} + 2(h_j + h_{j+1})c_j + h_j c_{j+1} = \frac{3}{h_j}(a_{j+1} - a_j) - \frac{3}{h_{j-l}}(a_j - a_{j-1}). \tag{G.2}$$

Here $c_0 = 0$, $c_n = 0$, and $j = 1, \ldots, n-1$.

The tridiagonal system is efficiently solved by Crout reduction [51], which involves factorization of the original matrix into a product of lower and upper triangular matrices. Since the matrix depends only on the spacing of the quadrature points, the factorization can be done once and then used several times for approximating different functions; the values of the approximated functions appear only on the right-hand side of the system.

For a matrix of the form

$$\begin{pmatrix} \alpha_1 & \beta_1 & 0 & 0 & 0 & \dots \\ \gamma_2 & \alpha_2 & \beta_2 & 0 & 0 & \dots \\ 0 & \gamma_3 & \alpha_3 & \beta_3 & 0 & \dots \\ 0 & 0 & . & . & . & \dots \\ 0 & 0 & 0 & . & . & \dots \\ . & . & . & . & . & \dots \end{pmatrix} \tag{G.3}$$

the factorization is

$$l_1 = \alpha_1, \;\; u_i = \beta_i / l_i, \;\; l_{i+1} = a_{i+1} - c_{i+1} u_i. \tag{G.4}$$

Write the right-hand side of the linear system as $(\delta_1, \delta_2, ..., \delta_{n-1})^T$, where the superscript T denotes the transpose. Then the solution $(c_1, c_2, \dots, c_{n-1})^T$ of the system is obtained from

$$\begin{aligned} z_1 &= \delta_1/l_1; \;\; z_i = (\delta_i - \gamma_i z_{i-1})/l_i, \;\; i = 2, \dots, n-1 \\ c_{n-1} &= z_{n-1}; \;\; c_i = z_i - u_i c_{i+1}, \;\; i = n-2, \dots, 1. \end{aligned} \tag{G.5}$$

The derivative of the function f at the point q_j^2 is then approximated by $s_j'(q_j^2) = b_j$.

Appendix H

TWO-PHOTON KERNELS

The two-photon contributions to the integral equation (6.7) for the two-particle wave function are represented by kernels that arise from the elimination of intermediate states with two photons. To keep the expressions compact, we write the kernel functions as

$$J^{(2)\mu\nu}_{ijs,i'j's'}(y,q_\perp;y',q'_\perp) = -\sum_a (-1)^{i'+j'+a}\frac{\sqrt{\xi_j\xi_{j'}}}{\sqrt{yy'}}\theta(1-y-y')J_2(\mu,\nu;s,s'), \qquad \text{(H.1)}$$

with the momentum arguments and most indices suppressed. The kernels are then determined by the following expressions, where the angular integrals $\mathcal{I}_n$ are defined in Eq. (6.6). As discussed in Appendix I, the integrals $\mathcal{I}_n$ are independent of the sign of n and only nonnegative values appear here. For some kernels, where there is division by $(1-y-y')^2$, some care is needed in the evaluation, and alternate forms to take this into account are listed at the end of this Appendix, beginning with Eq. (H.69).

The basic expressions for the kernel functions are

$$J_2(+,+,+\frac{1}{2},+\frac{1}{2}) = \mathcal{I}_0, \qquad \text{(H.2)}$$

$$J_2(+,-,+\frac{1}{2},+\frac{1}{2}) = \frac{(q_\perp^2+m_am_i)\mathcal{I}_0 + q_\perp q'_\perp\mathcal{I}_1}{(1-y)(1-y-y')}, \qquad \text{(H.3)}$$

$$J_2(+,(+),+\frac{1}{2},+\frac{1}{2}) = -\frac{q_\perp\mathcal{I}_1}{1-y}, \qquad \text{(H.4)}$$

$$J_2(+,(-),+\frac{1}{2},+\frac{1}{2}) = -\frac{q'_\perp\mathcal{I}_0 + q_\perp\mathcal{I}_1}{1-y-y'}, \qquad \text{(H.5)}$$

$$J_2(-,+,+\frac{1}{2},+\frac{1}{2}) = \frac{(q_\perp'^2 + m_a m_{i'})\mathcal{I}_0 + q_\perp q_\perp' \mathcal{I}_1}{(1-y')(1-y-y')}, \tag{H.6}$$

$$\begin{aligned} J_2(-,-,+\frac{1}{2},+\frac{1}{2}) &= -[(1-y)(1-y')(1-y-y')^2]^{-1} \\ &\times \left[(q_\perp^2 q_\perp'^2 + m_a^2 m_i m_{i'} + q_\perp^2 m_i m_{i'} + q_\perp'^2 m_i m_{i'})\mathcal{I}_0\right. \\ &\left.+(q_\perp^3 q_\perp' + q_\perp q_\perp'^3 + q_\perp q_\perp' m_a^2 + 2q_\perp q_\perp' m_i m_{i'})\mathcal{I}_1 + q_\perp^2 q_\perp'^2 \mathcal{I}_2\right], \end{aligned} \tag{H.7}$$

$$J_2(-,(+),+\frac{1}{2},+\frac{1}{2}) = -\frac{(q_\perp q_\perp'^2 + q_\perp m_a m_{i'})\mathcal{I}_1 + q_\perp^2 q_\perp' \mathcal{I}_2}{(1-y')(1-y)(1-y-y')}, \tag{H.8}$$

$$\begin{aligned} J_2(-,(-),+\frac{1}{2},+\frac{1}{2}) &= -[(1-y)(1-y')(1-y-y')^2]^{-1} \\ &\times \left[(q_\perp^2 q_\perp' y + q_\perp'^3 y - q_\perp^2 q_\perp' - q_\perp'^3 - q_\perp' m_a^2 + q_\perp' y m_a^2 + q_\perp' m_a m_i - q_\perp' y m_a m_i\right. \\ &- q_\perp' y' m_a m_i - q_\perp' m_i m_{i'} + q_\perp' y m_i m_{i'} + q_\perp' y' m_i m_{i'})\mathcal{I}_0 \\ &\left.+(2q_\perp q_\perp'^2 y - 2q_\perp q_\perp'^2 - q_\perp m_i m_{i'} + + q_\perp y m_i m_{i'} + q_\perp y' m_i m_{i'})\mathcal{I}_1\right], \end{aligned} \tag{H.9}$$

$$J_2((+),+,+\frac{1}{2},+\frac{1}{2}) = -\frac{q_\perp' \mathcal{I}_1}{1-y'}, \tag{H.10}$$

$$J_2((+),-,+\frac{1}{2},+\frac{1}{2}) = -\frac{(q_\perp^2 q_\perp' + q_\perp' m_a m_i)\mathcal{I}_1 + q_\perp q_\perp'^2 \mathcal{I}_2}{(1-y')(1-y)(1-y-y')}, \tag{H.11}$$

$$J_2((+),(+),+\frac{1}{2},+\frac{1}{2}) = \frac{q_\perp q_\perp' \mathcal{I}_2}{(1-y)(1-y')}, \tag{H.12}$$

$$J_2((+),(-),+\frac{1}{2},+\frac{1}{2}) = \frac{q_\perp q_\perp' \mathcal{I}_0 + q_\perp'^2 \mathcal{I}_1}{(1-y')(1-y-y')}, \tag{H.13}$$

$$J_2((-),+,+\frac{1}{2},+\frac{1}{2}) = -\frac{q_\perp \mathcal{I}_0 + q'_\perp \mathcal{I}_1}{1-y-y'}, \tag{H.14}$$

$$\begin{aligned} J_2((-),-,+\frac{1}{2},+\frac{1}{2}) &= -[(1-y)(1-y')(1-y-y')^2]^{-1} \\ &\times \big[(q_\perp^3 y' + q_\perp q_\perp'^2 y' - q_\perp^3 - q_\perp q_\perp'^2 - q_\perp m_a^2 + q_\perp y' m_a^2 + q_\perp m_a m_{i'} - q_\perp y m_a m_{i'} \\ &\quad - q_\perp y' m_a m_{i'} - q_\perp m_i m_{i'} + q_\perp y m_i m_{i'} + q_\perp y' m_i m_{i'})\mathcal{I}_0 \\ &\quad + (2q_\perp^2 q'_\perp y' - 2q_\perp^2 q'_\perp - q'_\perp m_i m_{i'} + q'_\perp y m_i m_{i'} + q'_\perp y' m_i m_{i'})\mathcal{I}_1\big], \end{aligned} \tag{H.15}$$

$$J_2((-),(+),+\frac{1}{2},+\frac{1}{2}) = \frac{q_\perp q'_\perp \mathcal{I}_0 + q_\perp^2 \mathcal{I}_1}{(1-y)(1-y-y')}, \tag{H.16}$$

$$\begin{aligned} J_2((-),(-),+\frac{1}{2},+\frac{1}{2}) &= -[(1-y)(1-y')(1-y-y')^2]^{-1} \\ &\times [(q_\perp q'_\perp - q_\perp q'_\perp y - q_\perp q'_\perp y' q_\perp q'_\perp y y')\mathcal{I}_0 \\ &+ (q_\perp^2 + q_\perp'^2 - q_\perp^2 y - q_\perp'^2 y - q_\perp^2 y' - q_\perp'^2 y' + q_\perp^2 y y' + q_\perp'^2 y y' \\ &+ m_a^2 - y m_a^2 - y' m_a^2 + y y' m_a^2 - m_a m_i + y m_a m_i + 2y' m_a m_i \\ &- y y' m_a m_i - y'^2 m_a m_i - m_a m_{i'} + 2y m_a m_{i'} - y^2 m_a m_{i'} + y' m_a m_{i'} - y y' m_a m_{i'} \\ &+ m_i m_{i'} - 2y m_i m_{i'} + y^2 m_i m_{i'} - 2y' m_i m_{i'} + 2y y' m_i m_{i'} + y'^2 m_i m_{i'})\mathcal{I}_1 \\ &+ (q_\perp q'_\perp + q_\perp q'_\perp y y' - q_\perp q'_\perp y - q_\perp q'_\perp y')\mathcal{I}_2], \end{aligned} \tag{H.17}$$

$$J_2(+,+,-\frac{1}{2},-\frac{1}{2}) = \mathcal{I}_1, \tag{H.18}$$

$$J_2(+,-,-\frac{1}{2},-\frac{1}{2}) = \frac{q_\perp q'_\perp \mathcal{I}_0 + (q_\perp^2 + m_a m_i)\mathcal{I}_1}{(1-y)(1-y-y')}, \tag{H.19}$$

$$J_2(+,(+),-\frac{1}{2},-\frac{1}{2}) = -\frac{q'_\perp \mathcal{I}_1 + q_\perp \mathcal{I}_2}{1-y-y'}, \tag{H.20}$$

$$J_2(+,(-),-\frac{1}{2},-\frac{1}{2}) = -\frac{q_\perp \mathcal{I}_0}{1-y}, \tag{H.21}$$

$$J_2(-,+,-\frac{1}{2},-\frac{1}{2}) = \frac{q_\perp q'_\perp \mathcal{I}_0 + (q'^2_\perp + m_a m_{i'})\mathcal{I}_1}{(1-y')(1-y-y')}, \tag{H.22}$$

$$\begin{aligned} J_2(-,-,-\frac{1}{2},-\frac{1}{2}) = &-[(1-y)(1-y')(1-y-y')^2]^{-1} \\ &\times \big[(q^3_\perp q'_\perp + q_\perp q'^3_\perp + q_\perp q'_\perp m_a^2 + q_\perp q'_\perp m_i m_{i'})\mathcal{I}_0 \\ &+(2q^2_\perp q'^2_\perp + q^2_\perp m_i m_{i'} + q'^2_\perp m_i m_{i'} + m_a^2 m_i m_{i'})\mathcal{I}_1 \\ &+q_\perp q'_\perp m_i m_{i'} \mathcal{I}_2\big], \end{aligned} \tag{H.23}$$

$$\begin{aligned} J_2(-,(+),-\frac{1}{2},-\frac{1}{2}) = &-[(1-y)(1-y')(1-y-y')^2]^{-1} \\ &\times \big[(q_\perp q'^2_\perp y - q_\perp q'^2_\perp)\mathcal{I}_0 \\ &+(q^2_\perp q'_\perp y + q'^3_\perp y - q^2_\perp q'_\perp - q'^3_\perp - q'_\perp m_a^2 + q'_\perp y m_a^2 + q'_\perp m_a m_i \\ &-q'_\perp y m_a m_i - q'_\perp y' m_a m_i - q'_\perp m_i m_{i'} + q'_\perp y' m_i m_{i'} + q'_\perp y m_i m_{i'})\mathcal{I}_1 \\ &+(q_\perp q'^2_\perp y - q_\perp q'^2_\perp + q_\perp y m_i m_{i'} + q_\perp y' m_i m_{i'} - q_\perp m_i m_{i'})\mathcal{I}_2\big], \end{aligned} \tag{H.24}$$

$$J_2(-,(-),-\frac{1}{2},-\frac{1}{2}) = -\frac{(q_\perp q'^2_\perp + q_\perp m_a m_{i'})\mathcal{I}_0 + q^2_\perp q'_\perp \mathcal{I}_1}{(1-y')(1-y)(1-y-y')}, \tag{H.25}$$

$$J_2((+),+,-\frac{1}{2},-\frac{1}{2}) = -\frac{q_\perp \mathcal{I}_1 + q'_\perp \mathcal{I}_2}{1-y-y'}, \tag{H.26}$$

$$J_2((+),-,-\frac{1}{2},-\frac{1}{2}) = -[(1-y)(1-y')(1-y-y')^2]^{-1} \tag{H.27}$$
$$\times \big[(q_\perp^2 q'_\perp y' - q_\perp^2 q'_\perp)\mathcal{I}_0$$
$$+(q_\perp^3 y' + q_\perp q_\perp'^2 y' - q_\perp^3 - q_\perp q_\perp'^2 - q_\perp m_a^2 + q_\perp y' m_a^2 + q_\perp m_a m_{i'} - q_\perp y m_a m_{i'}$$
$$-q_\perp y' m_a m_{i'} - q_\perp m_i m_{i'} + q_\perp y m_i m_{i'} + q_\perp y' m_i m_{i'})\mathcal{I}_1$$
$$+(q_\perp^2 q'_\perp y' - q_\perp^2 q'_\perp - q'_\perp m_i m_{i'} + q'_\perp y m_i m_{i'} + q'_\perp y' m_i m_{i'})\mathcal{I}_2\big]\,,$$

$$J_2((+),(+),-\frac{1}{2},-\frac{1}{2}) = -[(1-y)(1-y')(1-y-y')^2]^{-1} \tag{H.28}$$
$$\times [(q_\perp q'_\perp - q_\perp q'_\perp y - q_\perp q'_\perp y' + q_\perp q'_\perp yy')\mathcal{I}_1$$
$$+(q_\perp^2 + q_\perp'^2 - q_\perp^2 y - q_\perp'^2 y - q_\perp^2 y' - q_\perp'^2 y' + q_\perp^2 yy' + q_\perp'^2 yy'$$
$$+m_a^2 - y m_a^2 - y' m_a^2 + yy' m_a^2 - m_a m_i + y m_a m_i + 2y' m_a m_i - yy' m_a m_i$$
$$-y'^2 m_a m_i - m_a m_{i'} + 2y m_a m_{i'} - y^2 m_a m_{i'} + y' m_a m_{i'} - yy' m_a m_{i'}$$
$$+m_i m_{i'} - 2y m_i m_{i'} + y^2 m_i m_{i'} - 2y' m_i m_{i'} + 2yy' m_i m_{i'} + y'^2 m_i m_{i'})\mathcal{I}_2$$
$$+q_\perp q'_\perp (1-y)(1-y')\mathcal{I}_3]\,,$$

$$J_2((+),(-),-\frac{1}{2},-\frac{1}{2}) = \frac{q_\perp^2 \mathcal{I}_0 + q_\perp q'_\perp \mathcal{I}_1}{(1-y)(1-y-y')}, \tag{H.29}$$

$$J_2((-),+,-\frac{1}{2},-\frac{1}{2}) = -\frac{q'_\perp \mathcal{I}_0}{1-y'}, \tag{H.30}$$

$$J_2((-),-,-\frac{1}{2},-\frac{1}{2}) = -\frac{(q_\perp^2 q'_\perp + q'_\perp m_a m_i)\mathcal{I}_0 + q_\perp q_\perp'^2 \mathcal{I}_1}{(1-y')(1-y)(1-y-y')}, \tag{H.31}$$

$$J_2((-),(+),-\frac{1}{2},-\frac{1}{2}) = \frac{q_\perp'^2\mathcal{I}_0 + q_\perp q_\perp'\mathcal{I}_1}{(1-y')(1-y-y')}, \tag{H.32}$$

$$J_2((-),(-),-\frac{1}{2},-\frac{1}{2}) = \frac{q_\perp q_\perp'\mathcal{I}_1}{(1-y)(1-y')}, \tag{H.33}$$

$$J_2(+,+,+\frac{1}{2},-\frac{1}{2}) = 0, \tag{H.34}$$

$$J_2(+,-,+\frac{1}{2},-\frac{1}{2}) = \frac{q_\perp' m_i\mathcal{I}_0 + (q_\perp m_i - q_\perp m_a)\mathcal{I}_1}{(1-y)(1-y-y')}, \tag{H.35}$$

$$J_2(+,(+),+\frac{1}{2},-\frac{1}{2}) = 0, \tag{H.36}$$

$$J_2(+,(-),+\frac{1}{2},-\frac{1}{2}) = -\frac{(-m_a + ym_a + m_i - ym_i - y'm_i)\mathcal{I}_0}{(1-y)(1-y-y')}, \tag{H.37}$$

$$J_2(-,+,+\frac{1}{2},-\frac{1}{2}) = \frac{(q_\perp' m_a - q_\perp' m_{i'})\mathcal{I}_0 - q_\perp m_{i'}\mathcal{I}_1}{(1-y')(1-y-y')}, \tag{H.38}$$

$$\begin{aligned} J_2(-,-,+\frac{1}{2},-\frac{1}{2}) = &-[(1-y)(1-y')(1-y-y')^2]^{-1} \\ &\times \big[(q_\perp^2 q_\perp' m_i + q_\perp'^3 m_i + q_\perp' m_a^2 m_i - q_\perp^2 q_\perp' m_{i'})\mathcal{I}_0 \\ &+(2q_\perp q_\perp'^2 m_i - q_\perp^3 m_{i'} - q_\perp q_\perp'^2 m_{i'} - q_\perp m_a^2 m_{i'})\mathcal{I}_1 \\ &-q_\perp^2 q_\perp' \mathcal{I}_2 m_{i'}\big], \end{aligned} \tag{H.39}$$

$$J_2(-,(+),+\frac{1}{2},-\frac{1}{2}) = -\frac{(q_\perp q_\perp' m_a - q_\perp q_\perp' m_{i'})\mathcal{I}_1 - q_\perp^2 m_{i'}\mathcal{I}_2}{(1-y')(1-y)(1-y-y')}, \tag{H.40}$$

$$J_2(-,(-),+\frac{1}{2},-\frac{1}{2}) = -[(1-y)(1-y')(1-y-y')^2]^{-1} \tag{H.41}$$
$$\times \left[(q_\perp'^2 y m_i - (q_\perp'^2 m_i) + q_\perp'^2 y' m_i + q_\perp^2 m_{i'} + q_\perp'^2 m_{i'} - q_\perp^2 y m_{i'} - q_\perp'^2 y m_{i'}\right.$$
$$+m_a^2 m_{i'} - y m_a^2 m_{i'} - m_a m_i m_{i'} + y m_a m_i m_{i'} + y' m_a m_i m_{i'})\mathcal{I}_0$$
$$\left.+(q_\perp q_\perp' y m_i - q_\perp q_\perp' m_i + q_\perp q_\perp' y' m_i + 2 q_\perp q_\perp' m_{i'} - 2 q_\perp q_\perp' y m_{i'})\mathcal{I}_1\right],$$

$$J_2((+),+,+\frac{1}{2},-\frac{1}{2}) = \frac{(-m_a + y' m_a + m_{i'} - y m_{i'} - y' m_{i'})\mathcal{I}_1}{(1-y')(1-y-y')}, \tag{H.42}$$

$$J_2((+),-,+\frac{1}{2},-\frac{1}{2}) = -[(1-y)(1-y')(1-y-y')^2]^{-1} \tag{H.43}$$
$$\times [(q_\perp q_\perp' y' m_i - q_\perp q_\perp' m_i)\mathcal{I}_0$$
$$+(q_\perp^2 y' m_i + q_\perp'^2 y' m_i - q_\perp^2 m_i - q_\perp'^2 m_i - m_a^2 m_i + y' m_a^2 m_i + q_\perp^2 m_{i'} - q_\perp^2 y m_{i'}$$
$$-q_\perp^2 y' m_{i'} + m_a m_i m_{i'} - y m_a m_i m_{i'} - y' m_a m_i m_{i'})\mathcal{I}_1$$
$$+(q_\perp q_\perp' y' m_i - q_\perp q_\perp' m_i + q_\perp q_\perp' m_{i'} - q_\perp q_\perp' y m_{i'} - q_\perp q_\perp' y' m_{i'})\mathcal{I}_2],$$

$$J_2((+),(+),+\frac{1}{2},-\frac{1}{2}) = -\frac{q_\perp(-m_a + y' m_a + m_{i'} - y m_{i'} - y' m_{i'})\mathcal{I}_2}{(1-y)(1-y')(1-y-y')}, \tag{H.44}$$

$$J_2((+),(-),+\frac{1}{2},-\frac{1}{2}) = -[(1-y)(1-y')(1-y-y')]^{-1} \tag{H.45}$$
$$\times [(q_\perp y' m_i - q_\perp m_i + q_\perp m_{i'} - q_\perp y m_{i'})\mathcal{I}_0$$
$$+(q_\perp' y' m_i - q_\perp' m_i + q_\perp' m_{i'} - q_\perp' y m_{i'})\mathcal{I}_1],$$

$$J_2((-),+,+\frac{1}{2},-\frac{1}{2}) = 0, \tag{H.46}$$

$$J_2((-),-,+\frac{1}{2},-\frac{1}{2}) = -\frac{(q_\perp q'_\perp m_i - q_\perp q'_\perp m_a)\mathcal{I}_0 + q'^2_\perp m_i \mathcal{I}_1}{(1-y')(1-y)(1-y-y')}, \tag{H.47}$$

$$J_2((-),(+),+\frac{1}{2},-\frac{1}{2}) = 0, \tag{H.48}$$

$$J_2((-),(-),+\frac{1}{2},-\frac{1}{2}) = -\frac{q'_\perp(m_a - y m_a - m_i + y m_i + y' m_i)\mathcal{I}_1}{(1-y)(1-y')(1-y-y')}, \tag{H.49}$$

$$J_2(+,+,-\frac{1}{2},+\frac{1}{2}) = 0, \tag{H.50}$$

$$J_2(+,-,-\frac{1}{2},+\frac{1}{2}) = \frac{(q_\perp m_a - q_\perp m_i)\mathcal{I}_0 - q'_\perp m_i \mathcal{I}_1}{(1-y)(1-y-y')}, \tag{H.51}$$

$$J_2(+,(+),-\frac{1}{2},+\frac{1}{2}) = \frac{(-m_a + y m_a + m_i - y m_i - y' m_i)\mathcal{I}_1}{(1-y)(1-y-y')}, \tag{H.52}$$

$$J_2(+,(-),-\frac{1}{2},+\frac{1}{2}) = 0, \tag{H.53}$$

$$J_2(-,+,-\frac{1}{2},+\frac{1}{2}) = \frac{q_\perp m_{i'}\mathcal{I}_0 + (q'_\perp m_{i'} - q'_\perp m_a)\mathcal{I}_1}{(1-y')(1-y-y')}, \tag{H.54}$$

$$\begin{aligned} J_2(-,-,-\frac{1}{2},+\frac{1}{2}) = &-[(1-y)(1-y')(1-y-y')^2]^{-1} \\ &\times \big[(q^3_\perp m_{i'} + q_\perp q'^2_\perp m_{i'} - q_\perp q'^2_\perp m_i + q_\perp m^2_a m_{i'})\mathcal{I}_0 \\ &+(2q^2_\perp q'_\perp m_{i'} - q^2_\perp q'_\perp m_i - q'^3_\perp m_i - q'_\perp m^2_a m_i)\mathcal{I}_1 \\ &-q_\perp q'^2_\perp m_i \mathcal{I}_2\big], \end{aligned} \tag{H.55}$$

$$J_2(-,(+),-\frac{1}{2},+\frac{1}{2}) = -[(1-y)(1-y')(1-y-y')^2]^{-1} \tag{H.56}$$
$$\times [(q_\perp q'_\perp y m_{i'} - q_\perp q'_\perp m_{i'})\mathcal{I}_0$$
$$+(q'^2_\perp m_i + -q'^2_\perp y m_i - q'^2_\perp y' m_i - q^2_\perp m_{i'} - q'^2_\perp m_{i'} + q^2_\perp y m_{i'} + q'^2_\perp y m_{i'}$$
$$-m_a^2 m_{i'} + y m_a^2 m_{i'} + m_a m_i m_{i'} - y m_a m_i m_{i'} - y' m_a m_i m_{i'})\mathcal{I}_1$$
$$+(q_\perp q'_\perp m_i - q_\perp q'_\perp y m_i - q_\perp q'_\perp y' m_i - q_\perp q'_\perp m_{i'} + q_\perp q'_\perp y m_{i'})\mathcal{I}_2]\,,$$

$$J_2(-,(-),-\frac{1}{2},+\frac{1}{2}) = -\frac{(q_\perp q'_\perp m_{i'} - q_\perp q'_\perp m_a)\mathcal{I}_0 + q^2_\perp m_{i'}\mathcal{I}_1}{(1-y')(1-y)(1-y-y')}, \tag{H.57}$$

$$J_2((+),+,-\frac{1}{2},+\frac{1}{2}) = 0, \tag{H.58}$$

$$J_2((+),-,-\frac{1}{2},+\frac{1}{2}) = -\frac{(q_\perp q'_\perp m_a - q_\perp q'_\perp m_i)\mathcal{I}_1 - q'^2_\perp m_i \mathcal{I}_2}{(1-y')(1-y)(1-y-y')}, \tag{H.59}$$

$$J_2((+),(+),-\frac{1}{2},+\frac{1}{2}) = \frac{(q'_\perp(m_a - y m_a - m_i + y m_i + y' m_i)\mathcal{I}_2}{(1-y)(1-y')(1-y-y'))}, \tag{H.60}$$

$$J_2((+),(-),-\frac{1}{2},+\frac{1}{2}) = 0, \tag{H.61}$$

$$J_2((-),+,-\frac{1}{2},+\frac{1}{2}) = \frac{(m_a - y' m_a - m_{i'} + y m_{i'} + y' m_{i'})\mathcal{I}_0}{(1-y')(1-y-y')}, \tag{H.62}$$

$$J_2((-),-,-\frac{1}{2},+\frac{1}{2}) = -[(1-y)(1-y')(1-y-y')^2]^{-1} \tag{H.63}$$
$$\times \big[(q^2_\perp m_i + q'^2_\perp m_i - q^2_\perp y' m_i - q'^2_\perp y' m_i + m_a^2 m_i - y' m_a^2 m_i - q^2_\perp m_{i'}$$
$$+q^2_\perp y m_{i'} + q^2_\perp y' m_{i'} - m_a m_i m_{i'} + y m_a m_i m_{i'} + y' m_a m_i m_{i'})\mathcal{I}_0$$
$$+(2q_\perp q'_\perp m_i - 2q_\perp q'_\perp y' m_i - q_\perp q'_\perp m_{i'} + q_\perp q'_\perp y m_{i'} + q_\perp q'_\perp y' m_{i'})\mathcal{I}_1]\,,$$

$$J_2((-),(+),-\frac{1}{2},+\frac{1}{2}) = -[(1-y)(1-y')(1-y-y')]^{-1} \quad \text{(H.64)}$$
$$\times [(q'_\perp m_i - q'_\perp y' m_i - q'_\perp m_{i'} + q'_\perp y m_{i'})\mathcal{I}_0$$
$$+(q_\perp m_i - q_\perp y' m_i - q_\perp m_{i'} + q_\perp y m_{i'})\mathcal{I}_1]\,,$$

$$J_2((-),(-),-\frac{1}{2},+\frac{1}{2}) = \frac{q_\perp(-m_a + y' m_a + m_{i'} - y m_{i'} - y' m_{i'})\mathcal{I}_1}{(1-y)(1-y')(1-y-y'))}. \quad \text{(H.65)}$$

Most matrix elements contain division by one or two powers of $1-y-y'$; however, all are finite in the limit that $1-y-y'$ becomes zero. The first power is cancelled by a factor of $1-y-y'$ that is implicit in all $\mathcal{I}_n$, through the dependence on F and D_{ajb}, defined in Eq. (5.11). The second power can also be cancelled by a suitable rearrangement of the numerators, and this becomes necessary when $(1-y-y')$ is very small, as can happen for y near 0 and y' near 1 or vice-versa, and there can be large round-off errors in the evaluation of such matrix elements. Alternate expressions, where the extra divisor of $(1-y-y')$ is cancelled explicitly, then need to be used. These are obtained by using the recursion relation (I.4) for the integrals to reduce all terms to include only $\mathcal{I}_0$, writing $D \equiv D_{ajb}$ and F as

$$D = (m_a^2 + q_\perp^2 + q_\perp'^2)/(1-y-y') + D', \quad F = 2q_\perp q'_\perp/(1-y-y'), \quad \text{(H.66)}$$

with

$$D' = \frac{\mu_j^2 + q_\perp^2}{y} + \frac{\mu_b^2 + q_\perp'^2}{y'} - M^2, \quad \text{(H.67)}$$

and, where necessary, defining a new function of momenta, $\mathcal{J}_0$, related to the angular integral $\mathcal{I}_0$ by

$$\mathcal{I}_0 = \frac{1}{D}\left[1 + \frac{F^2}{2D^2}\mathcal{J}_0\right]. \quad \text{(H.68)}$$

This yields

$$J_2(-,-,+\frac{1}{2},+\frac{1}{2}) = [2(1-y)(1-y')(1-y-y')]^{-1} \tag{H.69}$$
$$\times \left[-2m_{i'}m_i + m_a^2 + q_\perp^2 + q_\perp'^2 + D'(1-y-y')\right] D'\mathcal{I}_0,$$

$$J_2(-,(-),+\frac{1}{2},+\frac{1}{2}) = [(1-y-y')^3 D^3(1-y)(1-y')]^{-1} \tag{H.70}$$
$$\times \left[D'm_a^4 q_\perp' - m_{i'}m_i m_a^4 q_\perp' + m_i m_a^5 q_\perp' + 2D'm_a^2 q_\perp^2 q_\perp' - 2m_{i'}m_i m_a^2 q_\perp^2 q_\perp'\right.$$
$$+\mathcal{J}_0 m_{i'}m_i m_a^2 q_\perp^2 q_\perp' + 2m_i m_a^3 q_\perp^2 q_\perp' + D'q_\perp^4 q_\perp' - m_{i'}m_i q_\perp^4 q_\perp'$$
$$+\mathcal{J}_0 m_{i'}m_i q_\perp^4 q_\perp' + m_i m_a q_\perp^4 q_\perp' + 2D'm_a^2 q_\perp'^3 - 2m_{i'}m_i m_a^2 q_\perp'^3$$
$$+2m_i m_a^3 q_\perp'^3 + 2D'q_\perp^2 q_\perp'^3 + 2D'\mathcal{J}_0 q_\perp^2 q_\perp'^3 - 2m_{i'}m_i q_\perp^2 q_\perp'^3$$
$$-\mathcal{J}_0 m_{i'}m_i q_\perp^2 q_\perp'^3 + 2m_i m_a q_\perp^2 q_\perp'^3 + 2\mathcal{J}_0 m_i m_a q_\perp^2 q_\perp'^3 + D'q_\perp'^5 - m_{i'}m_i q_\perp'^5$$
$$+m_i m_a q_\perp'^5 + 2D'^2 m_a^2 q_\perp'(1-y-y') - 2D'm_{i'}m_i m_a^2 q_\perp'(1-y-y')$$
$$+2D'm_i m_a^3 q_\perp'(1-y-y') + 2D'^2 q_\perp^2 q_\perp'(1-y-y')$$
$$-2D'm_{i'}m_i q_\perp^2 q_\perp'(1-y-y') + D'\mathcal{J}_0 m_{i'}m_i q_\perp^2 q_\perp'(1-y-y')$$
$$+2D'm_i m_a q_\perp^2 q_\perp'(1-y-y') + 2D'^2 q_\perp'^3(1-y-y')$$
$$-2D'm_{i'}m_i q_\perp'^3(1-y-y') + 2D'm_i m_a q_\perp'^3(1-y-y')$$
$$+D'^3 q_\perp'(1-y-y')^2 - D'^2 m_{i'}m_i q_\perp'(1-y-y')^2$$
$$+D'^2 m_i m_a q_\perp'(1-y-y')^2 - D'm_a^4 q_\perp' y - 2D'm_a^2 q_\perp^2 q_\perp' y - D'q_\perp^4 q_\perp' y$$
$$-2D'm_a^2 q_\perp'^3 y - 2D'q_\perp^2 q_\perp'^3 y - 2D'\mathcal{J}_0 q_\perp^2 q_\perp'^3 y - D'q_\perp'^5 y - 2D'^2 m_a^2 q_\perp'(1-y-y')y$$
$$\left.-2D'^2 q_\perp^2 q_\perp'(1-y-y')y - 2D'^2 q_\perp'^3(1-y-y')y - D'^3 q_\perp'(1-y-y')^2 y\right],$$

$$J_2((-),-,+\frac{1}{2},+\frac{1}{2}) = [(1-y-y')^3 D^3 (1-y)(1-y')]^{-1} \tag{H.71}$$
$$\times \big[D' m_a^4 q_\perp - m_{i'} m_i m_a^4 q_\perp + m_{i'} m_a^5 q_\perp + 2D' m_a^2 q_\perp^3 - 2 m_{i'} m_i m_a^2 q_\perp^3$$
$$+2 m_{i'} m_a^3 q_\perp^3 + D' q_\perp^5 - m_{i'} m_i q_\perp^5 + m_{i'} m_a q_\perp^5$$
$$+2D' m_a^2 q_\perp q_\perp'^2 - 2 m_{i'} m_i m_a^2 q_\perp q_\perp'^2 + \mathcal{J}_0 m_{i'} m_i m_a^2 q_\perp q_\perp'^2 + 2 m_{i'} m_a^3 q_\perp q_\perp'^2$$
$$+2D' q_\perp^3 q_\perp'^2 + 2D' \mathcal{J}_0 q_\perp^3 q_\perp'^2 - 2 m_{i'} m_i q_\perp^3 q_\perp'^2 - \mathcal{J}_0 m_{i'} m_i q_\perp^3 q_\perp'^2$$
$$+2 m_{i'} m_a q_\perp^3 q_\perp'^2 + 2\mathcal{J}_0 m_{i'} m_a q_\perp^3 q_\perp'^2 + D' q_\perp q_\perp'^4 - m_{i'} m_i q_\perp q_\perp'^4 + \mathcal{J}_0 m_{i'} m_i q_\perp q_\perp'^4$$
$$+ m_{i'} m_a q_\perp q_\perp'^4 + 2D'^2 m_a^2 q_\perp (1-y-y')$$
$$-2D' m_{i'} m_i m_a^2 q_\perp (1-y-y') + 2D' m_{i'} m_a^3 q_\perp (1-y-y')$$
$$+2D'^2 q_\perp^3 (1-y-y') - 2D' m_{i'} m_i q_\perp^3 (1-y-y')$$
$$+2D' m_{i'} m_a q_\perp^3 (1-y-y') + 2D'^2 q_\perp q_\perp'^2 (1-y-y')$$
$$-2D' m_{i'} m_i q_\perp q_\perp'^2 (1-y-y') + D' \mathcal{J}_0 m_{i'} m_i q_\perp q_\perp'^2 (1-y-y')$$
$$+2D' m_{i'} m_a q_\perp q_\perp'^2 (1-y-y') + D'^3 q_\perp (1-y-y')^2$$
$$-D'^2 m_{i'} m_i q_\perp (1-y-y')^2 + D'^2 m_{i'} m_a q_\perp (1-y-y')^2$$
$$-D' m_a^4 q_\perp y' - 2D' m_a^2 q_\perp^3 y' - D' q_\perp^5 y' - 2D' m_a^2 q_\perp q_\perp'^2 y' - 2D' q_\perp^3 q_\perp'^2 y'$$
$$-2D' \mathcal{J}_0 q_\perp^3 q_\perp'^2 y' - D' q_\perp q_\perp'^4 y' - 2D'^2 m_a^2 q_\perp (1-y-y') y'$$
$$-2D'^2 q_\perp^3 (1-y-y') y' - 2D'^2 q_\perp q_\perp'^2 (1-y-y') y' - D'^3 q_\perp (1-y-y')^2 y' \big] ,$$

$$J_2((-),(-),+\frac{1}{2},+\frac{1}{2}) = [(1-y-y')^2 D^2 (1-y)(1-y')]^{-1} \tag{H.72}$$
$$\times [\mathcal{J}_0 q_\perp q_\perp' (m_{i'} m_a + D'(1-y-y') - m_{i'} m_i (1-y-y')$$
$$+ m_i m_a (1-y-y') + D' y - m_{i'} m_a y$$
$$+ m_i m_a y - D'(1-y-y') y - D' y^2) \big] ,$$

$$J_2(-,-,-\frac{1}{2},-\frac{1}{2}) = -[(1-y-y')^3 D^3 (1-y)(1-y')]^{-1} \tag{H.73}$$
$$\times \big[D'(-(\mathcal{J}_0 m_{i'} m_i m_a^2 q_\perp q'_\perp + m_a^4 q_\perp q'_\perp - \mathcal{J}_0 m_{i'} m_i q_\perp^3 q'_\perp + 2m_a^2 q_\perp^3 q'_\perp + q_\perp^5 q'_\perp$$
$$-\mathcal{J}_0 m_{i'} m_i q_\perp q_\perp'^3 + 2m_a^2 q_\perp q_\perp'^3 + 2q_\perp^3 q_\perp'^3 + 2\mathcal{J}_0 q_\perp^3 q_\perp'^3$$
$$+q_\perp q_\perp'^5 - D'\mathcal{J}_0 m_{i'} m_i q_\perp q'_\perp (1-y-y') + 2D' m_a^2 q_\perp q'_\perp (1-y-y')$$
$$+2D' q_\perp^3 q'_\perp (1-y-y') + 2D' q_\perp q_\perp'^3 (1-y-y') + D'^2 q_\perp q'_\perp (1-y-y')^2\big],$$

$$J_2(-,(+),-\frac{1}{2},-\frac{1}{2}) = -[(1-y-y')^3 D^3 (1-y)(1-y')]^{-1} \tag{H.74}$$
$$\times \big[q_\perp(-(m_{i'} m_i m_a^4) + \mathcal{J}_0 m_{i'} m_i m_a^4 - 2m_{i'} m_i m_a^2 q_\perp^2 + 2\mathcal{J}_0 m_{i'} m_i m_a^2 q_\perp^2$$
$$-m_{i'} m_i q_\perp^4 + \mathcal{J}_0 m_{i'} m_i q_\perp^4 + D'\mathcal{J}_0 m_a^2 q_\perp'^2 - 2m_{i'} m_i m_a^2 q_\perp'^2$$
$$++\mathcal{J}_0 m_{i'} m_i m_a^2 q_\perp'^2 + \mathcal{J}_0 m_i m_a^3 q_\perp'^2 D'\mathcal{J}_0 q_\perp^2 q_\perp'^2 - 2m_{i'} m_i q_\perp^2 q_\perp'^2$$
$$+-\mathcal{J}_0 m_{i'} m_i q_\perp^2 q_\perp'^2 + \mathcal{J}_0 m_i m_a q_\perp^2 q_\perp'^2 + D'\mathcal{J}_0 q_\perp'^4 - m_{i'} m_i q_\perp'^4$$
$$+\mathcal{J}_0 m_i m_a q_\perp'^4 - 2D' m_{i'} m_i m_a^2 (1-y-y') + 2D'\mathcal{J}_0 m_{i'} m_i m_a^2 (1-y-y')$$
$$-2D' m_{i'} m_i q_\perp^2 (1-y-y') + 2D'\mathcal{J}_0 m_{i'} m_i q_\perp^2 (1-y-y')$$
$$+D'^2\mathcal{J}_0 q'^2_\perp (1-y-y') - 2D' m_{i'} m_i q'^2_\perp (1-y-y')$$
$$+D'\mathcal{J}_0 m_{i'} m_i q'^2_\perp (1-y-y') + D'\mathcal{J}_0 m_i m_a q'^2_\perp (1-y-y')$$
$$-D'^2 m_{i'} m_i (1-y-y')^2 + D'^2\mathcal{J}_0 m_{i'} m_i (1-y-y')^2$$
$$-D'\mathcal{J}_0 m_a^2 q'^2_\perp y - D'\mathcal{J}_0 q_\perp^2 q'^2_\perp y - D'\mathcal{J}_0 q'^4_\perp y - D'^2\mathcal{J}_0 q'^2_\perp (1-y-y')y\big],$$

$$J_2((+),-,-\frac{1}{2},-\frac{1}{2}) = -[(1-y-y')^3 D^3 (1-y)(1-y')]^{-1} \tag{H.75}$$
$$\times \left[q'_\perp(-(m_{i'} m_i m_a^4) + \mathcal{J}_0 m_{i'} m_i m_a^4 - 2 m_{i'} m_i m_a^2 q_\perp^2 + \mathcal{J}_0 m_{i'} m_i m_a^2 q_\perp^2 \right.$$
$$+\mathcal{J}_0 m_{i'} m_a^3 q_\perp^2 - m_{i'} m_i q_\perp^4 + \mathcal{J}_0 m_{i'} m_a q_\perp^4 - 2 m_{i'} m_i m_a^2 q_\perp'^2$$
$$+2\mathcal{J}_0 m_{i'} m_i m_a^2 q_\perp'^2 - 2 m_{i'} m_i q_\perp^2 q_\perp'^2 - \mathcal{J}_0 m_{i'} m_i q_\perp^2 q_\perp'^2 + \mathcal{J}_0 m_{i'} m_a q_\perp^2 q_\perp'^2$$
$$-m_{i'} m_i q_\perp'^4 + \mathcal{J}_0 m_{i'} m_i q_\perp'^4 - 2D' m_{i'} m_i m_a^2 (1-y-y')$$
$$+2D' \mathcal{J}_0 m_{i'} m_i m_a^2 (1-y-y') - 2D' m_{i'} m_i q_\perp^2 (1-y-y')$$
$$+D' \mathcal{J}_0 m_{i'} m_i q_\perp^2 (1-y-y') + D' \mathcal{J}_0 m_{i'} m_a q_\perp^2 (1-y-y')$$
$$+D' \mathcal{J}_0 m_a^2 q_\perp^2 (1-y-y') + D' \mathcal{J}_0 q_\perp^4 (1-y-y')$$
$$-2D' m_{i'} m_i q_\perp'^2 (1-y-y') + 2D' \mathcal{J}_0 m_{i'} m_i q_\perp'^2 (1-y-y')$$
$$+D' \mathcal{J}_0 q_\perp^2 q_\perp'^2 (1-y-y') - D'^2 m_{i'} m_i (1-y-y')^2$$
$$+D'^2 \mathcal{J}_0 m_{i'} m_i (1-y-y')^2 + D'^2 \mathcal{J}_0 q_\perp^2 (1-y-y')^2 + D' \mathcal{J}_0 m_a^2 q_\perp^2 y$$
$$\left. +D' \mathcal{J}_0 q_\perp^4 y + D' \mathcal{J}_0 q_\perp^2 q_\perp'^2 y + D'^2 \mathcal{J}_0 q_\perp^2 (1-y-y') y \right],$$

$$J_2((+),(+),-\frac{1}{2},-\frac{1}{2}) = -[(1-y-y')^3 D^3 (1-y)(1-y')]^{-1} \tag{H.76}$$
$$\times \left[(-m_a^4 + \mathcal{J}_0 m_a^4 - 2 m_a^2 q_\perp^2 + 2\mathcal{J}_0 m_a^2 q_\perp^2 - q_\perp^4 + \mathcal{J}_0 q_\perp^4 - 2 m_a^2 q_\perp'^2 \right.$$
$$+2\mathcal{J}_0 m_a^2 q_\perp'^2 - 2 q_\perp^2 q_\perp'^2 - q_\perp'^4 + \mathcal{J}_0 q_\perp'^4 - 2D' m_a^2 (1-y-y')$$
$$+2D' \mathcal{J}_0 m_a^2 (1-y-y') - 2D' q_\perp^2 (1-y-y') + 2D' \mathcal{J}_0 q_\perp^2 (1-y-y')$$
$$-2D' q_\perp'^2 (1-y-y') + 2D' \mathcal{J}_0 q_\perp'^2 (1-y-y') - D'^2 (1-y-y')^2$$
$$+D'^2 \mathcal{J}_0 (1-y-y')^2)(m_{i'} m_a + D'(1-y-y') - m_{i'} m_i (1-y-y')$$
$$+m_i m_a (1-y-y') + D' y - m_{i'} m_a y$$
$$\left. +m_i m_a y - D'(1-y-y') y - D' y^2 \right],$$

$$J_2(-,-,+\frac{1}{2},-\frac{1}{2}) = [(1-y-y')^3 D^3 (1-y)(1-y')]^{-1} \tag{H.77}$$
$$\times \big[-(D' m_i m_a^4 q'_\perp - D' \mathcal{J}_0 m_{i'} m_a^2 q_\perp^2 q'_\perp - 2D' m_i m_a^2 q_\perp^2 q'_\perp - D' \mathcal{J}_0 m_{i'} q_\perp^4 q'_\perp$$
$$- D' m_i q_\perp^4 q'_\perp - 2D' m_i m_a^2 q_\perp'^3 - D' \mathcal{J}_0 m_{i'} q_\perp^2 q_\perp'^3 - 2D' m_i q_\perp^2 q_\perp'^3$$
$$- 2D' \mathcal{J}_0 m_i q_\perp^2 q_\perp'^3 - D' m_i q_\perp'^5 - 2D'^2 m_i m_a^2 q'_\perp (1-y-y')$$
$$- D'^2 \mathcal{J}_0 m_{i'} q_\perp^2 q'_\perp (1-y-y') - 2D'^2 m_i q_\perp^2 q'_\perp (1-y-y')$$
$$- 2D'^2 m_i q_\perp'^3 (1-y-y') - D'^3 m_i q'_\perp (1-y-y')^2 \big] ,$$

$$J_2(-,(-),+\frac{1}{2},-\frac{1}{2}) = [2(1-y)(1-y')(1-y-y')]^{-1} \tag{H.78}$$
$$\times \big[-2D' m_{i'} - 2 m_{i'} m_i m_a + m_i m_a^2 + m_i q_\perp^2 - m_i q_\perp'^2$$
$$+ D' m_i (1-y-y') + 2D' m_{i'} y] \mathcal{I}_0,$$

$$J_2((+),-,+\frac{1}{2},-\frac{1}{2}) = -[(1-y-y')^3 D^3 (1-y)(1-y')]^{-1} \tag{H.79}$$
$$\times \big[(q_\perp q'_\perp(\mathcal{J}_0 m_{i'} m_i m_a^3 + m_{i'} m_a^4 - \mathcal{J}_0 m_{i'} m_a^4 + \mathcal{J}_0 m_{i'} m_i m_a q_\perp^2$$
$$+2m_{i'} m_a^2 q_\perp^2 - \mathcal{J}_0 m_{i'} m_a^2 q_\perp^2 + m_{i'} q_\perp^4 + \mathcal{J}_0 m_{i'} m_i m_a q_\perp'^2$$
$$+2m_{i'} m_a^2 q_\perp'^2 - 2\mathcal{J}_0 m_{i'} m_a^2 q_\perp'^2 + 2m_{i'} q_\perp^2 q_\perp'^2 + \mathcal{J}_0 m_{i'} q_\perp^2 q_\perp'^2$$
$$+m_{i'} q_\perp'^4 - \mathcal{J}_0 m_{i'} q_\perp'^4 + D' \mathcal{J}_0 m_{i'} m_i m_a (1-y-y')$$
$$+2D' m_{i'} m_a^2 (1-y-y') - 2D' \mathcal{J}_0 m_{i'} m_a^2 (1-y-y')$$
$$+D' \mathcal{J}_0 m_i m_a^2 (1-y-y') + 2D' m_{i'} q_\perp^2 (1-y-y')$$
$$-D' \mathcal{J}_0 m_{i'} q_\perp^2 (1-y-y') + D' \mathcal{J}_0 m_i q_\perp^2 (1-y-y')$$
$$+2D' m_{i'} q_\perp'^2 (1-y-y') - 2D' \mathcal{J}_0 m_{i'} q_\perp'^2 (1-y-y')$$
$$+D' \mathcal{J}_0 m_i q_\perp'^2 (1-y-y') + D'^2 m_{i'} (1-y-y')^2$$
$$-D'^2 \mathcal{J}_0 m_{i'} (1-y-y')^2 + D'^2 \mathcal{J}_0 m_i (1-y-y')^2$$
$$+D' \mathcal{J}_0 m_i m_a^2 y + D' \mathcal{J}_0 m_i q_\perp^2 y$$
$$+D' \mathcal{J}_0 m_i q_\perp'^2 y + D'^2 \mathcal{J}_0 m_i (1-y-y')y)\big] ,$$

$$J_2(-,-,-\frac{1}{2},+\frac{1}{2}) = -[(1-y-y')^3 D^3 (1-y)(1-y')]^{-1} \tag{H.80}$$
$$\times \big[-D' m_{i'} m_a^4 q_\perp - 2D' m_{i'} m_a^2 q_\perp^3 - D' m_{i'} q_\perp^5 - 2D' m_{i'} m_a^2 q_\perp q_\perp'^2$$
$$-D' \mathcal{J}_0 m_i m_a^2 q_\perp q_\perp'^2 - 2D' m_{i'} q_\perp^3 q_\perp'^2 - 2D' \mathcal{J}_0 m_{i'} q_\perp^3 q_\perp'^2 - D' \mathcal{J}_0 m_i q_\perp^3 q_\perp'^2$$
$$-D' m_{i'} q_\perp q_\perp'^4 - D' \mathcal{J}_0 m_i q_\perp q_\perp'^4 - 2D'^2 m_{i'} m_a^2 q_\perp (1-y-y')$$
$$-2D'^2 m_{i'} q_\perp^3 (1-y-y') - 2D'^2 m_{i'} q_\perp q_\perp'^2 (1-y-y')$$
$$-D'^2 \mathcal{J}_0 m_i q_\perp q_\perp'^2 (1-y-y') - D'^3 m_{i'} q_\perp (1-y-y')^2\big] ,$$

$$J_2(-,(+),-\frac{1}{2},+\frac{1}{2}) = -[(1-y-y')^3 D^3 (1-y)(1-y')]^{-1} \tag{H.81}$$
$$\times \left[q_\perp q'_\perp (-D' \mathcal{J}_0 m_{i'} m_a^2 - \mathcal{J}_0 m_{i'} m_i m_a^3 - m_i m_a^4 + \mathcal{J}_0 m_i m_a^4 \right.$$
$$-D' \mathcal{J}_0 m_{i'} q_\perp^2 - \mathcal{J}_0 m_{i'} m_i m_a q_\perp^2 - 2 m_i m_a^2 q_\perp^2 + 2 \mathcal{J}_0 m_i m_a^2 q_\perp^2$$
$$-m_i q_\perp^4 + \mathcal{J}_0 m_i q_\perp^4 - D' \mathcal{J}_0 m_{i'} q_\perp'^2 - \mathcal{J}_0 m_{i'} m_i m_a q_\perp'^2$$
$$-2 m_i m_a^2 q_\perp'^2 + \mathcal{J}_0 m_i m_a^2 q_\perp'^2 - 2 m_i q_\perp^2 q_\perp'^2 - \mathcal{J}_0 m_i q_\perp^2 q_\perp'^2$$
$$-m_i q_\perp'^4 - D'^2 \mathcal{J}_0 m_{i'} (1-y-y') - D' \mathcal{J}_0 m_{i'} m_i m_a (1-y-y')$$
$$-2D' m_i m_a^2 (1-y-y') + 2D' \mathcal{J}_0 m_i m_a^2 (1-y-y')$$
$$-2D' m_i q_\perp^2 (1-y-y') + 2D' \mathcal{J}_0 m_i q_\perp^2 (1-y-y')$$
$$-2D' m_i q_\perp'^2 (1-y-y') + D' \mathcal{J}_0 m_i q_\perp'^2 (1-y-y')$$
$$-D'^2 m_i (1-y-y')^2 + D'^2 \mathcal{J}_0 m_i (1-y-y')^2$$
$$+D' \mathcal{J}_0 m_{i'} m_a^2 y + D' \mathcal{J}_0 m_{i'} q_\perp^2 y$$
$$\left. +D' \mathcal{J}_0 m_{i'} q_\perp'^2 y + D'^2 \mathcal{J}_0 m_{i'} (1-y-y') y) \right],$$

$$J_2((-),-,-\frac{1}{2},+\frac{1}{2}) = -[2(1-y)(1-y')(1-y-y')]^{-1} \tag{H.82}$$
$$\times \left[2 m_{i'} m_i m_a - m_{i'} m_a^2 + m_{i'} q_\perp^2 - m_{i'} q_\perp'^2 - D' m_{i'} (1-y-y') \right.$$
$$\left. +2D' m_i (1-y-y') + 2D' m_i y \right] \mathcal{I}_0.$$

The remaining divisors of $1-y-y'$ are cancelled by factors contained within D and $\mathcal{I}_0$.

Appendix I

ANGULAR INTEGRALS

Calculation of the two-photon kernels requires the integrals

$$\mathcal{I}_n = \int_0^{2\pi} \frac{d\phi}{2\pi} \frac{e^{-in\phi}}{D + F\cos\phi}, \tag{I.1}$$

first defined in Eq. (6.6). Here the original integration variable ϕ' has been shifted by the independent angle ϕ and the prime then dropped for simplicity of notation in this Appendix. The factor F is always positive, but D can be negative. If the bare fermion mass m_0 is less than the physical mass m_e, we can have $|D| < F$; in this case, $\mathcal{I}_n$ is defined by a principal value, as in the one-photon sector. If either photon has zero transverse momentum, F will be zero, and any pole due to a zero in D will not involve the angular integration. The numerical quadrature is chosen to never use grid points where a photon transverse momentum is zero, so that the principal-value prescription can always be invoked for the angular integral, where it is easily handled analytically.

The imaginary part of $\mathcal{I}_n$ is zero. This follows from the even parity of the denominator and the odd parity of $\sin n\phi$. As a consequence, $\mathcal{I}_{-n} = \mathcal{I}_n$, and we evaluate (I.1) for only nonnegative n.

The real part is nonzero and most easily calculated from combinations of the related integrals

$$\bar{\mathcal{I}}_n = \int_0^{2\pi} \frac{d\phi}{2\pi} \frac{\cos^n\phi}{D + F\cos\phi}. \tag{I.2}$$

Of course, for $n = 0$ and 1, the two integrals are identical. For $n = 2$ and 3 we have $\cos 2\phi = 2\cos^2\phi - 1$ and $\cos 3\phi = 4\cos^3\phi - 3\cos\phi$. Therefore, the integral

combinations are

$$\mathcal{I}_0 = \bar{\mathcal{I}}_0, \;\; \mathcal{I}_1 = \bar{\mathcal{I}}_1, \;\; \mathcal{I}_2 = 2\bar{\mathcal{I}}_2 - \bar{\mathcal{I}}_0, \;\; \mathcal{I}_3 = 4\bar{\mathcal{I}}_3 - 3\bar{\mathcal{I}}_1. \tag{I.3}$$

Larger values of n do not appear in the two-photon kernels.

The integrals $\bar{\mathcal{I}}_n$ are connected by a simple recursion for $n > 0$:

$$\bar{\mathcal{I}}_n = \int_0^{2\pi} \frac{d\phi}{2\pi} \frac{\cos^{n-1}\phi}{F} \frac{(D + F\cos\phi - D)}{D + F\cos\phi} = \frac{1}{F}\int_0^{2\pi} \frac{d\phi}{2\pi} \cos^{n-1}\phi - \frac{D}{F}\bar{\mathcal{I}}_{n-1}. \tag{I.4}$$

The first term is zero when n is even. For $n = 1$, it is $1/F$, and for $n = 3$, this term is $1/2F$. The only other integral that must be evaluated directly is $\bar{\mathcal{I}}_0 = \mathcal{I}_0$.

The determination of $\mathcal{I}_0$, with or without the presence of poles, is conveniently done by contour integration around the unit circle in terms of a complex variable $z = e^{i\phi}$. We then have

$$\mathcal{I}_0 = \frac{1}{i\pi F}\oint \frac{dz}{z^2 + 2\frac{D}{F}z + 1} = \frac{1}{i\pi F}\oint \frac{dz}{(z - z_+)(z - z_-)}. \tag{I.5}$$

There are simple poles at

$$z_\pm = -\frac{D}{F} \pm \sqrt{\frac{D^2}{F^2} - 1} = -\frac{D}{F} \pm i\sqrt{1 - \frac{D^2}{F^2}} = -e^{\mp i\cos^{-1}(D/F)} \tag{I.6}$$

When D is greater than F, one pole, z_+, is inside the contour and the other outside, as illustrated in Fig. I.1. Evaluation of $2\pi i$ times the residue yields

$$\mathcal{I}_0 = \frac{1}{\sqrt{D^2 - F^2}} \;\text{ for }\; D > F. \tag{I.7}$$

Similarly, when D is less than $-F$, the pole at z_- is inside the contour, and we have

$$\mathcal{I}_0 = -\frac{1}{\sqrt{D^2 - F^2}} \;\text{ for }\; D < -F. \tag{I.8}$$

When $|D|$ is less than F, the poles move to the contour, and the integral is defined by the principal value. This is evaluated by distorting the contour to include semicircles

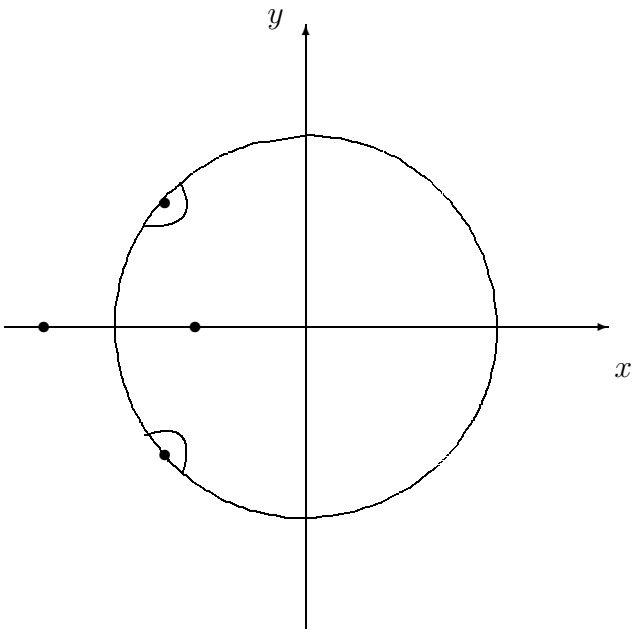

Figure I.1. Integration contour for evaluation of $\mathcal{I}_0$. The locations of the poles at $z_\pm$ depend upon the magnitude and sign of D/F. The semicircles are used when $|D|/F < 1$ and the poles are on the contour.

of radius ϵ around each pole, as shown in Fig. I.1, and subtracting the contributions from the semicircles after taking the $\epsilon \to 0$ limit. The choice of inward semicircles makes the integral around the closed contour simply zero. For the semicircle around $z_\pm$, we have $z = z_\pm + \epsilon e^{i\theta}$ and a contribution, as ϵ goes to zero, of

$$\frac{2}{iF}\int \frac{\epsilon i e^{i\theta} d\theta}{\epsilon e^{i\theta}(\epsilon e^{i\theta} \mp 2i\sqrt{1 - D^2/F^2})} \longrightarrow \frac{\pm \int d\theta}{F\sqrt{1 - D^2/F^2}}. \tag{I.9}$$

Thus the contributions from the two semicircles are of opposite sign and cancel, so that the net result is also zero. Therefore, we have

$$\mathcal{I}_0 = \begin{cases} \frac{1}{\sqrt{D^2 - F^2}}, & D > F \\ 0, & |D| < F \\ -\frac{1}{\sqrt{D^2 - F^2}}, & D < -F. \end{cases} \tag{I.10}$$

The case where D equals F represents an integrable singularity for the transverse momentum integrations and can be ignored. When F is zero, we have simply

$$\mathcal{I}_n = \int_0^{2\pi} \frac{d\phi}{2\pi D} e^{-in\phi} = \frac{1}{D}\delta_{n0}. \tag{I.11}$$

When F/D is small, the expressions for the integrals $\mathcal{I}_n$ are best evaluated from expansions in powers of F/D, to avoid round-off errors due to cancellations between large contributions. The expansions used are

$$\mathcal{I}_0 \simeq \frac{1}{128D}\left[128 + 64\left(\frac{F}{D}\right)^2 + 48\left(\frac{F}{D}\right)^4 + 40\left(\frac{F}{D}\right)^6 + 35\left(\frac{F}{D}\right)^8\right], \tag{I.12}$$

$$\mathcal{I}_1 \simeq -\frac{1}{128D}\left(\frac{F}{D}\right)\left[64 + 48\left(\frac{F}{D}\right)^2 + 40\left(\frac{F}{D}\right)^4 + 35\left(\frac{F}{D}\right)^6\right], \tag{I.13}$$

$$\mathcal{I}_2 \simeq \frac{1}{128D}\left(\frac{F}{D}\right)^2\left[32 + 32\left(\frac{F}{D}\right)^2 + 30\left(\frac{F}{D}\right)^4\right], \tag{I.14}$$

$$\mathcal{I}_3 \simeq -\frac{1}{128D}\left(\frac{F}{D}\right)^3\left[16 + 20\left(\frac{F}{D}\right)^2\right]. \tag{I.15}$$

REFERENCES

[1] T. Kinoshita and M. Nio, Phys. Rev. D **73**, 013003 (2006).

[2] S.J. Brodsky, J.R. Hiller, and G. McCartor, Phys. Rev. D **58**, 025005 (1998).

[3] S.J. Brodsky, J.R. Hiller, and G. McCartor, Phys. Rev. D **60**, 054506 (1999).

[4] S.J. Brodsky, J.R. Hiller, and G. McCartor, Phys. Rev. D **64**, 114023 (2001).

[5] S.J. Brodsky, J.R. Hiller, and G. McCartor, Ann. Phys. **296**, 406 (2002).

[6] S.J. Brodsky, J.R. Hiller, and G. McCartor, Ann. Phys. **305**, 266 (2003).

[7] S.J. Brodsky, V.A. Franke, J.R. Hiller, G. McCartor, S.A. Paston, and E.V. Prokhvatilov, Nucl. Phys. B **703**, 333 (2004).

[8] S.J. Brodsky, J.R. Hiller, and G. McCartor, Ann. Phys. **321**, 1240 (2006).

[9] C. Lanczos, J. Res. Nat. Bur. Stand. **45**, 255 (1950); J.H. Wilkinson, *The Algebraic Eigenvalue Problem* (Clarendon, Oxford, 1965); B.N. Parlett, *The Symmetric Eigenvalue Problem* (Prentice-Hall, Englewood Cliffs, NJ, 1980); D.S. Scott, in *Sparse Matrices and their Uses*, edited by I.S. Duff (Academic Press, London, 1981), p. 139; G.H. Golub and C.F. van Loan, *Matrix Computations* (Johns Hopkins University Press, Baltimore, 1983); J. Cullum and R.A. Willoughby, in *Large-Scale Eigenvalue Problems*, eds. J. Cullum and R.A. Willoughby, *Math. Stud.* **127** (Elsevier, Amsterdam, 1986), p. 193; Y. Saad, Comput. Phys. Commun. **53**, 71 (1989); S.K. Kin and A.T. Chronopoulos, J. Comp. and Appl. Math. **42**, 357 (1992).

[10] J. Cullum and R.A. Willoughby, J. Comput. Phys. **44**, 329 (1981); *Lanczos Algorithms for Large Symmetric Eigenvalue Computations* (Birkhauser, Boston, 1985), Vol. I and II.

[11] W. Pauli and F. Villars, Rev. Mod. Phys. **21**, 434 (1949).

[12] B. Grinstein, D. O'Connell, and M.B. Wise, Phys. Rev. D **77**, 025012 (2008); C.D. Carone and R.F. Lebed, JHEP **0901**:043 (2009).

[13] P.A.M. Dirac, Rev. Mod. Phys. **21**, 392 (1949).

[14] For reviews and additional references, see M. Burkardt, Adv. Nucl. Phys. **23**, 1 (2002); S.J. Brodsky, H.-C. Pauli, and S.S. Pinsky, Phys. Rep. **301**, 299 (1998).

[15] T. Maskawa and K. Yamawaki, Prog. Theor. Phys. **56**, 270 (1976).

[16] P.P. Srivastava and S.J. Brodsky, Phys. Rev. D **61**, 025013 (1999); **64**, 045006 (2001); **66**, 045019 (2002).

[17] S.S. Chabysheva and J.R. Hiller, Phys. Rev. D **79**, 096012 (2009) and references therein.

[18] R.P. Feynman, in *The Quantum Theory of Fields* (Interscience Publishers, New York, 1961).

[19] S.D. Drell and H.R. Pagels, Phys. Rev. **140**, B397 (1965).

[20] J.R. Hiller and S.J. Brodsky, Phys. Rev. D **59**, 016006 (1998).

[21] For a perturbative analysis using light-cone quantization, see A. Langnau, Ph.D. thesis, SLAC Report 385, 1992; A. Langnau and M. Burkardt, Phys. Rev. D **47**, 3452 (1993).

[22] I. Tamm, J. Phys. (Moscow) **9**, 449 (1945); S.M. Dancoff, Phys. Rev. **78**, 382 (1950).

[23] R.J. Perry, A. Harindranath, and K.G. Wilson, Phys. Rev. Lett. **65**, 2959 (1990); R.J. Perry and A. Harindranath, Phys. Rev. D **43**, 4051 (1991).

[24] K.G. Wilson, T.S. Walhout, A. Harindranath, W.-M. Zhang, R.J. Perry, and St.D. Głazek, Phys. Rev. D **49**, 6720 (1994);

[25] A. Harindranath and R.J. Perry, Phys. Rev. D **43**, 492 (1991); **43**, 3580(E) (1991); D. Mustaki, S. Pinsky, J. Shigemitsu, and K.G. Wilson, *ibid.* **43**, 3411 (1991); A. Langnau, Ph.D. thesis, SLAC Report 385, 1992; A. Langnau and S.J. Brodsky, J. Comput. Phys. **109**, 84 (1993); R.J. Perry, Phys. Lett. **B300**, 8 (1993); W.-M. Zhang and A. Harindranath, Phys. Rev. D **48**, 4868 (1993); **48**, 4881 (1993); **48**, 4903 (1993); N.E. Ligterink and B.L.G. Bakker, Phys. Rev. D **52**, 5917 (1995); 5954 (1995); N.C.J. Schoonderwoerd and B.L.G. Bakker, Phys. Rev. D **57**, 4965 (1998); **58**, 025013 (1998).

[26] H.-C. Pauli and S.J. Brodsky, Phys. Rev. D **32**, 1993 (1985); **32**, 2001 (1985).

[27] K. Hornbostel, S. J. Brodsky and H. C. Pauli, Phys. Rev. D **41**, 3814 (1990).

[28] Y. Matsumura, N. Sakai, and T. Sakai, Phys. Rev. D **52**, 2446 (1995); O. Lunin and S. Pinsky, AIP Conf. Proc. **494**, 140 (1999); J. R. Hiller, S. S. Pinsky, N. Salwen and U. Trittmann, Phys. Lett. B **624**, 105 (2005) and references therein.

[29] L.C.L. Hollenberg, K. Higashijima, R.C. Warner, and B.H.J. McKellar, Prog. Th. Phys. **87**, 441 (1992).

[30] C. Bouchiat, P. Fayet, and N. Sourlas, Lett. Nuovo Cim. **4**, 9 (1972); S.-J. Chang and T.-M. Yan, Phys. Rev. D **7**, 1147 (1973); M. Burkardt and A. Langnau, Phys. Rev. D **44**, 1187 (1991).

[31] O.W. Greenberg and S.S. Schweber, Nuovo Cim. **8**, 378 (1958).

[32] A.C. Tang, S.J. Brodsky, and H.-C. Pauli, Phys. Rev. D **44**, 1842 (1991).

[33] J. Schwinger, Phys. Rev. **73**, 416 (1948); **76**, 790 (1949).

[34] C.M. Sommerfield, Phys. Rev. **107**, 328 (1957); A. Petermann, Helv. Phys. Acta. **30**, 407 (1957).

[35] S.A. Paston and V.A. Franke, Theor. Math. Phys. **112**, 1117 (1997) [Teor. Mat. Fiz. **112**, 399 (1997)]; S.A. Paston, V.A. Franke, and E.V. Prokhvatilov, Theor. Math. Phys. **120**, 1164 (1999) [Teor. Mat. Fiz. **120**, 417 (1999)];

[36] S. Dalley and G. McCartor, Ann. Phys. **321**, 402 (2006), hep-ph/0406287.

[37] See, for example, S. Capstick and N. Isgur, Phys. Rev. D **34**, 2809 (1986); S. Godfrey and N. Isgur, Phys. Rev. D **32**, 189 (1985).

[38] M.M. Brisudova, R.J. Perry, and K.G. Wilson, Phys. Rev. Lett. **78**, 1227 (1997).

[39] S. J. Brodsky and G. F. de Teramond, Phys. Rev. Lett. **96**, 201601 (2006).

[40] S. D. Głazek and J. Mlynik, Phys. Rev. D **74**, 105015 (2006), S. D. Głazek, Phys. Rev. D **69**, 065002 (2004), S. D. Głazek and J. Mlynik, Phys. Rev. D **67**, 045001 (2003); St.D. Głazek and M. Wieckowski, Phys. Rev. D **66**, 016001 (2002).

[41] V. A. Karmanov, J. F. Mathiot and A. V. Smirnov, Phys. Rev. D **75**, 045012 (2007); Nucl. Phys. Proc. Suppl. **161**, 160 (2006).

[42] For reviews, see M. Creutz, L. Jacobs and C. Rebbi, Phys. Rep. **93**, 201 (1983); J.B. Kogut, Rev. Mod. Phys. **55**, 775 (1983); I. Montvay, *ibid.* **59**, 263 (1987); A.S. Kronfeld and P.B. Mackenzie, Ann. Rev. Nucl. Part. Sci. **43**, 793 (1993); J.W. Negele, Nucl. Phys. **A553**, 47c (1993); K.G. Wilson, Nucl. Phys. B (Proc.

Suppl.) **140**, 3 (2005); J.M. Zanotti, PoS **LAT2008**, 007 (2008). For recent discussions of meson properties and charm physics, see for example C. McNeile and C. Michael (UKQCD Collaboration), Phys. Rev. D **74**, 014508 (2006); I. Allison *et al.* [HPQCD Collaboration], Phys. Rev. D **78**, 054513 (2008).

[43] M. Burkardt and S. Dalley, Prog. Part. Nucl. Phys. **48**, 317 (2002) and references therein; S. Dalley and B. van de Sande, Phys. Rev. D **67**, 114507 (2003); D. Chakrabarti, A.K. De, and A. Harindranath, Phys. Rev. D **67**, 076004 (2003); M. Harada and S. Pinsky, Phys. Lett. B **567**, 277 (2003); S. Dalley and B. van de Sande, Phys. Rev. Lett. **95**, 162001 (2005); J. Bratt, S. Dalley, B. van de Sande, and E. M. Watson, Phys. Rev. D **70**, 114502 (2004). For work on a complete light-cone lattice, see C. Destri and H.J. de Vega, Nucl. Phys. **B290**, 363 (1987); D. Mustaki, Phys. Rev. D **38**, 1260 (1989).

[44] C.D. Roberts and A.G. Williams, Prog. Part. Nucl. Phys. **33**, 477 (1994); P. Maris and C.D. Roberts, Int. J. Mod. Phys. **E12**, 297 (2003); P.C. Tandy, Nucl. Phys. B (Proc. Suppl.) **141**, 9 (2005).

[45] S.S. Chabysheva and J.R. Hiller, Phys. Rev. D **79**, 114017 (2009).

[46] G.P. Lepage and S.J. Brodsky, Phys. Rev. D **22**, 2157 (1980).

[47] S.N. Gupta, Proc. Phys. Soc. (London) **A63**, 681 (1950); K. Bleuler, Helv. Phys. Acta **23**, 567 (1950).

[48] N.N. Bogoliubov and D.V. Shirkov, *Introduction to the Theory of Quantized Fields,* (Interscience, New York, 1959); S. Schweber, *An Introduction to Relativistic Quantum Field Theory,* (Harper & Row, New York, 1961); C. Itzykson and J.-B. Zuber, *Quantum Field Theory,* (McGraw–Hill, New York, 1980).

[49] S.J. Brodsky, R. Roskies, and R. Suaya, Phys. Rev. D **8**, 4574 (1973).

[50] S.J. Brodsky and S.D. Drell, Phys. Rev. D **22**, 2236 (1980).

[51] R.L. Burden and J.D. Faires, *Numerical Analysis*, 3rd ed., (Prindle, Weber & Schmidt, Boston, 1985).

[52] D. Klabucar and H.-C. Pauli, Z. Phys. C **47**, 141 (1990); M. Kaluža and H.-C. Pauli, Phys. Rev. D **45**, 2968 (1992); M. Krautgärtner, H.C. Pauli, and F. Wölz, *ibid.* **45**, 3755 (1992); U. Trittmann and H.-C. Pauli, hep-th/9704215; hep-th/9705021; U. Trittmann, hep-th/9705072; hep-th/9706055.

[53] J.C. Ward, Phys. Rev. **78**, 1824 (1950); Y. Takahashi, Nuovo Cim. **6**, 370 (1957).

[54] W. Pauli, Rev. Mod. Phys. **15**, 175 (1943).